Ministry of Agriculture, Natural Resources and Environment
Cyprus Geological Survey Department

Investigation of Rocks that may Contain Asbestos Minerals in the Troodos Region (GSD/2008/26)

Final Report

For the period December 2008 – November 2010

November 2010

TABLE OF CONTENTS

LIST OF FIGURES

LIST OF TABLES

LIST OF ANNEXES

1 INTRODUCTION

1.1 Purpose and Scope of the Report

The purpose of this report is to present to the Geological Survey Department (Ministry of Agriculture, Natural Resources and Environment) a draft final report of Project GSD/2008/26, pursuant to the terms and conditions of the contract dated 1st December 2008, between the Geological Survey Department (GSD) and the Consortium Ecorem N.V. (Belgium) - Atlantis Consulting Cyprus Ltd.

Aiming primarily at the investigation of fibrous minerals of the Troodos Plutonic Complex, Project GSD/2008/26 was carried out by the consortium from December 2008 to November 2010. The bulk of the work performed and the results obtained by the Project are described in two intermediate reports dated August 2009 and April 2010, respectively.

The present report gives a full account on the Project and describes thoroughly the methodology, the work performed and the results obtained. It makes particular reference to the geology, asbest mineralization and distribution, the findings of laboratory work and the assessment of potential risk of asbestos bearing rocks, leading to conclusions and recommendations.

1.2 Project Objectives

The primary objective of the Project is to map and record all types of fibrous minerals occurring in the ultrabasic rocks of the Troodos Ophiolite Complex, within an area of approximately 500 sq. km. centered on Mt.Olympus **(Figure 1)**.

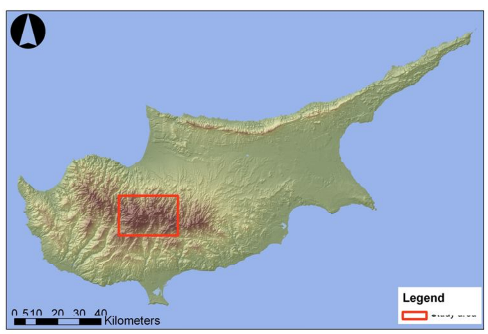

Figure 1: Study Area

For the achievement of the Project objectives, the specific tasks and goals were the following:

- Compilation and evaluation of all available relevant data and information.
- Geological mapping with particular emphasis on the ultrabasic rocks.
- Petrographical, mineralogical and spectrographic analysis of samples.
- Delineation of areas containing asbestos minerals and preparation of potential risk maps.
- Establishment of GIS-database and map preparation.

- Training of GSD staff, on the petrographical and mineralogical techniques in the analysis of asbestiform minerals.

1.3 Project background

The study area comprises hilly and mountainous villages, which administratively belong to the districts of Nicosia and Limassol. In these villages there is a rapid agricultural, tourist and residential development. During this development, extensive excavations for building and growing major rural areas are conducted.

The transportation in these areas uses a relatively adequate road network, which includes both asphalted and graded roads. These deployments occur on the rocks of the Troodos Ophiolite, which may contain asbestos fibres. Therefore, there is a possibility that asbestos fibres are released into the air, and so endangering human health.

During the rehabilitation of the abandoned Amiantos Asbestos Mine, a risk analysis was conducted for possible dangers emanating from the existence of the abandoned mine. From air samples of this study, both within the mine area and the wider region of Troodos, the measured asbestos fibres had a significant variability in different places. Although the values of asbestos concentrations reported by the latter analysis fell within acceptable limits, it was felt that there was a need to further study the rocks of the wider environment of the asbestos mine and assess the risk from any atmospheric release of asbestos fibres from the rocks.

In August 2008, the Geological Survey Department (GSD) procured a tender with the title “Investigation of Rock that May Contain Asbestos Minerals in the Troodos Region”, project code GSD/2008/26. The contract was awarded to Consortium Ecorem N.V. - Atlantis Consulting Cyprus Ltd and was signed on December 1st 2008 with the GSD.

Project Team:

Key Experts

- Dr. S.Helsen, Geologist, Project Leader
- Ing. E. Vermaut , Environmental Expert
- Dr. K. Louca, Sr Geological Expert
- Dr. P.Dumortier Asbestos Mineralogist

Supporting Staff

- Dr. B.Hermans, Environmental Expert
- Dr. T. Rommens, Geomorphologist & Database Expert
- Ing. E. De Smedt Environmental Expert
- Ch. Panayiotou M.Sc., Local Coordinator & Environmental Expert
- E. Ypsilanti, Field Geologist
- T.Toumazi B.Sc., Geologist

Subcontractors

Catholic University of Leuven
- Prof. Dr. N.Vandenberghe, Geologist & Head of Laboratory
- Prof. Dr. R.Swennen, Petrographical Expert
- Prof. Dr. M.Sintubin Structural Geologist

University of Athens
- Prof. Dr. M.Stamatakis, Mineralogist & Head of Section
- Dr. P.Kotsovitis, Petrographical Expert
- Dr. I.Mitsis, Mineralogist
- Mr. E.Michailides, Main Laboratory Assistant

2 BACKGROUND INFORMATION

2.1 General Statement and Definitions

The term "asbestos" has different definitions in common, regulatory, and mineralogical usage. It is used to identify a group of six commercially important silicate minerals of fibrous or asbestiform type (Clinckenbeard et al, 2002). These minerals all have specific properties of high tensile strength, flexibility, chemical resistance, and heat resistance. Because of these properties, asbestos has been used in many manufactured products and industrial processes during the twentieth century.

The six types of asbestos are:

- **chrysotile** (also called "white asbestos"),
- **crocidolite** (asbestiform riebeckite, also called "blue asbestos"),
- **amosite** (asbestiform cummingtonite-grunerite, also called "brown asbestos"),
- asbestiform **tremolite**,
- asbestiform **actinolite**, and
- asbestiform **anthophyllite**.

The terms "crocidolite" and "amosite" are varietal or trade names rather than formal mineral names. However, they are common in the literature regarding the regulation and health effects of asbestos. Chrysotile has been, and is, the most commonly used type of asbestos and probably accounts for 90% to 95% of the worldwide historic asbestos production. Crocidolite, and amosite make up most of the rest of the world's historic production but small amounts of anthophyllite-asbestos, tremolite-asbestos, and actinolite-asbestos have also been produced (Ross, 1981; Ross et al., 2001).

Naturally Occurring Asbestos (NOA) is the term applied to the natural geological occurrence of any of the six types of asbestos minerals.

Medical studies have shown that there is an association between certain diseases and asbestos exposure (e.g., Senyigit et al., 2000; Pan et al., 2005). Initial concern over the health effects of asbestos arose from studies of workers in the asbestos related industries (e.g., Camus et al., 1998). Much of the medical data on asbestos related diseases come from these studies. They involved workers in the asbestos industries, and showed that the workers were exposed to six asbestiform minerals. Since the initial studies on industrial asbestos exposure, other studies have investigated also the non-occupational exposures to asbestos minerals and the potential health effects of other mineral fibres.

In recent years, there is a rising concern over potential public exposure to Naturally Occurring Asbestos. Consequently, for many regions the need was felt to evaluate the NOA potential prior to land-use decisions, land acquisition, or property development (e.g., INVIS, 2007, Roggli, 2007, Burragato, 2002). In this respect, reliable geological information is crucial for regulatory decision-making, especially for activities such as excavation and levelling in areas where NOA may be present.

Geologic information is also useful in designing site development to avoid potential long-term exposure to NOA or in developing monitoring or mitigation plans to minimize potential short-term NOA exposures during construction activities.

2.2 Literature Review

While the processes by which the asbestos minerals cause lung cancer and mesothelioma have been studied, no general consensus has been reached by the medical community regarding the exact mechanism, or combination of mechanisms, by which these materials cause these diseases. There is also not a general consensus among the medical community about the potency of different fibre sizes, relative potency of different asbestos species, and potential health effects of cleavage fragments vs. fibres. Some of these issues are controversial, and this contributes to the overall complexity of the asbestos issue. However, it is widely recognized that asbestos is a human carcinogen, and all six of the asbestos types are considered to be potentially hazardous.

The first scientific report on the health hazards of asbestos was published in the early 1900s (Murray, 1907), first case reports of asbestos-related malignancies in the 1930s (Lynch et al., 1935) and the first epidemiological studies on asbestos-related lung cancer and mesothelioma in 1955 and 1960, respectively (Doll, 1955; USDHHS, 1960). Despite of these findings, the first system-wide actions for reduction of the use were initiated about 40 years ago in most countries and implemented in full scale as late as in the 1970s and 1980s.

At present, the main illnesses known to be caused by airborne asbestos are:

- nonmalignant lung and pleural disorders including interstitial pulmonary fibrosis (asbestosis), pleural plaques, pleural thickening, and pleural effusions;
- pleural and peritoneal mesothelioma;
- lung cancer.

Asbestos fibres may enter the body after inhalation or oral exposure. **The deposition and fate of the fibre is largely dependent on its size and shape.** Human and animal studies indicate that when asbestos fibres are inhaled, thick fibres (diameter > 2-5 µm) are deposited in the upper airways, whereas thinner fibres are carried deeper into the alveolar regions of the lung (USDHHS, 2001, Lippman, 1994, Wylie et al., 1993). Fibres that are deposited in the respiratory tract may be removed (e.g. by swallowing and mucociliary transport), or they may be retained in the lung. Very few of the long fibres are likely to move through the lungs and be distributed to tissues other than the mesothelium. Fibre width is a key determinant of access of fibres to the lung and pleural cavity, and thus of fibre toxicity.

Longer fibres that are retained in the lung may undergo a number of processes including translocation, dissolution, fragmentation, splitting, or protein encapsulation. Fibres that are encapsulated in protein can form a so-called "asbestos body" (the term "ferruginous body" is used when the nature of the core fibre is not known).

Fibres that are retained in the lung or mesothelium for long periods of time are capable of producing chronic inflammation and fibrotic and tumorigenic effects. Fibres that enter the gastrointestinal tract, either by ingestion or mucociliary transport from the lungs, are mostly excreted in the feces, although a small fraction of the fibres may become lodged in cells or penetrate the gastrointestinal lining and enter other tissues. Small number of fibres may reach the lymph system or be transported to the pleura and peritoneum. Dissolution of fibres by alveolar macrophages is also thought to play a role in eliminating asbestos fibres from the lung, especially for chrysotile fibres.

Some fibres are not cleared from the lung, which leads to a gradual accumulation. There is evidence in animals that long fibres are retained in the lungs for longer periods than short fibres (e.g., Coin et al., 1992, Davis, 1989). But analysis of autopsied human lung or parietal tissue for retained fibres often shows higher numbers of short (< 5µm) fibres than long fibres (Dodson et al., 1997, Sebastien et al., 1980).

There is also evidence that amphibole fibres are retained for longer periods than chrysotile fibres (Albin et al, 1994*,* Davis et al., 1989, Churg, 1993, Wagner et al., 1974). The apparent longer retention of amphibole fibres in lung tissue has been proposed as a partial explanation of why amphibole asbestos appears to be more potent in producing mesothelioma than chrysotile (Mossman et al., 1990).

The main determinants of asbestos toxicity include exposure concentration, duration, and frequency, and fibre dimensions and durability. Long and thin fibres are expected to reach the lower airways and alveolar regions of the lung, to be retained in the lung longer, and to be more toxic than short and wide fibres or particles. Wide particles are expected to be deposited in the upper respiratory tract and not to reach the lung and pleura, the sites of asbestos induced toxicity. Short, thin fibres, however, may also play a role in asbestos pathogenesis. Fibres of amphibole asbestos such as tremolite asbestos, actinolite asbestos, and crocidolite asbestos are reported to be retained longer in the lower respiratory tract than chrysotile fibres of similar dimension (USDHHS, 2001).

Although it is generally agreed that fibres of amphibole asbestos are retained longer in the lower respiratory tract than chrysotile fibres, there is no general consensus on the fact that amphiboles should be more carcinogenic than chrysotile. Most international organisations state that exposure to any asbestos type can increase the likelihood of lung cancer, mesothelioma and nonmalignant lung and pleural disorders.

2.2.1 Asbestos Types

Asbestos is a generic term for a group of six naturally-occurring, fibrous silicate minerals that have been widely used in commercial products (USDHHS, 2001). **Asbestos minerals** fall into two groups or classes: **serpentine asbestos** and **amphibole asbestos**. It should be noted that serpentine and amphibole minerals **also occur in nonfibrous or nonasbestiform forms**. These nonfibrous minerals are not asbestos, and are much more common and widespread than the asbestiform varieties. Regulatory or health agencies such as the European Union, WHO, ILO, U.S. EPA and OSHA only focus on the risks associated with the asbestiform type of the above mentioned minerals.

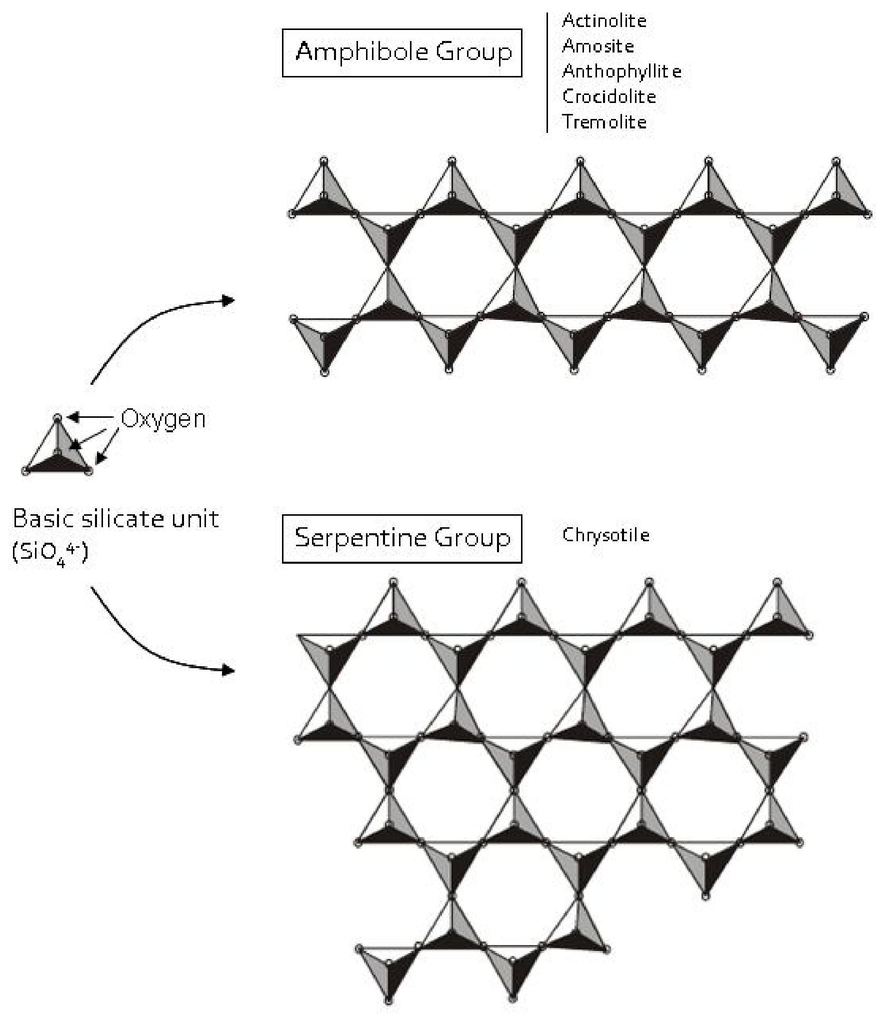

Figure 2: Basic polysilicate structures of asbestos (Adapted from Hurlbut and Klein, 1977).

For the **amphibole class** of asbestos (amosite, crocidolite, tremolite, anthophyllite, and actinolite), the polymeric structure consists of a **linear double chain** (**Figure 2**). These chains crystallize into **long, thin, straight fibres**, which are the characteristic structure of this type of asbestos. For the **serpentine class** (chrysotile), the polymeric form is an **extended sheet**. This extended sheet tends to wrap around itself forming a **tubular fibre structure**. These fibres are usually **curved** ("serpentine"), in contrast to the straight morphometry of the amphiboles. The long crystalline serpentine fibres are capable of being woven. The crystalline amphibole fibres are substantially more brittle than serpentine asbestos. Asbestos from the Amphibole group is therefore more limited in being fabricated.

Table 1 lists common synonyms and chemical formulas for the six individual asbestos minerals.

Table 1: Asbestos types – common names and chemical structure.

Asbestos type	Synonyms	Chemical formula
Amphibole Group		
Amosite	Mysorite; Brown asbestos; Fibrous cummingtonite / grunerite	$[(Mg,Fe)_7Si_8O_{22}(OH)_2]_n$
Tremolite*	Silicic acid; calcium magnesium salt (8:4)	$[Ca_2Mg_5Si_8O_{22}(OH)_2]_n$
Actinolite*	No data	$[Ca_2(Mg,Fe)_5Si_8O_{22}(OH)_2]_n$
Anthophyllite	Ferroanthophyllite; Azbolen asbestos	$[(Mg,Fe)_7Si_8O_{22}(OH)_2]_n$
Crocidolite	Blue asbestos	$[NaFe_3^{2+}Fe_2^{3+}Si_8O_{22}(OH)_2]_n$
Serpentine Group		
Chrysotile	Serpentine asbestos; White asbestos	$[(Mg_3Si_2O_5(OH)_4]_n$

** Tremolite and Actinolite form a continuous mineral series in which Mg and Fe(II) can freely substitute with each other while retaining the same 3-dimensional crystal structure. Tremolite contains little or no iron, while actinolite contains iron (Jolicoeur et al., 1992)*

Asbestos minerals form under special physical conditions that promote the growth of fibres that are loosely bonded in a parallel array (fibre bundles) or matted masses. The individual fibrils, which are readily separated from the bundles of fibres, are finely acicular, rodlike crystals. Deposits of fibrous minerals are generally found in veins, in which the fibres are at right angles to the walls of the vein. In the general mineralogical definition, fibre size is not specified.

Fibres are defined by the US ATDSR[1], as well as in EU directives, as those particles of asbestos minerals that have lengths **> 5 µm** and **length:width ratios > 3:1**. It should be noted that other agencies use different definitions of asbestos fibres for counting purposes. For example, the US Environmental Protection Agency defines a fibre as any particle with aspect ratio > 5:1.

Most amphibole and serpentine minerals in the earth's crust are of nonfibrous forms and are therefore not asbestiform. Fibrous forms may occur together with nonfibrous forms in the same deposits. Nonasbestiform amphiboles may occur in many diverse forms, including flattened prismatic and elongated crystals and cleavage fragments. When large pieces of nonfibrous amphibole minerals are crushed, as may occur in mining and milling of ores, microscopic fragments may be

[1] Agency for Toxic Substances and Disease Registry: agency of the US Department of Health and Human Services.

formed that have the appearance of fibres but are generally shorter and have smaller length:width ratios (i.e., particle length >5 μm and a length:width ratio >3:1). These fragments are thus most often not considered as fibres by health regulatory agencies. However, some cleavage fragments may fall within the dimensional definition of a fibre and be counted as an asbestos fibre in air samples or biological samples, unless evidence is provided that the particles are nonasbestiform.

Asbestos fibres are chemically inert (or nearly so). They do not evaporate, dissolve, burn or undergo significant ractions with most chemicals. In acid and neutral aqueous media, magnesium is lost from the outer brucite layer of chrysotile. Amphibole fibres are more resistant to attack by alkalis (WHO, 1998).

2.2.2 Health Risks related to Asbestos

2.2.2.1 Benign Pleural Disease

The most common asbestos-related abnormalities are pleural plaques. They are discretely elevated grey-white areas of connective tissue, rich in collagen and situated in the parietal pleura of the chest wall, diaphragm, pericardium or towards mediastinum. Asbestos and erionite fibres are the only established causative agents for typical pleural plaques and the latency time from the onset of exposure to the occurrence of pleural plaques is several decades. **In some instances pleural plaques are found in endemic areas after environmental exposure to asbestos from the soil, but outside these areas 80-90% of pleural plaques are attributable to occupational asbestos exposure.** Pleural plaques do not cause pulmonary function impairment, but they are frequently identifiable in the chest X-ray of exposed individuals and even more frequently in computed tomographies or autopsies. Pleural plaques can be caused by low exposure to asbestos and they are as such not considered to indicate an important risk of lung cancer, while they are a reliable marker of some level of past exposure to asbestos (International group of experts, 1997).

Additional observations adding to the evidence that long-term environmental exposure to airborne **tremolite fibres** can lead to development of nonmalignant changes in the lung and pleura include:

- high prevalences of pleural calcification among residents of villages in Greece (Bazas et al., 1985, Bazas, 1987, Constantopoulos et al., 1985, 1987), Turkey (Baris et al., 1988, Coplu et al., 1996, Dumortier et al., 2001, Metintas et al., 1999, Yazicioglu et al., 1980), and Corsica (Boutin et al., 1989, Rey et al., 1993, Peto et al., 1999) where whitewashes containing tremolite asbestos have been used domestically or where there are abundant surface deposits rich in tremolite asbestos, and;
- progressive pulmonary fibrogenic reactions in the lungs of rats and mice after exposure to tremolite asbestos by inhalation or intratracheal instillation (Davis et al., 1985).

2.2.2.2 Asbestosis

Asbestosis refers to a diffuse pulmonary fibrosis caused by inhalation of asbestos fibres. The traditional criteria for asbestosis included (a) a history of exposure to asbestos and a sufficient latency time between the onset of exposure and the occurrence of the disease (usually more than 15 years), (b) pulmonary fibrosis in the chest X-ray, and (c) a restrictive pattern of pulmonary function impairment (American Thoracic Soc., 1986). Neither the clinical features nor the architectural tissue abnormalities of asbestosis sufficiently differ from those of other causes of interstitial fibrosis to allow confident diagnosis without a history of significant asbestos exposure or detection of asbestos fibres or bodies in lung tissue greatly in excess of that commonly seen in the general population (International Group of Experts, 1997).

The risk of asbestosis is linearly related to the cumulative exposure, but in case of a low level of asbestos exposure, radiological, pathological and clinical evidence of lung fibrosis is generally absent. This suggests the existence of a threshold below which, asbestosis will not occur. The value commonly proposed for cumulative exposure is 25 fibre-years per cubic centimetre (Bofetta, 1998).

2.2.2.3 Mesothelioma

Mesothelioma is a cancer which is most commonly found in the pleura, less frequently in the peritoneum and occasionally also in the pericardium or tunica vaginalis testis. Mesothelioma used to be a rare tumor. The background incidence is assumed to be as low as 1-2 per million (Bofetta, 1998). During the recent decades, however, its incidence has increased steeply in the industrialized countries and was around 10-25 per million in the early 1990s in most Western European countries (Peto et al, 1999). **The great majority (about 80% in men) of mesotheliomas are caused by asbestos and most of them are due to occupational exposure, but cases caused by environmental exposure or exposure through a family member's work have been reported.** Most patients have been first exposed 30 or more years before the diagnosis (Camus et al., 1998).

The only established causative agents for mesothelioma are asbestos and erionite fibres. Dose-response analyses indicate that even relatively low exposures increase the risk (Iwatsubo et al. 1998) and there is no safe level of exposure. Of the asbestos fibres crocidolite fibres are the most potent followed by amosite, tremolite and anthophyllite (Bofetta, 1998). There is still scientific disagreement on the contribution of chrysotile to overall mesothelioma incidence. Some authors have concluded that although less potent than crocidolite and amosite, chrysotile could still be the main cause of mesothelioma world-wide due to its wider use (Cullen, 1998). Others have argued that very few mesotheliomas are caused by pure chrysotile (McDonald et al. 1997). Decisive evidence is difficult to reach as most workers have been exposed both chrysotile and amphiboles.

Mesothelioma is one of the most numerous entities in most occupational disease compensation schemes, but is also known to be heavily underdiagnosed as an occupational disease. The bulk of the mesothelioma epidemic does not result from the asbestos production industry, but from the downstream use of asbestos products in construction sites, shipyards and other industries (Peto et al. 1995). Indirect bystander exposures in such occupations are the most difficult challenge in mapping the exposure history of a mesothelioma patient.

Additional evidence indicates a causal relationship between long-term exposure to airborne tremolite asbestos and mesothelioma, which is a rare fatal cancer accounting for 2,87 deaths per million within the U.S. white male general population in 1996 (NIOSH, 1999). The evidence includes elevated prevalences of mesothelioma deaths (of about 1/100 to 2/100) among groups of Libby, Montana, vermiculite workers (Amandus & wheeler, 1987; McDonald et al. 1986b), among residents of Greek (Constantopoulos et al. 1987, 1991; Langer et al. 1987; Sakellariou et al. 1996), Turkish (Baris et al. 1988, Erzen et al. 1991; Metintas et al. 1999; Schneider at al. 1998;Yazicioglu et al. 1980), and New Caledonia (Luce et al. 1994, 2001) villages that used tremolite-asbestos whitewashes on interior walls, and in regions of northeastern Corsica that have abundant surface deposits of tremolite asbestos (Magee et al. 1986; Rey et al. 1993). Strong supporting evidence comes from animal studies showing increased incidences of pleural tumors resembling human mesotheliomas in rats (Stanton et al. 1981; Wagner et al. 1982) and hamsters (Smith et al. 1979) exposed to tremolite asbestos by intrapleural implantation, in rats exposed to tremolite asbestos or actinolite asbestos samples by intraperitoneal injection (Davis et al. 1991; Pott et al. 1989; Roller et al. 1996, 1997), and in rats exposed to airborne tremolite asbestos (Davis et al. 1985a).

2.2.2.4 Lung cancer

Lung cancer is numerically the most important cancer in the world. Tobacco smoke is by far the most important cause of lung cancer, but several work-related factors also contribute to the global lung cancer burden. **Of the work-related causes of lung cancer, exposure to asbestos is the most important, accounting for about one half of the occupational lung cancer burden** (Nurminen and Karjalainen, 2001).

Most lung cancers among asbestos-exposed workers occur in smokers or ex-smokers and a multiplicative model of interaction between smoking and exposure to asbestos has been introduced although a review of studies in the interaction between asbestos and tobacco revealed a somewhat variable pattern of interaction ranging from supramultipicative to less than additive (Vainio and Boffetta, 1994).

There is very little data on the dose-response at low levels of exposure (Health Effects Institute, 1991). A question closely related to the dose-response relationship is how much the risk is increased among those exposed individuals who don't have asbestosis. Several recent studies indicate that there is an increased risk of lung cancer among such individuals, although the risk is not as high as among those with asbestosis (who have a relatively high exposure) (International Group of Experts, 1997). Asbestos increases the risk for lung cancer of all sites and all histological types, but the increase may be slightly greater for lower lobe cancers and adenocarcinomas than for upper lobe cancers and squamous cell carcinomas.

Additional evidence relevant to the Amiantos mine and similar situations indicates that repeated exposure to airborne tremolite asbestos can lead to increased risk for the development of lung cancer. This includes observations of statistically significantly increased rates of mortality from lung cancer in groups of Libby Montana vermiculite workers compared with rates for the general population (Amandus & Wheeler, 1987; McDonald et al. 1986b), statistically significant relationships between cumulative fibre exposure measures and prevalence of lung or respiratory cancer among Libby vermiculite workers, and increased incidences of lung tumors in rats exposed to tremolite asbestos by inhalation (Davis et al. 1985a) or intratracheal instillation (Pott et al. 1994). The weight of the human evidence for tremolite asbestos-induced lung cancer is limited by the inability to adjust for likely confounding factors from smoking in the Libby vermiculite workers.

Most concern exists for the airborne asbestos and breathing in the tiny fibres. The fibres that are most dangerous to human health are those fibres that are longer than 5 microns and especially those longer than 10 microns, with a length:width ratio of 5:1. The tremolite-actinolite fibres may also be more chemically reactive, making them even more toxic to people's lungs. Although people can also be exposed to asbestos by ingestion (eating, drinking) or possibly on the skin, these are not major exposure routes and do not pose nearly as great a risk as inhalation (EPA, 2000).

2.2.3 Exposure

Although asbestos is neither volatile nor soluble, small fibres or clumps of fibres may occur in suspension in both **air and water**. These fibres are very stable and do not undergo significant degradation in the environment. Large fibres are removed from air and water by gravitational settling at a rate dependent upon their size, but small fibres may remain suspended for long periods of time.

No estimates of the amounts of asbestos released to the air from natural sources is available. Asbestos is much more likely to be released to the atmosphere when asbestos deposits are disturbed—as in mining operations. In Canada, over 95% of asbestos is mined in open-mining operations that involve drilling and blasting, and this contributes more air emissions than underground mining operations (Sebastien et al. 1984).

The general population is exposed to low levels of asbestos primarily by inhalation. Small quantities of asbestos fibres are ubiquitous in air. They may arise from **natural sources** (e.g., **weathering** of asbestos containing minerals), from **windblown soil**, from hazardous **waste sites** where asbestos is not properly stored, and from deterioration of **automobile clutches and brakes** or breakdown of asbestos-containing (mainly chrysotile) materials, such as **insulation**. Tremolite asbestos is a contaminant in some vermiculite and talc. These sources would also contribute to asbestos levels in air.

Other anthropogenic sources of asbestos emissions besides mining are the crushing, screening, and milling of the ore, the processing of asbestos into products, the use of asbestos-containing materials, and the transport and disposal of asbestos-containing wastes. Higher levels of airborne asbestos therefore occur near **asbestos mines** and may occur **near industries that produced asbestos-containing products** (Case 1991; WHO 1998).

Soils may be contaminated with asbestos by the weathering of natural asbestos deposits, or by land-based disposal of waste asbestos materials.

Higher exposure levels may result when asbestos is released from **asbestos-containing building materials** such as insulation, ceiling tiles, and floor tiles that are in poor condition or disturbed. In general, levels of asbestos in air inside and outside buildings with undisturbed asbestos-containing materials are low, but indoor levels may be somewhat higher than outside levels.

In most cases, the exposure of the general population to asbestos has been found to be very low. The concentrations of asbestos fibres in outdoor air are highly variable, ranging from below 0.1 ng/m3 (equivalent to $3x10^{-6}$ f/mL) in rural areas to over 100 ng/m^3 ($3x10^{-3}$ f/mL) near specific industrial sources such as asbestos mines. Typical concentrations are $1x10^{-5}$ f/mL in rural areas and up to an order of magnitude higher in urban areas. In the vicinity of an asbestos mine or factory, levels may reach 0.01 f/mL or higher. The concentration of fibres in indoor air is also highly variable, depending on the amount and condition of asbestos-containing materials in the building. Typical concentrations range from 1 to 200 ng/m3 ($3x10^{-5}$ to $6x10^{-3}$ f/mL) (Nicholson 1987). For a human exposed for a lifetime (70 years), this range of exposures corresponds to cumulative doses of approximately 0.002–0.4 f-yr/mL. Children may be exposed to asbestos in the same ways that adults are exposed outside the workplace—from asbestos in air, especially near emission sources or in buildings with deteriorating asbestos-containing material. Since children are more apt to play in dirt, they may be exposed to higher levels of asbestos if the dirt they are playing in contains asbestos and they inhale the dust.

Fibres in **water** arise mainly by **erosion of natural deposits** of asbestos or waste piles, or by corrosion of fibres from **pipes** made with asbestos-containing cement and disintegration of asbestos roofing materials. Waste water from asbestos-related industries may also carry significant burdens of asbestos fibres (EPA 1976). Asbestos concentrations in most water supplies are less than 1 million fibres per liter (MFL), but may exceed 100 MFL in some cases.

The relationship between **workplace exposure** to airborne asbestos fibres and respiratory diseases is one of the most widely studied subjects of modern epidemiology. It was not until the early 1960s that researchers firmly established an epidemiologic correlation between worker excess exposure to asbestos fibres and respiratory cancer diseases. This finding triggered a significant research effort to unravel important issues such as the influence of fibre size, shape, crystal structure, and chemical composition; the relationship between exposure levels and diseases; the consequences of exposure to asbestos fibres in different types of industries, or from different types of products; and the development of technologies to reduce worker exposure. The research efforts resulted in a consensus in some areas, although controversy still remains in other areas (Virta, 2001).

Asbestos fibres are nonvolatile and insoluble, so their natural tendency is to settle out of air and water, and deposit in soil or sediment. However, some fibres are sufficiently small that they can remain in suspension in both air and water and be transported long distances. For example, fibres with aerodynamic diameters of 0.1–1 μm can be carried thousands of kilometers in air, and transport of fibres over 75 miles has been reported in the water of Lake Superior (EPA). Adsorptive interactions between the fibres and natural organic contaminants may favor coagulation and precipitation of the fibres.

Studies generally indicate the strong effects of non-occupational exposure like domestic exposure, environmental exposure from industrial pollution (mines, mills, factories, etc.), environmental exposure from asbestos in soil, etc. on human health.

According to Goldberg (2001), non-occupational circumstances of exposure include domestic exposure to asbestos contaminated materials, environmental exposure from industrial pollution, environmental exposure from asbestos in the soil and environmental non-occupational exposure in buildings.

The conditions in which **environmental and/or domestic exposure** occurs are the **presence of tremolite- and chrysotile-bearing rocks (serpentinites, ophiolites) and soils** and/or the local use of white soil. The existence of dry or Mediterranean climate probably also plays a role. These conditions can be used as a preliminary basis for the identification of geographical areas at risk (Dumortier et al., 1998).

The environmental exposure epidemiological studies all indicate the existence of a strong effect of non-occupational exposures (domestic, industrial and natural). There appeared to be no difference between men and women and also no apparent effect of age at first exposure could be observed. **Concerning the fibre types it could be concluded that in most of the cases amphiboles (crocidolite, tremolite) play an important role**. **However, chrysotile is almost always present in lung samples of the cancer cases.**

This co-exposure of chrysotile was also reported by Dumortier et al. (1998). The main type of asbestos fibre in broncheoalveolar lavage fluid (BALF) reported in Turkey was tremolite. Together with tremolite, elevated concentrations of chrysotile were detected in a small number of Turkish cases showing that for some cases environmental co-exposure to chrysotile also occurs. Elevated amounts of chrysotile were observed in cases with ongoing or recent exposures, but data accumulated over the past 25 year demonstrate that it is difficult to relate chrysotile lung burden to estimated exposure owing to its faster clearance rate compared with amphiboles. Churg and Wright (1994) estimated that the preferential clearance of chrysotile, leading to its lower biopersistence when compared with amphiboles, must occur and be completed within weeks to months of exposure.

3 GENERAL PROJECT CHARACTERISTICS

3.1 Location and Climate of Troodos

Cyprus is the third largest Island in the Mediterranean (9.251 km^2). The Troodos Mountains occupy an area of approximately 3.200 km^2 in the central and western part of the island (**Figure 3**). The highest point is Mount Olympus, which peaks at 1.951 m above sea level. Several torrents spring radially from the range ending in the sea. The pine forests covering the Troodos area, combined with the steep slopes and precipices and narrow valleys and crevices, create a beautiful scenery. The hard igneous rocks are surrounded by a lower belt of dome-shaped volcanics, which levels gradually towards the coast.

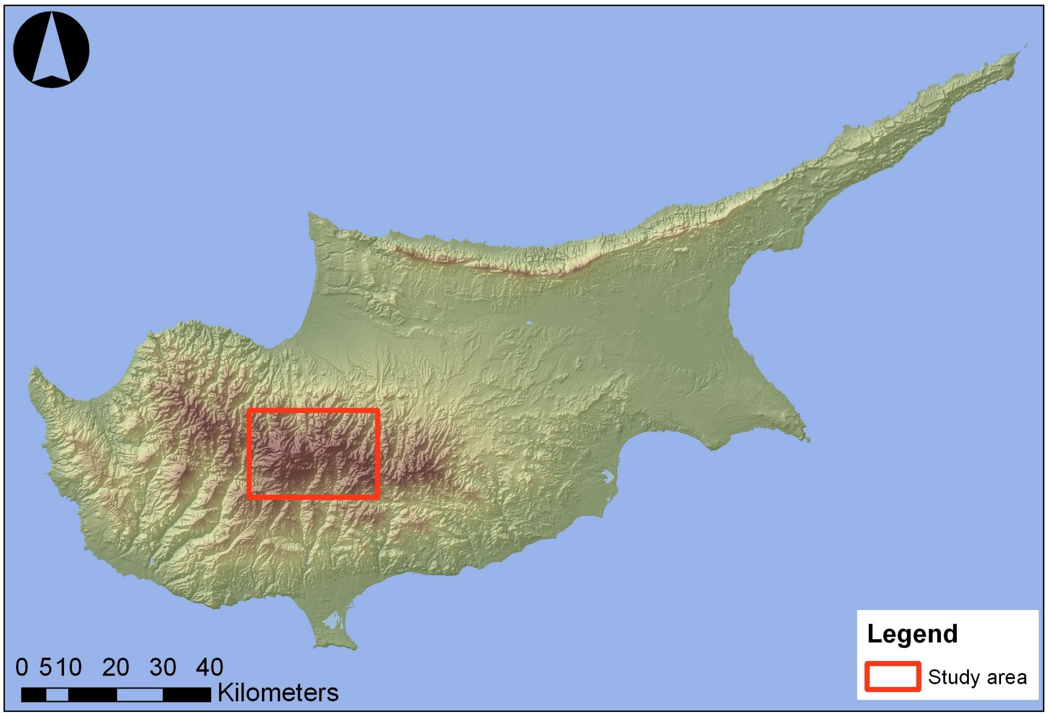

Figure 3: Location of the study area.

Cyprus has a typical Mediterranean Climate, characterized by hot and dry summers and mild winters. The average rainfall is 406 mm. Climate is however depending on altitude. As a result, the Troodos Mountains have a cooler and wetter climate. The air is cooler during summer, and occasionally, showers occur. From December until March, snow falls frequently, covering the area for about ten weeks of the year. In the Troodos Area winds come mainly from the NNE and NW. South of the mountains and near the coast westerly winds are dominant.

3.2 Regional Geological Setting

Occupying the core of the Troodos Ophiolite, the Project Area is exclusively underlain by plutonic and intrusive rocks units of the Troodos Ophiolite. The ophiolite forms the backbone of Cyprus and together with its extension beneath the Mesaoria Plain represents the most extensive and important geotectonic zone of the island **(Figure 4)**

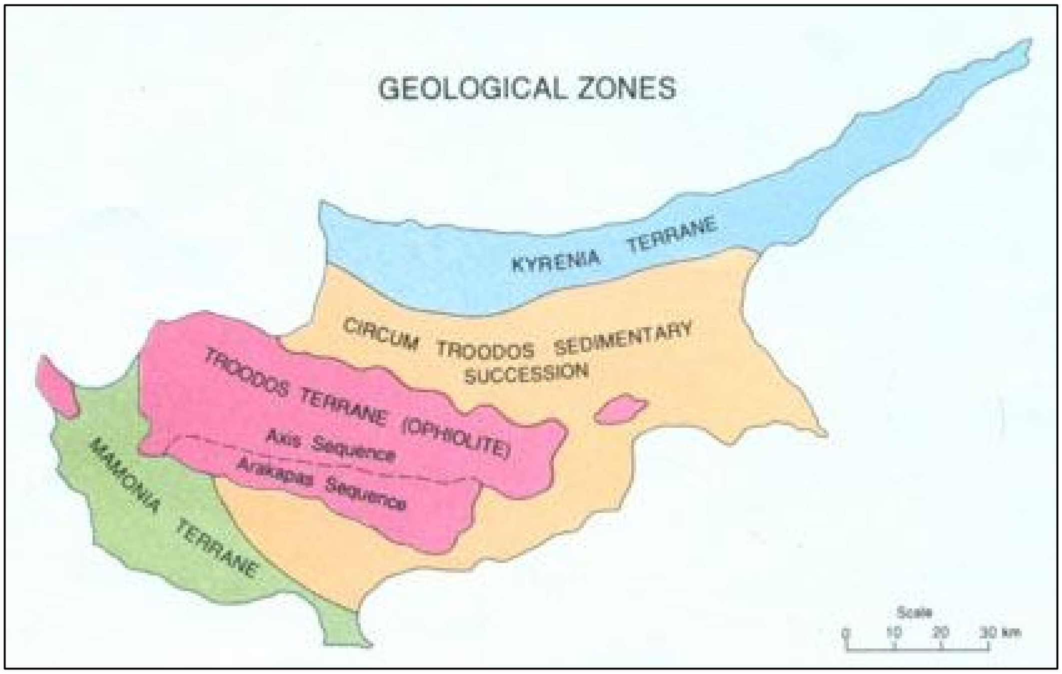

Figure 4: Main geological zones in Cyprus (*Source: GSD*).

The Troodos Ophiolite is probably the most intensively studied and best known ophiolite in the world and has been the object of two international symposiums held in Nicosia in 1979 and 1987. It is regarded as a classic occurrence of the relatively few complete and least deformed and non-disrupted ophiolite sequences available for investigation. Data and interpretations produced by investigation of its unique structure have contributed to our understanding of ophiolites and oceanic lithosphere (Greenbaum D. 1972, George R.P. 1975, Coleman R.G. 1977, Panayiotou A. 1980, Malpas J. 1990, Gas I.G. 1990).

There is a consensus that the Troodos Ophiolite has been formed at several spreading axes in a supra-subduction zone environment resulting from the collision of the African and Eurasian Plates in the Late Cretaceous (Malpas et al, 1990). The complex processes involved consumption of plate margins, oceanic crust accretion, partial melting of mantle sources and development of multiple and independent gabbro chambers. These magma chambers produced a Sheeted Dyke Complex and associated extrusive sequence at a series of spreading axes (Robinson and Malpas 1990, Moores et al. 1990).

Structurally, the Troodos Ophiolite is sub-divided into a Mantle Sequence and a Crustal Sequence, the two being divided by a Petrological Moho. The Mantle

Sequence consists largely of variably serpentinized and tectonised peridotites, mainly harzburgites with associated sporadic bodies of lherzolite and dunite. The Crustal Sequence consists, from the base upward, of deformed and underformed layered ultrabasic and basic plutonic rocks (dunite, pyroxenites, wehrlite and gabbro) overlain by non-layered plutonic rocks (high level gabbros and plagiogranites), a Sheeted Dyke Complex and an Extrusive Sequence consisting of three lithographic units of lavas. The uppermost volcanic unit is capped by manganoan, pelagic sediments.

On the basis of their cross cutting relationships, relative ages of deformation and magmatism, the plutonic sequence of the Troodos Complex can be divided in an Early Suite and a Late Suite (Malpas, 1990). Characterised by penetrative deformation, the Early Suite consists of tectonised harzburgite and peridotite, dunite, layered olivine pyroxenite and gabbro. A domal structure formed by solid-state diapirism in the Early Suite was intruded by an extensive Later Suite of plutons. These Late Suite underformed plutons comprise poikilitic wehrlites with pyroxene, oikocrysts, plagioclase wehrlites, amphibole gabbro-norites and plagiogranites.

As a result of the combined effects of solid-state mantle diapirism, Late Suite intrusions, tectonic uplift and post Ophiolite emplacement serpentinite diapirism, the Troodos Ophiolite Complex has developed an elongate, east oriented domal structure of which Mount Olympus marks the centre.

Episodic uplift coupled by intense erosion of the massif has resulted in the topographic inversion of the Ophiolite stratigraphy. The lowest stratigraphic units of the Ophiolite are exposed in the central portion of the domal structure, while the higher stratigraphic units are confined concentrically outwards around the dome.

3.3 Amiantos Asbestos Mine

Cyprus has a long mining history including among other copper and asbestos. This history dates back to prehistoric times. Especially during the Roman Era, Cyprus was considered as one of the main sources of asbestos. Asbestos was excavated and used for multiple purposes, such as: incineration sheets for corpses, shoes, protective surfaces for houses, etc. After 1904, chrysotile asbestos was used in the bricks and flat stones industry. Around that time, a major exploitation phase for asbestos began and some villages took advantage of the presence of this natural resource in the Troodos Mountains.

Chrysotile asbestos fibres, naturally occurring in the highly serpentinized ultrabasic rocks of the Troodos Range in Cyprus, have been mined for hundreds of years. The **Amiantos asbestos mine** in the centre of the Troodos area was successfully operated until the early 1980's. After 1982 both the demand and the price of asbestos decreased dramatically because of the international campaign against the use of asbestos. As a result, the mining company (Cyprus Asbestos Mines Ltd.) faced financial problems. After some difficult years, the company was granted (for free) to Limassol Metropolis in 1986. Finally, in 1990, Cyprus Asbestos Mines Ltd. was liquidated. The mine's lease ended in 1992.
It is estimated that from 1904 until 1988, when the mining activities were terminated, about 130.000.000 tons of rock were mined and 1.000.000 tons of

asbestos fibres were produced and exported to several European and other countries, resulting in a revenue of 75.000.000 Cyprus Pounds (CP) (former currency). Thousands of people were employed in the mining industry and its derived activities. At first (until 1950) the production of asbestos was done manually (digging and picking) by a great number of miners, who lived near the mine. That is for example how the communities of Pano Amiantos and Kato Amiantos came into existence. After 1950, large scale mechanisation was applied for the mining process. Great excavation machinery was used and old mills were replaced by a factory. Pano Amiantos was deserted.

The mine waste resulting from the first mining operations (early 20th century) was disposed in the **Livadhin valley** at the lowermost part of the slopes. Substantial amounts were washed downstream. The waste dump that was formed during the early years of operation covered an area of some 35 ha and the maximum depth of the waste was in the order of 25-30 m. Later, when mechanisation was applied, huge volumes of waste materials were produced which the steep slopes of the existing dumps could not accommodate. Therefore, the waste material was dumped nearby the **Loumata valley**. For drainage purpose a 1,3 km long concrete gallery was built along the valley bottom and waste was dumped over the gallery infilling the valley. It is estimated that about 60 million cubic metres of waste were dumped in this valley. The waste tips in the Loumata valley are known as the “new tips” and they consist of the lower level tip at the elevation of 1.350 m and the upper level tip at the elevation of 1.450 m.

The mining activities from 1904 until 1988 resulted in large volumes of waste tips resting on steep slopes and infilling side valleys, a badly designed mine pit and pollution with fibres of the soil, the surface water and air with possible consequences on the safety and health of the people.

For the rehabilitation of the landscape, profiling works were started, aiming at the stabilization of the waste tips (Kyrou and Petrides, 2004). In addition, a form of reprofiling was needed to intercept surface water flows, preventing flow of fibres in the valley streams. Reprofiling works also aimed to reduce the sharp contrast between the artificial slopes and the natural slopes and the general topography of the neighbouring area. Furthermore, due to the alkaline nature of the waste, which prevents the grow of any form of vegetation, fertile soil was transported with lorries and the area is being planted and irrigated. Following consultations with the experts from the Forestry Department it was decided that the maximum slope that would facilitate grow of vegetation would be 2 horizontal: 1 vertical. In addition, berms 8 m wide at 15 m elevation intervals would be required for the planting of trees. In this way, typical slopes with a total height in excess of 240 m were constructed.

The earthworks have been performed under medium sized contracts. Earthworks commenced in 1996. In 2004, seven contracts were completed, representing about 70% of the total earthworks and involving the excavation and placement of some 3,6 million cubic m of material.

The reforestation of the mine lease area was planned and is being executed by the Forestry Department, after consultation with the Technical Committee (**Figure 5**). The work is being performed in stages. All surfaces are covered with fertile topsoil. It is estimated that about 4.000 cubic metres of topsoil are required for the reforestation of a hectare. Planting is being carried out along trenches and secondary terraces. All other surfaces are being sown with a mixture of seeds from different perennial plant species. The seeds of plants used both in planting and sowing are collected from plants growing around the mine. Traditional thatching is being used for protecting seeds sown on sloped ground from being washed away by rainwater. Ground preparation works are being carried out all year round. Sowing is being done from the beginning of September together with thatching. Planting is being performed from early October through December.

Figure 5: Reforested slopes in the Amiantos mine area (*Photo: T.Toumazis, Atlantis Consulting Cyprus Ltd*).

Other issues that need to be addressed in the overall rehabilitation programme are the badly designed mine pit and the preservation and cleaning of the houses and buildings (old fibre mills, office and warehouse as well as staff houses in the adjacent areas). The ultimate aim is to produce a long term master plan for the optimal development of the area.

3.4 Previous Research Concerning Amiantos Asbestos Mine

The old Amiantos asbestos mine is obviously an important source of asbestos. In the "Risk Assessment for the Amiantos Asbestos Mine (2003-06)" Ecorem n.v. investigated on behalf of the Geological Survey Department the past and current environmental impact of this asbestos mine in the Troodos area.

From the results obtained in air monitoring stations, partly concentrated inside and in the immediate area of the mine, and partly extended towards the greater Troodos area, it was concluded that for the Amiantos area, the mine can be considered as a temporary single source for the observed asbestos burden. Inside and in the immediate area of the mine, air samples showed frequently asbestos concentrations between 0,1 - 1 fibres/l. During dry summer days, when a lot of dust raising activities (rehabilitation works and associated vehicle traffic) take place, concentrations may even be higher. Mainly **chrysotile fibres** were observed inside the mine, however, fibres of **actinolite** were generally present as well.

For the greater Troodos area, airborne asbestos concentrations of 0,1 - 1 fibres/l were detected most frequently, but also concentrations of 1 - 10 fibres/l were abundant near Troodos Square, College Forest and up to Kyperounta. During the summer surveys of 2005, the highest concentrations, up to 40 fibres/l, were measured in the greater Troodos area. Here, fibrous actionolite predominated.

Five surface water surveys were executed, spread over the three years. Also groundwater samples were collected at various existing springs and wells around the mining area. From the water monitoring surveys it was concluded that the concentrations of asbestos fibres in the **surface water and groundwater** were **relatively low**.

Soil and rock samples were taken inside the mine at rehabilitated and non-rehabilitated tailings, at the dry river beds and at different geological formations from the greater area. The samples included also some stucco material, bricks and dust samples from inside the mining buildings.

Chrysotile fibres were detected in almost all superficial soil samples collected in the mine. Asbestos concentrations up to 40%v were found in the superficial soil samples taken near the dirt roads and up to 80%v in the dust samples collected inside the buildings. No difference in asbestos concentration could be observed between samples from original and rehabilitated tailings (range of 1 - 20%v). It was demonstrated that asbestos fibres were also common in the superficial soil samples from the surrounding area (< 1%v - 10%v). Due to prevailing winds and dust deposits over more than hundred years, chrysotile fibres could become widespread, also in areas with different geology. **Most of the rock samples show asbestos concentrations lower than 10% by volume**. The **asbestos fibres were only of the chrysotile type**, with the exception of a sample containing tremolite from the packing building wall.

The data set of airborne asbestos collected during these extended surveys was evaluated and related to local geological conditions, local topography and local meteorological conditions by means of dispersion modelling and some additional geological investigation in order to identify trends and distribution patterns, and other potential sources for fibre release.

It was concluded that peak concentrations of airborne asbestos in the sampling period 2003 - 2005 were characteristic for the northwestern area of the mine. Two factors have contributed to this distribution. One factor was the relative abundance of the restoration works and important truck traffic in this area. The other factor that favored the high concentrations in the northwestern mine area was the wind direction.

A dispersion model was applied in order to examine the distribution of airborne fibres in a typical summer day, and also to assess risk to the nearby areas of Kato Amiantos and Troodos Square in terms of the maximum potential concentrations that may occur under worst case scenarios. From this analysis, it became clear that peak values in the surrounding areas diminish quickly to less than 10% of peak values within 1-2 km from the mine. It was concluded that the area of influence of the mine is limited to the area between Kato Amiantos to the east and Troodos Square to the west. It was concluded that **for the greater area, the influence of the mine was negligible, and other local sources of asbestos were to be considered, such as the natural outcrops of serpentinized harzburgite and the weathered uralite gabbro occurring at various locations.**

The mine area itself could be considered as a temporary single source for the observed asbestos burden. The highly **serpentinized harzburgite**, covered with loose **serpentinite** materials from the ceased mining activities, constituted the main source of **chrysotile asbestos fibres in the air**. Especially the truck transport and earthworks on the recent burial place for asbestos waste materials has raised a lot of fine asbestos dust. During rehabilitation works in the mining area other type of rocks and soil have been imported, among them **weathered uralite gabbro**. Airborne **fibrous actinolite**, recorded at various places in the mine, might be related to the **leveling works**. However, other sources, including the highly uralite gabbro outcrops in the surrounding area, could not be fully excluded.

For Kato Amiantos, life-time exposure to the highest observed concentrations could result in a risk for developing cancer between 1/100.000 to 1/10.000. For the surrounding area of Kyperounta, a risk of up to 1/1.000 exists if life-time exposure to the observed peak concentrations occurs. Near Troodos Square the highest concentrations observed could result in a risk of more than 1/1.000 if exposed continuously. For the area of the College Forest, risk was found to vary between 1/10.000 to 1/1.000. Similarly to the mine, the elevated concentrations of airborne asbestos in the greater Troodos area were characteristic for summer conditions, and were not considered as averages for life-time exposure.

From the above results it was concluded that the mine area was a potentially hazardous territory which under circumstances might impose a risk to human health, and could be a concern to inhabitants, workers, and visitors. Additional baseline mapping of soils and rocks were recommended to point out if any actions need to be undertaken to reduce potential sources.

4 WORK SCHEDULE AND WORK PERFORMED

The project became operational in December 2008 with the preparation of the inception report, data collection and project meetings with the Geological Survey Department. The project management and working schedule are illustrated in **Figure 6.**

The first three months of 2008 involved intensive preparatory work including the preparation of base field maps, acquisition of an aerial photographs database and reconnaissance field surveys.

A first phase of systematic rock and soil sampling was initiated in April 2009 and was completed in November 2009. The work involved the collection of a total of 283 samples. Samples were collected and selected for analysis by T. Toumazis, under the supervision of K. Louca, Ch. Panayiotou or St. Helsen. After a first macroscopic evaluation, 197 samples were sent to the laboratory for further analysis. The sampling scheme is depicted in **Figure 7**.

The first phase of the Geological mapping was completed on schedule in October 2009 and was confined to traverses related directly to the sample locations.

Following the remarks of the GSD after submission of the 2nd Intermediate Report in May 2010, 69 extra samples were selected for the preparation of thin sections and petrographical analysis. As such, a final number of 200 thin sections, has been achieved.

With the completion of the petrographic determinations, geological mapping was extended over the entire project area.

Investigation of Rocks that may Contain Asbestos Minerals in the Troodos Region
(GSD/2008/26)

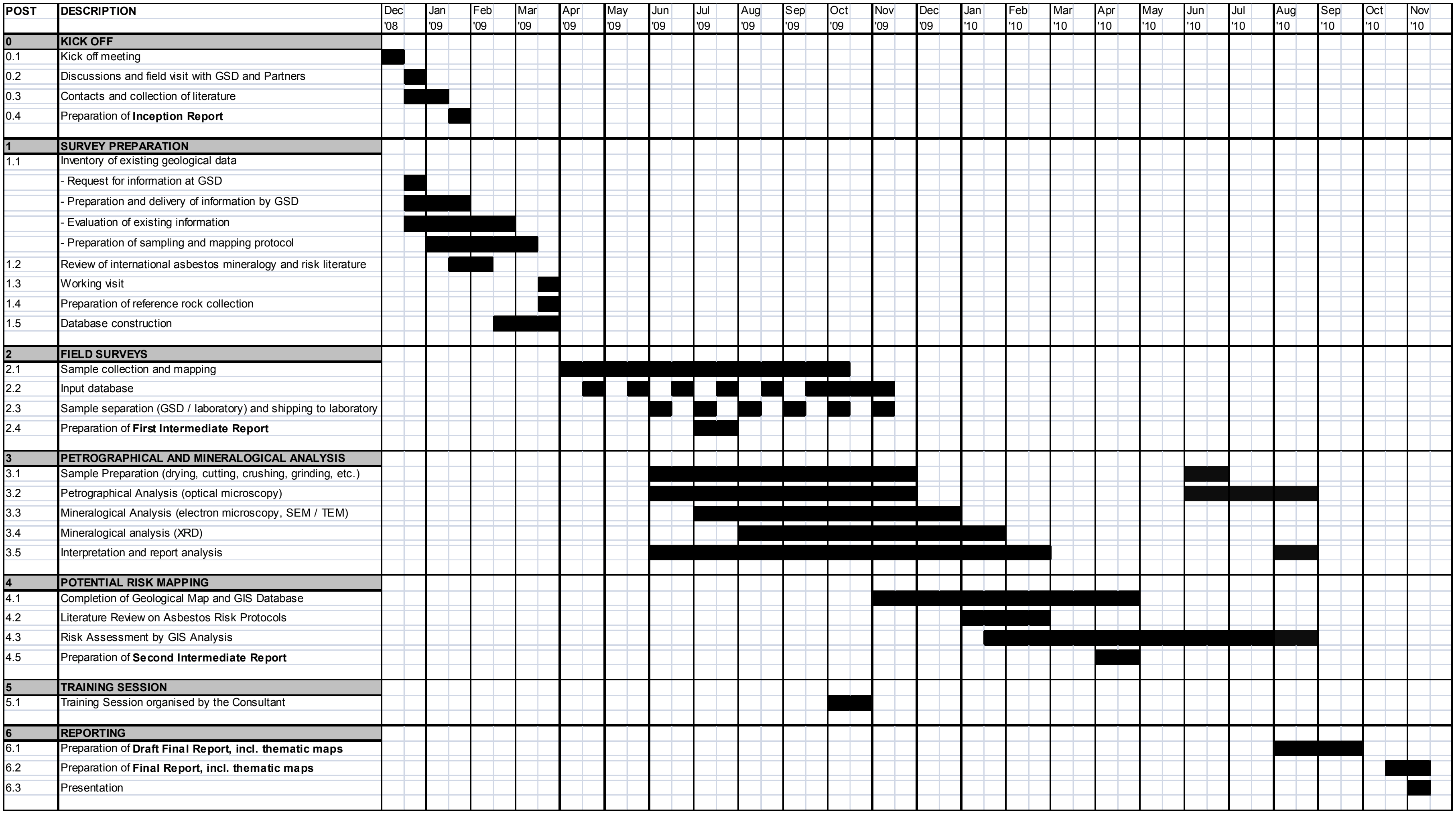

Figure 6: Project management and working schedule.

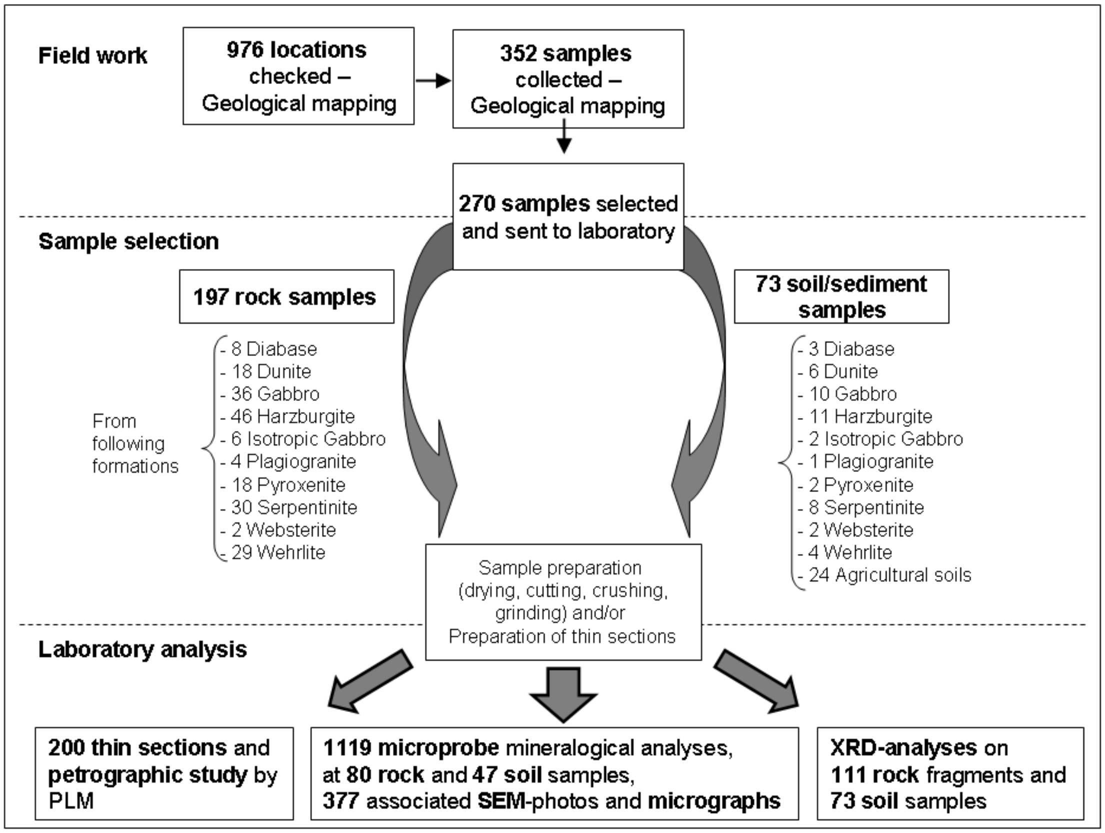

Figure 7: Sampling and petrographical analysis scheme.

5 METHODOLOGY

5.1 General Information

Field surveys started in April 2009, after a thorough preparation and selection of the sampling sites based on aerial photographs, satellite images and geological maps (April 2009) **(Figure 8 & 9)**.

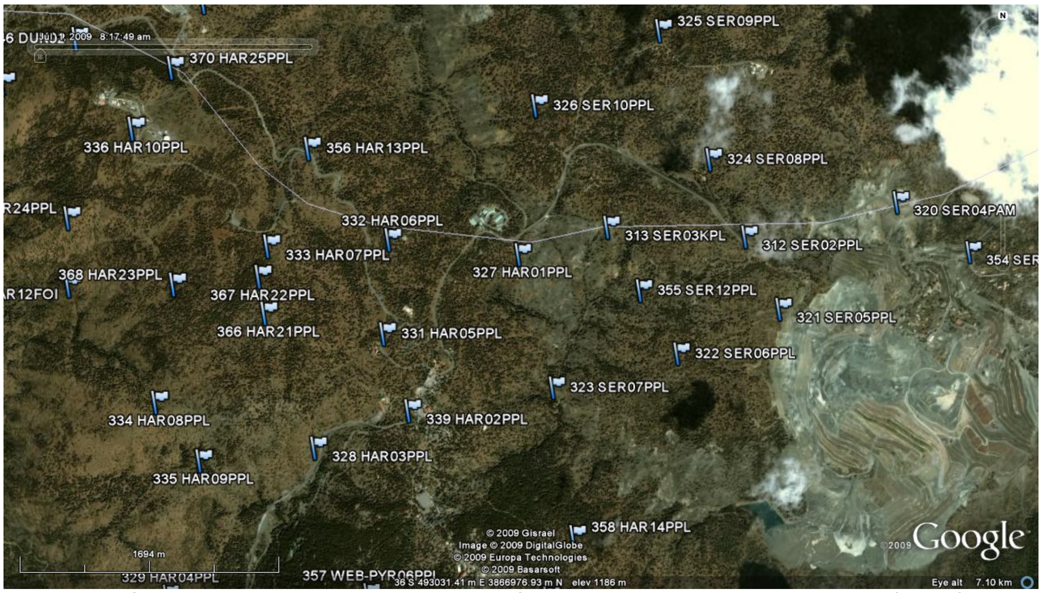

Figure 8: Google Earth showing a section of the study area with indication of the foreseen sampling locations, as prepared for the field surveys

The sampling areas were selected in a first phase from Satellite images and Google Earth images. The number of samples from each geological formation, needed for a representative sampling pattern, was initially estimated taking into account the area that was covered by each formation. Each formation area was then sub-divided into a number of sub-areas. Sampling locations were selected in such a way that a good spatial distribution was obtained (in the first place), taking into account the accessibility to the area (in the second place). During the collection of the samples in the field, if another area appeared to be geologically different and interesting, an additional sample from that particular area was taken.

Whenever was considered necessary, the sampling point was thus moved, affecting this way the desired spatial distribution pattern. The samples were mainly collected from road cuts on main roads, dirt roads, and also from natural trails.

At one sampling point, different types of rocks could occur. In such a case, the dominant formation rock type was considered representative for the sampling location. Rock samples were generally taken from the least weathered rock exposed on the sampling site.

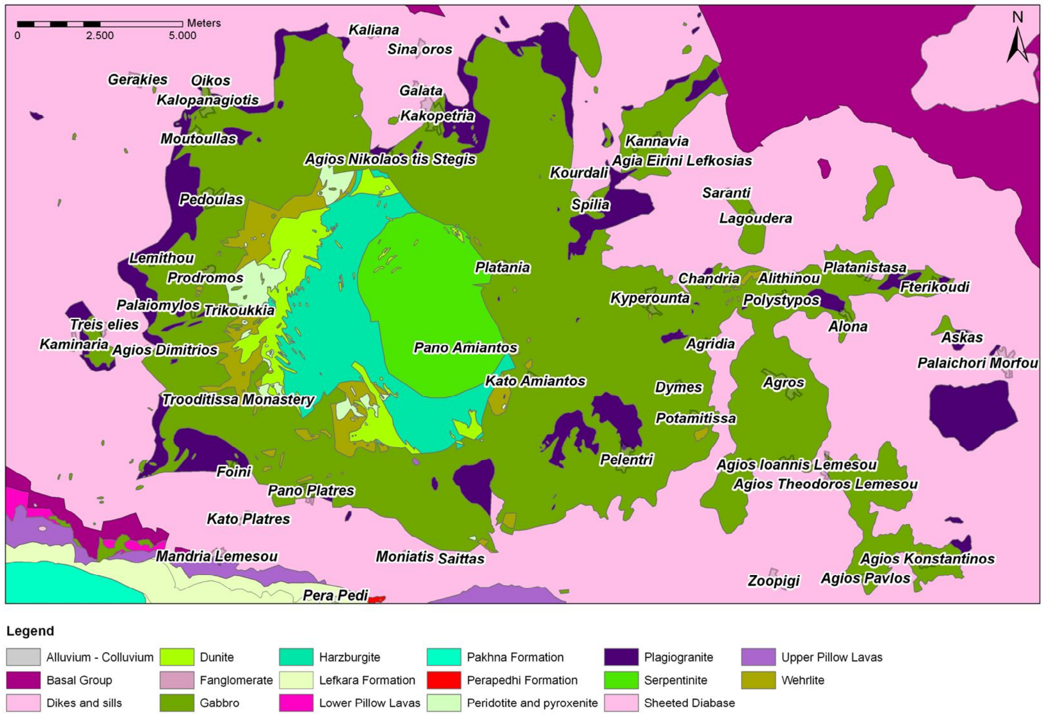

Figure 9: Geological map of the Troodos area. (*GIS Data layer GSD.*)

The study area was regularly visited by the geologist and the senior expert of the team in order to map rock formations and collect samples (**Table 2**).

Table 2: Calendar of working visits.

Date	Geologist	Location	Aim
14/04/2009	K. Louca Ch. Panayiotou	Kakopetria - Troodos	Sample Collection
12/05/2009	K. Louca T. Toumazis	Troodos – Mt. Olympus	Sample Collection
14/05/2009	T. Toumazis Ch. Panayiotou	Kakopetria - Amiantos – Troodos	Sample Collection
15/05/2009	T. Toumazis Ch. Panayiotou	Mt Olympus Dirt Roads	Sample Collection
19/05/2009	T. Toumazis Ch. Panayiotou	Mt Olympus – Kakopetria Dirt Road	Sample Collection
27/05/2009	T. Toumazis St. Helsen	Atalanta Natural Trail	Sample Collection
04/06/2009	T. Toumazis St. Helsen	Troodos – Platres Dirt Road	Sample Collection
15/06/2009	T. Toumazis Ch. Panayiotou	Artemis Natural Trail	Sample Collection
18/06/2009	K. Louca T. Toumazis	Prodromos-Platres-Troodos	Sample Collection
07/07/2009	T. Toumazis Ch. Panayiotou	Troodos area	Sample Collection

Date	Geologist	Location	Aim
11/08/2009	T. Toumazis Ch. Panayiotou	Kalidonia falls	Sample Collection
13/08/2009- 26/08/2009	T. Toumazis K. Louca	West Troodos area	Sample Collection
01/09/2009- 16/09/2009	T. Toumazis Ch. Panayiotou	East Troodos area	Sample Collection
18/09/2009- 08/10/2009	K. Louca T. Toumazis	NW Troodos area	Sample Collection-Mapping
20/10/2009- 29/10/2009	T. Toumazis St. Helsen	NE Troodos area	Sample Collection - Mapping
10/11/2009- 27/11/2009	T. Toumazis Ch. Panayiotou	North Troodos area	Sample Collection - Mapping
11/01/2010- 27/04/2010	K. Louca T. Toumazis	Troodos area	Mapping
11/05/2010	K. Louca T. Toumazis	Troodos area	Mapping
25/05/2010- 27/05/2010	K. Louca T. Toumazis	Troodos area	Mapping
01/06/2010- 09/06/2010	K. Louca T. Toumazis	Troodos area	Mapping
15/06/2010- 23/06/2010	K. Louca T. Toumazis	Troodos area	Additional Sample Collection

5.2 Sampling practises

The geological formations of the existing published maps used for sampling purposes were the following:

- **Diabase**: sheeted dykes;
- **Plagiogranite Group**: Trondhjemites, Granophyres, Microgabbro, Epidosites and Quartz granulite;
- **Isotropic Gabbro**: Pyroxene and hornblende gabbro
- **Gabbro**: Olivine and layered gabbro
- **Pyroxenite Group**
  - Pyroxenite
  - Websterite
- **Wehrlite**
- **Dunite**
- **Harzburgite:** tectonised Harzburgites with dunite and lherzolite bodies;
- **Serpentenite:** highly serpentinized and tectonised Harzburgite, bastite serpentinite

In total, 197 rock samples, 49 samples of residual soils, (originating from highly weathered parent material) and 24 soil samples from agricultural fields were selected for further petrographical and mineralogical analysis. Their distribution over the different geological formations is illustrated in **Table 3**. Photographs of each sampling location can be found in **Annex 2**.

Sampling locations are illustrated in **Annex 1**.

Table 3: Samples selected for laboratory analysis.

Formation	Total number of selected samples	Rock	Soil
Diabase	11	8	3
Dunite	24	18	6
Gabbro	46	36	10
Harzburgite	57	46	11
Isotropic Gabbro	8	6	2
Plagiogranite	5	4	1
Pyroxenite	20	18	2
Serpentinite	38	30	8
Websterite	4	2	2
Wehrlite	33	29	4
Agricultural soil	24		24
Total	**270**	**197**	**73**

5.3 Geological Mapping

Geological mapping at the scale of 1:10.000 was initially carried out in 2009, along traverses, during the course of the rock sampling program. Subsequently, geological mapping was extended to areas with completed petrographic work and finally in the spring of 2010, it was undertaken in a systematic manner along roads and forestry trails. A number of discrepancies found between the initial mapping and petrographic rock determination were verified and corrected through re-examination of duplicate sub-samples, and their comparison with the rocks at the sampling site.

Air-photo interpretation using two different tonal patterns of colour photographs at a scale of 1:20.000 was performed in two phases: The first-phase interpretation and analysis involved annotation of structural elements, such as joint patterns, major fracture systems, faults and other linear features.

Conducted in the spring of 2010 in conjunction with the geological mapping, the second-phase air photo interpretation aimed at the recognition of boundaries between contrasting lithological units. All sources of data, including ground information, were combined to complement each other on final maps at the scale of 1:20.000

With a strong consideration to the generally accepted subdivision of the Trooodos Plutonic Complex and the results of the Project petrographic study, the mappable units adopted by the mapping program are the following: serpentinite, harzburgite, peridotite, dunite, pyroxenite, wehrlite, olivine gabbro, hornblendic-pyroxenic gabbro, plagiogranites and diabase.

The overall geological work was highly facilitated by the availability of the published geological maps of the Geological Survey Department, especially of Wilson (1959). During the course of the geological mapping the findings of detailed investigations carried out within the framework of the deep drilling program of the International Crustal Research Drilling Group (ICRDG) in Cyprus, from 1982 to 1985, were also taken into consideration.

A part of the draft geological map is illustrated in **Figure 10**.

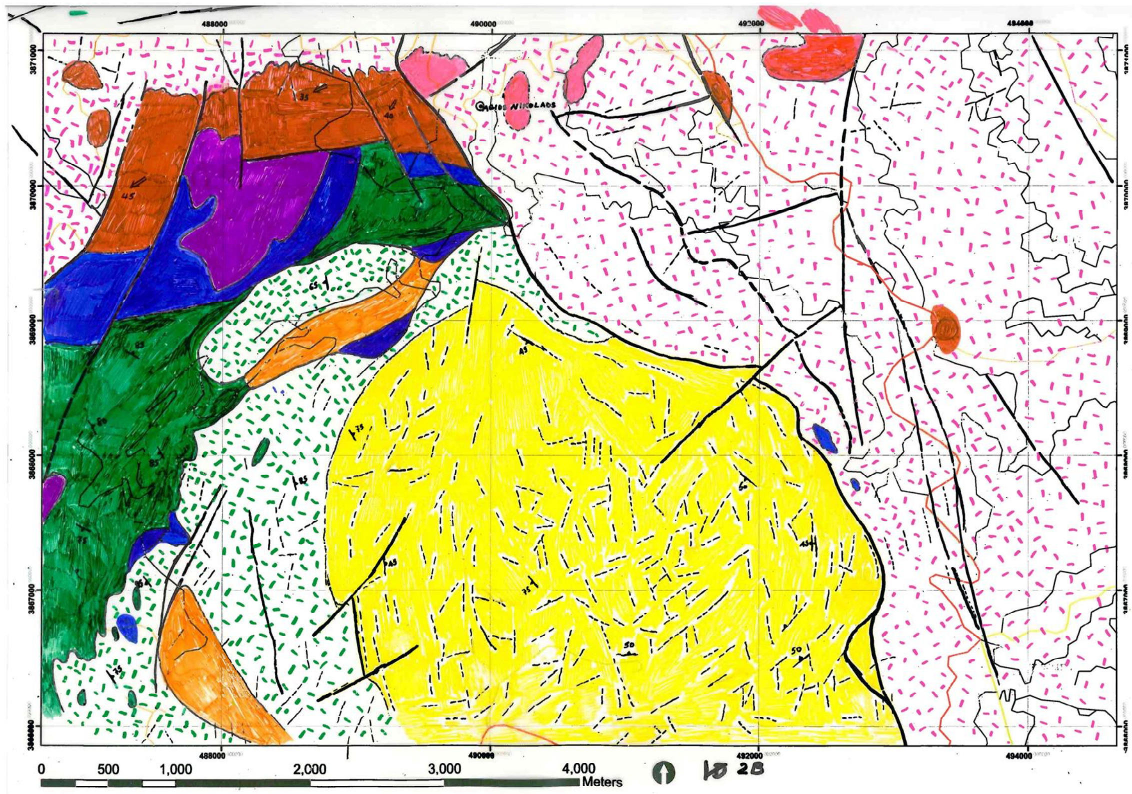

Figure 10: Draft geological map (part of the area near the Amiantos Mine).

5.4 Preparation and dispatch of field samples

Batches of samples were sent to the laboratory of the National and Kapodistrian University of Athens on four different dates (17/06/2009, 31/08/2009 and 16/12/2009 and 28/06/2010). Samples were split so that half of the sampled material could be stored in the Atlantis offices in Cyprus.

Hard rock and soil samples were packed in plastic bags and then placed in plastic containers for the dispatch **(Figure 11)**.

Figure 11: Plastic bags for rock and soil samples and plastic containers for dispatch

5.5 Preparation of reference rock collection

Representative samples for each geological formation were collected in order to prepare a reference rock collection. These reference samples were collected during field surveys with the Senior Geologist Expert (K. Louca). All the different geological formations in the project area where thus visited.

The resulting collection consists of Serpentinite, Harzburgite, Dunite, Wehrlite, Websterite-Pyroxenite, Peridotite, Plagiogranite, Olivinic Gabbro, Hornblendic Gabbro, Isotropic Gabbro and Diabase. Two collections were created: one for the field team and one that will be presented to GSD at the end of the project.

5.6 Petrographical and Mineralogical analysis

5.6.1 Introduction

The physical and chemical properties of NOA in geological formations are usually more complex and variable than asbestos encountered in manufactured products. Rock samples may also contain asbestiform minerals other than the six types of asbestos commonly found in manufactured products. Additionally, the matrix of rock samples is likely to be different and may be more variable than those in manufactured products. However, the identification of asbestiform minerals in a rock sample is usually relatively clear. Quantification of the amount of asbestiform minerals in a rock sample is more difficult.

Unequivocal identification of asbestos minerals requires information on morphology, chemical composition, and crystal structure. Several analytical methods may be applicable to soil and rock samples in studies on Naturally Occurring Asbestos. **Table 4** summarizes these various methods, the information they provide, and their advantages and disadvantages. The principal methods used by laboratories to identify asbestos are polarized light microscopy (PLM) and electron microscopy (TEM/SEM) (**Figure 12**).

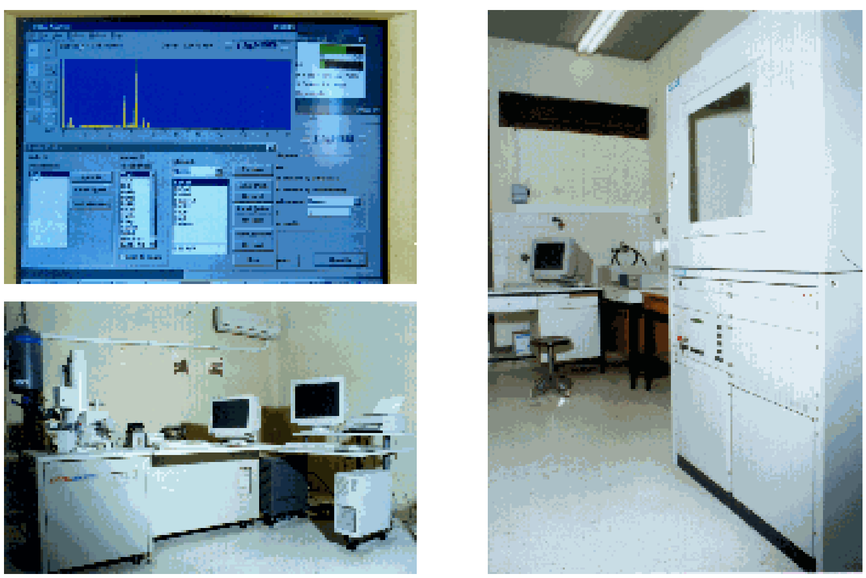

Figure 12: Laboratory equipment at the University of Athens: left: SEM-; right: XRD-devices.

Table 4: Available analytical techniques for asbestos samples.

Analytical Technique	Abbreviation	Information provided	Comments	Sample characteristics and size
Polarized Light Microscopy	PLM	The presence or absence and type of asbestos in a sample, and the particle morphology (asbestiform vs. non-asbestiform) can be determined. Estimation of the percent of asbestos (usually as area or particle percents) by visual or point counting methods is possible.	Used with thin sections for rock type characterization; used with grain mounts and immersion oils (dispersion staining) for mineral identification; grain mounts are better suited for asbestos identification than thin sections; difficult to use on very small particles – 1 micron practical resolution limit; relatively rapid and inexpensive compared to electron microscopy.	Thin sections and mineral grains or particles.
Scanning Electron Microscope	SEM	High magnification imaging of particle and fibre morphology. Qualitative or semi-quantitative chemical analysis of areas on individual mineral particles is possible if the SEM has EDS (energy dispersive spectroscopy) capabilities. Chemical composition information can be used for mineral identification.	High magnification imaging of mineral particle surfaces allows examination of smaller sized particles than PLM; chemical analysis by EDS is rapid but semi-quantitative and may not be sufficient for distinguishing different minerals with similar chemical compositions.	Sub-mm to 1 cm sized mineral particles and rock fragments. Particles with irregular surfaces may be utilized.
Transmission Electron Microscope *(not used in this study)*	TEM	High magnification of particle morphology, semi-quantitative chemical analysis by EDS, and crystal structure information by Selective Area Electron Diffraction (SAED) can all be used to aid in positively identifying mineral grains and fibres. Some methods allow determination of asbestos percentages.	Slower and more complex to use than PLM for asbestos analysis, but definitive for asbestos mineral identification. TEM my be used to analyze much smaller particles than can be analyzed by PLM and chemical analyses are of much smaller volumes than SEM or EPMA. TEM can be used for either qualitative or quantitative determination of the asbestos content of samples.	Very small sample quantities may be analyzed; mineral particles must be thin enough (sub-micron) to allow electron beam transmission.
X-ray Powder Diffraction	XRD	Identification of the major mineral types present in bulk samples; may be used to estimate mineral abundance.	Allows rapid determination of the major minerals present in a sample, provided there is not too much overlap between the different mineral diffraction patterns. The method has relatively high detection limits for minerals. No information is provided about morphology (asbestiform vs. non-asbestiform). This method has been used for quantitative determinations of asbestos abundance in samples.	Sample must be powdered; about 0.1 to 1 g of sample are used for the analysis, depending on the type of mounting method used.

5.6.2 Sample preparation

The following steps are involved in sample preparation:

- All rock samples are cut.
- After cutting, half of the sample is pulverized for XRD (Powder X-Ray Diffraction) analysis.
- The rest of each sample is then examined macroscopically and filed. After that, a petrographic specimen (thin section) is made, suitable for PLM (Polar Light Microscopy) microscope and SEM and/or EMPA (Scanning Electron Microscopy and/or Electron Microprobe Analyses) study. Non-used parts of the sample are stored.
- All soil samples are dried at 60°C.
- The dried soil-samples are sieved and the 3 mm-200 mesh fraction is examined under a binocular microscopy (to check the presence of asbestos minerals).
- Half of this fraction is pulverized for subsequent XRD analysis, and the rest is stored.
- The other half is stored for eventual SEM examination.

5.6.3 Optical microscopy

Optical techniques may be applied both to the description of thin sections for the purpose of petrographic description and classification of rock samples and to grain mounts (soil/sediment) for identification of individual mineral grains. Discussion of the general techniques of optical mineralogy can be found in Nesse (1991) and Bloss (1999).

Examination of thin sections of rock samples provides information on rock-type, mineralogy, texture, alteration, and metamorphic grade – all of which may be useful in the investigation of naturally occurring fibrous minerals. Because individual asbestos fibres are much thinner than the thickness of the thin section, numerous fibres may overlap in a vein, or other minerals may underlie asbestos fibres, which makes identification of individual asbestos fibres difficult.

Isolation in refractive index oil on a glass slide immediately distinguishes chrysotile (refractive index less than 1.57) from the amphibole-asbestos minerals (refractive indices above 1.59). However, this may not immediately separate the serpentine minerals from other potentially asbestiform minerals with refractive indices less than or equal to 1.57 such as palygorskite, sepiolite, brucite, or erionite. Nor will it exclude potentially asbestiform, non-regulated amphibole species that may have refractive indices greater than or equal to 1.59. The identification of the non-asbestiform serpentine minerals (chrysotile, lizardite, and antigorite) generally requires X-ray diffraction methods.

A limitation of the PLM method is the size of fibres that can be resolved. Although modern optical microscopes can resolve fibres with diameters less than 1 micron using special illumination techniques, the practical resolution limit when using the PLM method is somewhat greater than 1 micron (McCrone, 1987). Some individual asbestos fibres may have diameters smaller than this practical limit and, in a given sample, such fibres may not be observed or identified by this method. This may be of particular concern with soil samples where fibre size may have been reduced by chemical and physical weathering or by transport. In such cases, because of the small fibre size, PLM may not adequately document the presence of asbestos in some soil samples. In that case, other methods such as scanning electron microscopy are applied.

The analysis of a sample begins by performing a macroscopic and/or microscopic examination of the sample using a simple stereomicroscope. For rock and soil samples this step allows the analyst to assess the sample and to select specific areas of the sample for further analysis

5.6.4 SEM

SEM can be considered as a powerful backup for optical microscopy because it allows much greater magnifications than optical microscopy and also allows semi-quantitative chemical analysis of the imaged material. Therefore, the SEM is used to evaluate both the morphological and chemical composition of asbestiform minerals. SEM produces images by scanning a finely focused beam of electrons across the surface of the sample. The interaction of the electron beam and the sample produces a variety of signals that can be used to image and chemically characterize the sample.

With SEM fibres adhering to other mineral surfaces can easily be observed. SEM images can provide a permanent record of grain sizes, shapes and aspect ratios, all of which are important to the characterization of asbestos minerals. Further information on the theory and application of the SEM and electron microprobe can be found in Potts (1987) and Goldstein et al. (1981).

SEM can be used for observation of asbestos fibres in a variety of matrices, e.g., mineral, bulk construction materials, air and water. However, standard analytical methods for quantitative analysis of asbestos have been difficult to develop, primarily because of the difficulty in standardizing the many operating parameters that are controlled by the SEM microscopist.

Electron microprobes are instruments designed specifically to produce quantitative elemental analyses of small point locations on a sample (Electorn Microprobe Analysis – EMPA). Like the SEM, the electron microprobe uses a finely focused electron beam to analyze very small portions of the sample. In the electron microprobe, quantitative elemental analyses are obtained through the use of focusing wavelength-dispersive X-ray spectrometers and by optimizing the electron beam-sample-detector geometry by using flat, polished samples. EMPA is utilized to obtain the quantitative elemental analyses needed for mineral identification and is routinely used for amphibole mineral identification in geologic research.

5.6.5 XRD

X-ray powder diffraction (XRD) is a widely used analytical technique for identifying minerals and characterizing their crystal structure. When an incident beam of X-rays strikes a sample of finely crushed mineral particles, the X-rays are diffracted in specific ways depending on the atomic structure of the minerals present. Each mineral thus has a corresponding unique X-ray diffraction pattern. Consequently, the XDR-diagrams allow determining the presence or absence of particular minerals.

Sample preparation for XRD requires that the rock or soil sample is first pulverized to the consistency of a fine powder. Generally, about 0.5 to 1 gram of sample is needed for analysis. The sample powder is not destroyed during the XRD process and may be retained for future reference if desired.

Mineral identification by X-ray powder diffraction works best for samples that are mono-mineralic or contain a small number of different minerals. Minerals must typically be present in at least several weight percent in a sample to be detected by XRD. If multiple minerals are present they should ideally have distinctly different reference patterns (i.e., limited or no diffraction peak overlaps). For example, a serpentine group mineral in a diffraction pattern is easily distinguished from an amphibole group mineral. However, correctly determining which serpentine or amphibole mineral is present may be difficult or impossible from XRD data alone because the diffraction patterns of minerals with closely related structures are very similar (O’Hanley, 1996, p. 65; Veblen and Wylie, 1993, p. 123; Wicks and O’Hanley, 1988, pp. 124-128).

5.6.6 Working schedule

The petrographical and mineralogical analysis of the samples was started up at the end of June. The final report was drafted in early March 2010. In June-August, 2010, an extra batch of samples was petrographically analysed. Sample preparation and analysis are time-consuming processes. In general, the work flow for sample preparation is as follows:

- Cutting-polishing of the samples: maximum 10 samples/day;
- Examining of samples by light microscopy: 6 samples/day;
- Examining samples by SEM: 4 samples/day;

The laboratory and analytical work comprised:

- Cutting and preparation of **200** thin sections, for **197** rock-samples. (A few samples were cut at two planes);
- Pulverizing: **111** rock-samples and **73** soil-samples;
- Sieving: **73** soil-samples;
- Petrographic study of all thin sections by PLM with 333 associated photos.
- Carrying out **1119** microprobe mineralogical analyses, at **80** rock and **47** soil samples, together with **310 rock** and **67 soil** associated and explanatory SEM-photos and micrographs.
- XRD-analyses on **111** rock fragments and **73** soil samples: **184** XRD diagrams were thus calculated on the pulverized samples. In addition, **22** duplicates

were made for certain soil samples. (XRD measurements using different parameters for the scans.)

Results of this analytical work are summarized and presented in the tables in the **Annexes 3**. The complete final progress reports are included in **Annex 7** and **Annex 8**.

5.7 GIS and database preparation

5.7.1 Data formats

An Excel-database format was built, stored on the Ecorem-server, and made accessible for the project collaborators in Cyprus and Belgium through a secured VPN-connection. This largely facilitated the data-transfer between the project partners.

The database format was compatible with the survey datasheets that were used in the field and with the reports that were produced by the laboratory at the University of Athens. (Annex 1)

Finally, geological mapping results were digitized in ArcInfo, and information from the database was linked to the geographical data in the GIS **(Annex 4)**.

5.7.2 GIS structure

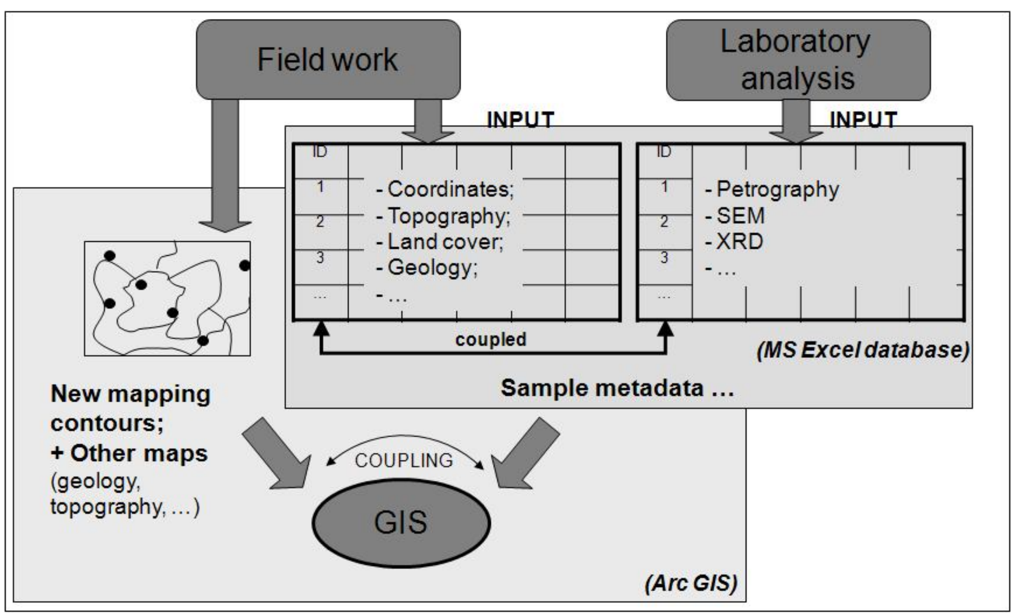

Figure 13: Methodology for database and GIS compilation.

Sample information which was collected in the field and obtained from the laboratory analyses, was regularly put into the database by the field geologist and project engineer. As a result, the GIS structure summarizes all information obtained in the course of the project:

- The refined geological map for the Troodos area and other geographical reference layers (topography, roads, villages, …);
- Sampling locations;
- Field observations from the surveys;
- Petrographical and mineralogical analysis results.

5.8 Training in laboratory techniques

From Monday 22/11/2009 to Friday 27/11/2009, Mr. Stelios Nicolaides and Mr. Andreas Zisimos from the Cyprus Geological Survey department received training at the laboratories of Prof. Stamatakis at the National & Kapodistrian University of Athens.

First, they went through the theoretical aspect of various analytical techniques and then used the SEM, the microprobe, the XRD and the optical microscope on samples from the Troodos area. A number of samples were analyzed by both GSD staff, so that they could examine the fibrous minerals on the SEM and the PLM.

The first-hand experience of these two geologists will be of great value to the GSD, as it will allow them to better understand the outcomes of the project.

6 PROJECT RESULTS

6.1 Geological Mapping

6.1.1 General Information

The overall geological picture of the area as mapped by the Project, is quite similar, except for some minor changes, to that portrayed by the published geological maps of the Geological Survey Department at the scale of 2 inches to 1 mile and 1:250.000. Notable differences between these maps and the Project's mapping exist in the eastern part of the investigated area, on the map sheets east of Amiantos asbestos mine. The Project's geological map on these sheets substantiates the bulk of the features reflected on the Amiantos-Palechori Map at the scale of 1:10.000, published by the Geological Survey Department in 1987 in conjunction with the 1987 Ophiolite Symposium

Although Sheet 1, of the Xeros-Troodos geological map at the scale of 2" to 1mile (Wilson, 1959) is admittedly quite accurate in terms of lithological boundaries, significant differences have been found by the Project in the definition of lithological units, in rock relationships and the stratigraphic position of certain units. With respect to mappable lithologies, the major differences are given below:

Wilson (1959) Map	Project (GSD/2008/26) Map
Enstatite-Olivinite	Tectonised harzburgite and peridotite
Harzburgite-Wehrlite	Wehrlite
Menalogabbro	Olivine gabbro
Uralite gabbro	Gabbro-norite, hornblendic gabbro

Differences in the general stratigraphic positions of the major lithological units are the following:

Wilson (1959) Map	Project (GSD/2008/26) Map
Diabase	Diabase
Granophyres (plagiogranites)	Granophyres (plagiogranites)
Gabbro	Gabbro
Wehrlite	Granophyres (plagiogranites)
Harzburgite	Gabbro
Dunite	Wehrlite
	Layered gabbro
	Pyroxenite
	Dunite
	Harzburgite, Peridotite

The Project's maps at the scale of 1:20.000 are included in **Annex 4** and a reduced map is shown in **Figure 13.**

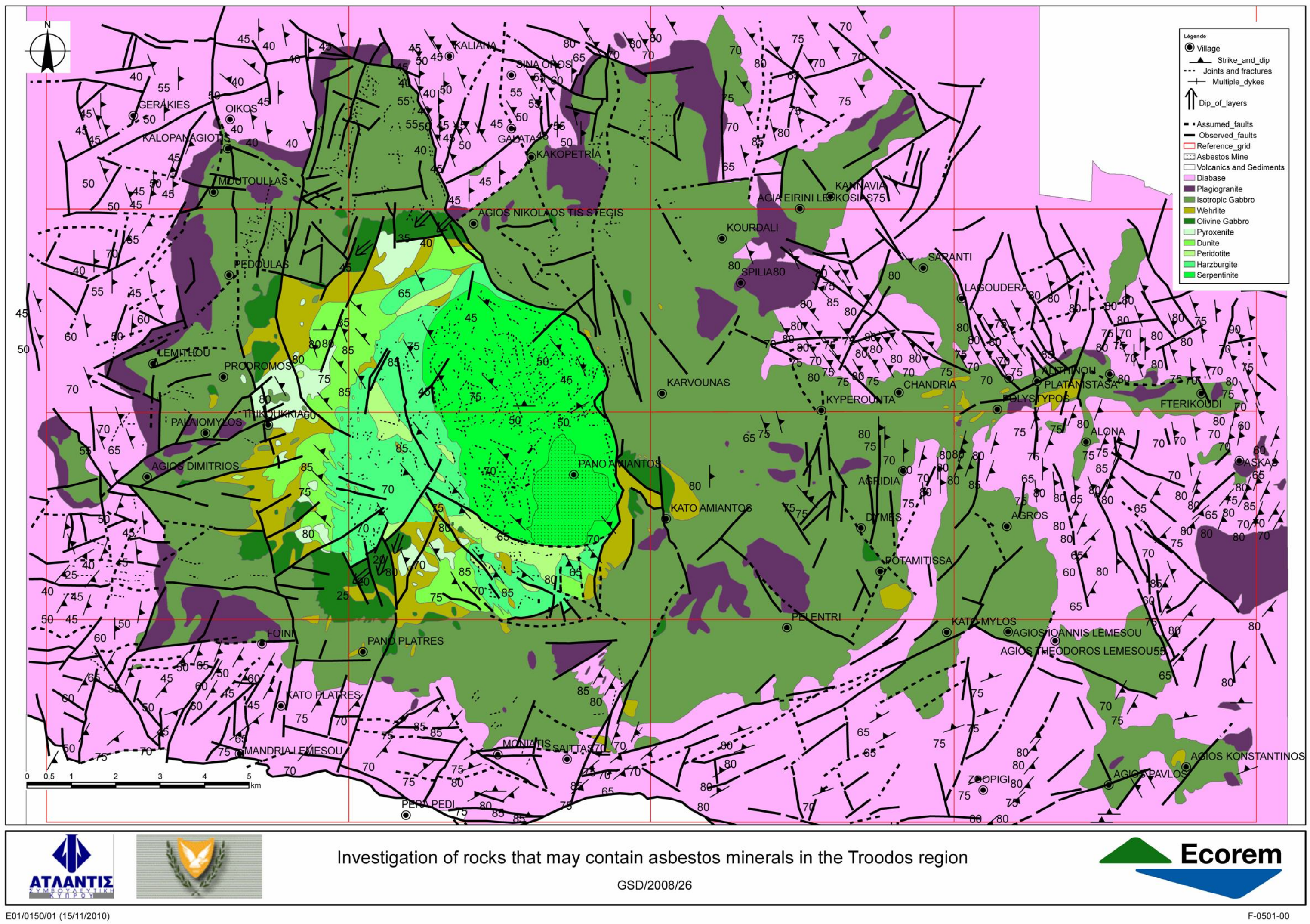

Figure 14. Project's study area

6.1.2 Lithological Units

6.1.2.1 Bastite Serpentinite

Occupying an oval shape of roughly 5.4 x 3.5 km in the central and highest portion of the Troodos dome, this unit represents a brecciated and smashed zone in serpentinite, serpentinized harzburgite and serpentinized peridotite. Small dunite lenses within this zone are completely crushed and serpentinized. The eastern contact of this zone is marked by a major reverse fault or thrust fault (Malpas, 1990) which emplaces the bastite serpentinite over the gabbros. Its southern contact is also sharp and probably faulted, while in the west it displays a gradation to relatively undisturbed harzburgite.

The zone is characterized by multi-directional shear planes and joints, narrow powdery crushed zones and development of chrysotile and picrolite veining. Varying in thickness from less than a millimetre to 5 cm, the chrysotile asbestos veins are most likely contemporaneous with the serpentinisation. Vein networks are most common in serpentinites, particularly within the Amiantos mine, where serpentinisation is well developed.

6.1.2.2 Harzburgite

Forming the base of the Troodos pluton, the tectonised harzburgite together with associated enclosed small masses and lenses of dunite, lherzolites and other peridotites, occupy the highest portion of the Troodos dome around Mt.Olympus, as well as a semi-circular area west of the Bastite-Serpentinites. Serpentinized harzburgite forms about 80% of the total outcrop while the remaining 20% is made of subordinate rocks.

Harzburgites are medium to coarse-grained rocks composed of 75-85% olivine, 15-20% orthopyroxene bastites and accessory chrome spinel and magnetite. Clinopyroxene is rare in the harzburgites but more common in the peridotites. The harzburgites and the enclosed rocks have undergone pervasive tectonic foliation and variable degree of serpentinisation. Tectonic foliation and metamorphic segregation impressed on the harzburgite has resulted in the planar alignment of orthopyroxene and sub-parallel segregation of olivine-orthopyroxene-rich bands.

Commonly elongated in the foliation direction of the host rock with sharp and folded contacts, the sporadically occurring dunite bodies are composed of >95% olivine and less than 5% chrome spinel and magnetite.

The boundaries between the harzburgite and the overlying Dunite Unit as mapped by the Project, are irregular and seldom diffuse but can in most places be closely defined by the abrupt absence of orthopyroxene crystals on the side of dunite and their presence on the side of harzburgite.

6.1.2.3 Peridotites

These peridotites and their smashed equivalent in the Bastite Serpentinite have been identified on he basis of the results of the petrographical investigations. They are enclosed within the tectonised harzburgites in the form of elongate discontinuous masses aligned in the direction of the regional tectonic foliation.

Petrographically, the rocks are similar in most aspects to the tectonised harzburgites but contain additionally small amounts of clinopyroxene (diopside). Their rock forming minerals are olivine, orthopyroxene, orthopyroxene bastites and accessories of spinel and magnetite. Locally, they contain prehnite and chlorite. Olivines are highly replaced by serpentine forming mesh textures.

The rocks have suffered similar tectonic fabric as the harzburgites. Their boundaries with the latter are difuse and are not easy to define accurately. In most cases there is nothing that may suggest a contact surface.

6.1.2.4 Dunite

Forming the base of the cumulate sequence of the Troodos Ophiolite, the dunite surrounds discontinually the tectonised harzburgites. It outcrops as a semi-circular belt of variable width within the western, northern and southern mass and forms an irregular boundary with the harzburgites along the western flank of Mt. Olympus. On this side, dunite with accessory pyroxene grades over greater distances into the harzburgites. These structures are often concordant with the mineral banding.

The dunites are black to bottle green on fresh surfaces, and are generally medium-grained. They are composed of olivine (>95%) which has been moderately to pervasively serpentinized. Accessory minerals are chromite and magnetite. The rocks have suffered penetrative deformation that has led to the transposition of layering parallel to the tectonic fabric. In some outcrops, dunite displays shearing and in others is heavily cleaved as a result of plastic deformation.

Relationships with the other members of the cumulate sequence are quite complex. Contacts with the overlying pyroxenite show variations, being interbanded or gradational. Interdigitating boundaries, with pyroxenite extending downwards into dunite, do also occur. Interlayered dunite and pyroxenite on a few centimetres scale marks the upward passage of dunite, into pyroxenite bodies.

Owing to poor exposures no actual contacts have been observed with the wehrlite. As will be discussed in Section 6.1.2.7, an intrusive relationship in evidenced on the basis of xenoliths of dunite in the margins of wehrlite.

6.1.2.5 Pyroxenites

Relatively large bodies of pyroxenite are those that occur on the northwestern flank of Mt.Olympus and due west of St.Nicholas. Isolated smaller bodies occur on the southern flanks of Troodos dome. Within the cumulate sequence the pyroxenites form an intermediate zone between the underlying dunite and the overlying layered gabbros.

They range in composition from websterites to clinopyroxenites with olivine sub-types and they include facies of pyroxene-rich rocks that cannot be distinguished from each other in the field. The olivine-bearing sub-types are weakly serpentinized. They are generally medium to coarse-grained rocks (5-10mm, in length) but pegmatite facies do also occur. Mineral banding caused by the segregation of olivine can be observed near their contacts with the underlying dunite, particularly within interlayered horizons with the latter.

The relationship of the pyroxenites, namely of olivine rich websterites with the overlying olivine gabbros is enhanced by interlayering and concordant mineral banding. An intrusive relationship with the wehrlite is suggested by the presence of frequent xenoliths of pyroxenite, particularly within their contact zone. This is further addressed in Section 6.1.2.7.

Nevertheless, local occurrences of pyroxenite and wehrlite interlayered on a centimetre scale, found beyond the limits of the main ultramafic mass, may belong to a stratigraphically higher layered horizon associated with pyroxene gabbro.

6.1.2.6 Olivine gabbros

Although the olivine gabbros have been mapped collectively as one mappable unit, they may not belong to the same stratigraphic horizon. The bulk of the exposed olivine gabbros are confined to the stratigraphically lower and main layered sequence of the Troodos dome, previously divided into the melanogabbros and olivine gabbro. (Wilson,1959). They occur as discontinuous zones and sporadic outcrops around the ultramafic pluton. Small outliers occur in pyroxenite and other ultramafic rocks.

Smaller and isolated outcrops of olivine gabbro, most probably associated with stratigraphically higher small layered units, are found in the pyroxene gabbro.

Olivine gabbros range in composition from olivine-rich gabbros and gabbro-norites to olivine-deficient varieties. They are fine to medium-grained rocks consisting of plagioclase, hypersthene, clinopyroxene and olivine and they display ophitic and cumulous textures. The rocks described previously as melanogabbros are medium to coarse-grained rocks, and compositionally are transitional rocks between a wehrlite and an olivine gabbro.

Prominent banding is displayed in the basic portion of the olivine-gabbro, particularly in the vicinity of pyroxenites and consists of alternating felspathic or pyroxene-gabbro bands with olivine rich bands. The latter bands vary from a few millimetres to more than a metre in thickness.

Deformation fabrics produced by viscious or plastic flow and transpotition of original cumulate layering in folds is exhibited in a number of outcrops aroung the ultrabasic pluton. Recrystallisation is also a common phenomenon within the deformed olivine gabbro.

Intruding the deformed olivine gabbros are the wehrlite unit and isotropic gabbros. Extensive outcrops of deformed olivine gabbros immediately east of Pano Amiantos village have been heavily intruded by multiple dykes of isotropic gabbro (hornblendic gabbro and pyroxenic gabbro), rendering this way difficult their separation.

6.1.2.7 Wehrlite Unit

The bulk of the wehrlite forms extensive and irregular belts along the margins of the ultabasic plutonic mass of the Troodos dome. These massive outcrops range up to 3 km in length and 1 km in width. Isolated small bosses occur with the other ultrabasic units. Relations with these rock are intrusive and are evidenced by the presence of xenoliths and large masses of deformed ultrabasic rocks within the wehrlite unit. North of Mt. Olympus, the wehrlite truncates the contacts between harzburgite and dunite, between dunite and pyroxenite and between pyroxenite and olivine gabrro. West of Mt. Olympus the wehrlite intrudes the older mafic and ultramafic rocks and is bordered by isotropic gabbro. Southeast of Mt. Olympus the wehrlite intrudes mainly dunite and olivine gabbro and encloses small bodies of pyroxenite and dunite.

Much smaller and isolated bodies of wehrlite have a sporadic distribution within the isotropic gabbro, particularly in the Polystipos region. Their relation with the wehrlite that occurs on the margins of the ultrabasic pluton has not been established.

The wehrlite group comprises poikilitic wehrlites with pyroxene oikocrysts and poikilitic plagioclase wehrlite. Both types have a distinctive poikilitic texture and under the microscope they exhibit cumulate textures. The wehrlites contain 60 to 70% olivine, clinopyroxene (diopsidic) and accessory spinels, enstatite and magnetite. Local lithological sub-types include umappable masses of diopside peridotite in which there is a relative decrease of olivine and an increase of diopside and enstatite.

In general, the rocks are moderately serpentinized. Otherwise the rocks do not exhibit the deformation fabric that characterises the older ultrabasic rocks.

The contact relationship between the wehrlite, the isotropic and uralite gabbro is complex and have not yet been established at high confidence levels. Veining of uralite gabbro into the wehrlite characterises a number of contacts while other sharp intrusive contacts are chilled on the side of the isotropic gabbro.

In general, the findings of the Project's mapping support the views of Malpas (1990), that the wehrlite may belong to a late suite pluton that intrudes an early suite pluton consisting of penetratively deformed harzburgite tectonite, dunite, layered olivine clinopyroxenite and gabbro.

6.1.2.8 Undifferentiated Gabbros

This is an assemblage of pyroxenic gabbros (gabbronorites) and hornblendic gabbros (uralite gabbro and hornblende gabbronorite) that forms a continuous belt around the Troodos ultrabasic pluton. Wilson (1959) divided these gabbros into pyroxene gabbro and uralite gabbro, considering the latter as being highest in the sequence. Subsequent investigations carried within the framework of the International Crustal Research Drilling Group (ICRDG) project have not substantiated Wilson's view but recognized the distribution of the uralite gabbro throughout the plutonic section (Malpas, 1990).

Consequently, it seems that some gabbros are cogenetic with the ultramafic cumulates while others are "high level gabbros" as referred in most ophiolites. Being beyond the scope and the financial capability of the Project, both types of gabbro have been mapped collectively.

The pyroxene gabbros are typically massive (isotropic) to very poorly layered, mesocratic rocks consisting of plagioclase, hypersthene and diopsidic augite. Quartz, is only locally present and common accessories are spinels. They are medium-grained rocks with common ophitic textures and less frequent cumulate textures. These are the most widespread of all the gabbro types of the Troodos Pluton.

The uralite or hornblendic gabbro consists of zoned plagioclase, clinopyroxene (augite), uralitic hornblende, magnetite and quartz. They are basically medium to coarse-grained hornblende gabbronorites which are locally pegmatitic, particularly near the contacts with the granophyres (diorites and plagiogranites).

The intrusive relations of the gabbros with surrounding diabase and plagiogranites are very complex posing this way difficulties in defining accurately their contacts. This is particularly valid in areas with gabbro and diabase roughly in equal proportions, showing mutual intrusive relations. Older generation gabbros are intruded by younger generation gabbros, the latter being intuded by plagiogranites and diabase.

6.1.2.9 Plagiogranites and Diorites (Granophyres)

The distribution of these rocks as mapped collectively by the Project, with a few minor modifications, remains the same as reflected on the published geological maps of the Geological Survey Department. These siliceous rocks range in composition from diorite to plagiogranite. They compise hornblende-trondhjemite, epidote trondhjemite and other hybrid dioritic rocks resulting from the differentiation sequence from gabbro to plagiogranite and the assimilation of hydrated diabase and microgabbro. They are composed essentially of sodic plagioclase felspar (albite) quartz, hornblende and epidote and show a variety of micrographic and granophyric intergrowth textures.

Being the most evolved rocks in the sequence they intrude diabase and gabbro and are locally cut by younger diabase and microgabbro dykes. Their contacts are often clear, particularly at the gabbro/diabase contacts but quite difficult to determine in areas with equal proportion of plagiogranite and diabase dykes.

6.1.2.10 Diabase

Separating the plutonic complex from the extrusive volcanic sequence, the Diabase Sheeted Dyke Complex surrounds the gabbro and the ultrabasic rocks on all sides. Mapping of its contacts was relatively accurate in areas where the diabase was in sharp contact with intruding plutonic rocks. Its boundaries are usually inferred in areas where the diabase intrudes the plutonic rocks, producing zones of mixed dykes and plutonic screens which occupy large areas of outcrops.

6.1.3 Structure

On the basis of the present project work and with due consideration to the findings of the previous multiple investigations on the Troodos Ophiolite Complex, the principal structural elements of the project area are summarized below:

- The region is dominated by the central dome structure of Troodos formed by the ultrabasic massif and surrounded in turn by gabbro and sheeted Diabase complex. The structure is cored by highly tectonised bastite serpentinite and harzburgite and the general disposition of its cumulate rocks in that of increasing basicity with depth. Characterized by multidirectional fracture patterns and completely crushed dunite lenses with serpentinized shear planes, the bastite serpentinite is perhaps the most striking feature of the Troodos dome structure.
- Block faulting typifies the overall tectonic pattern of the project area with characteristic repeated movements along many faults. Considerable faulting and brecciation characterize many lithological contacts and have a pronounced effect on the Troodos massif and the original form of the plutonic complex.
- Steeply dipping fractures of variable trends dominate in the area but a number of low angled faults or thrust faults do also occur in the area. One such important low angled fault or thrust with considerable displacement bounds the Troodos ultrabasic massif in the east, bringing the ultrabasic rocks against the pyroxene gabbro. It swings from NE-SW direction in the vicinity of Kato Amiantos village to a NNW-SSE direction at St.Nikolas monastery and has a dip of about 30^{o} to the west and southwest maintaining a constant NNW-SSE direction north of St.Nikolas monastery this fault brings the gabbro against the diabase sheeted dyke complex.
- Numerous cross-cutting faults and oblique systems of fractures occur around the greater portion of the plutonic massif. Many faults tend to coincide with the boundaries between the gabbro and the ultrabasic rocks and between the gabbro and the diabase. Both the north and south sides of Troodos appear to be bounded by steeply dipping fractures trending roughly in an E-W direction and which are offset by N-S transcurrent faults. Such E-W dislocations are dominant on the southern margin of the massif but they appear also to severely displace the lithological contacts on the western side of the massif.
- Banded structures having intermediate to steep dips and showing a variety of strike directions occur within the ultrabasic rocks and gabbros. High

temperature penetrative deformation of older rocks (harzburgite-peridotite group) is characterized by L-S fabrics that are generally parallel to the compositional layering. Oblique and cross-cutting relationships between these planar elements are common at the margins of the individual plutons.

- The strike of the diabase dykes swings from a regional NNW-SSE direction through NE-SW to an E-W direction on the south side of Troodos massif. Abrupt changes in the regional strike of dykes are marked by faulting and brecciation.
- Presence of multiple magma chambers and cross-cutting relationships between the plutonic sequence and the sheeted dyke complex and between different plutonic bodies.

6.1.4 Distribution of Asbestos Minerals

Asbestos mineralization within the Project Area is represented by the serpentine fibrous silicate chrysotile which occurs together with other non-asbestiform serpentine minerals (lizardite and picrolite) in pervasively serpentinized portions of the ultrabasic rocks of Troodos massif. Poorly fibrous tremolite and other colourless amphibole are subordinate in amount and distribution and they occur principally in association with amphibolitised pegmatitic pyroxenite and gabbroic veins.

Formed at the expense of olivine by hydration, the asbestiform chrysotile mineralization takes the form of hair-like stringers less than a millimeter in thickness to veinlets of about one centimeter in cross section. Their extension, strike and dip are most irregular and the majority of the individual veinlets comprise short-fibred varieties. The individual veinlets are discontinuous and may be traced for distances from a few tens of centimeters to a few metres.

The bulk of the veins are composite veinlets consisting of parallel stringers of both chrysotile and picrolite. These constituents of the veinlets pinch and swell or thin out over short distances.

Stockworks of cross-fiber chrysotile veinlets and stringers are confined to the bastite serpentinite and particularly to its highly brecciated and smashed portions within the Amiantos quarries and its immediate vicinity. Further north, the frequency of the chrysotile network within the serpentinite decreases proportionally with th intensity of brecciation.

Subordinate occurrences of chrysotile hair-like stringers may be observed in pervasively serpentinized zones and irregular masses of other ultrabasic rocks, particularly within the harzburgite. The locations of these sites are illustrated on the map of **Annex 5**.

6.2 Laboratory Results

6.2.1 Petrographical Study

The results of the petrographic study of 200 standard size thin-sections of rock samples substantiate the classification of lithological units adopted by the geological mapping. The bulk of the petrographic descriptions confirmed the field determinations of rocks but at of the same time they introduced significant differences which were taken into consideration by the mapping.

Whereas the Bastite Serpentinite, as mapped by the Project, was inferred to have derived by the metamorphic alteration of Harzburgite, the microscopic study of thin-sections revealed additionally protoliths of lherzolite and peridotite. Similarly, within the Harzburgite Unit, the petrographic study indicated the presence of small bodies of lherzolite and irregular masses of peridotite. Also, within the Wehrlite Unit as mapped by the Project team, wehrlite looking rocks proved to be local differentiates of diopsidic peridotite or wehrlitic periodotite.

The definition of intermediate rocks between wehrlite and olivine gabbro and between highly pyroxenic gabbros and pyroxenites has also been facilitated by the study of thin-sections. With respect to the olivine gabbros as collectively mapped by the Project, the petrographic study identified rock types such as olivine gabbro, olivine gabbronorite and troctolite.

Under the microscope the ultrabasic rocks show cumulate textures and where are highly serpentinized they exhibit mesh and pseudomorphic textures. Ophitic and locally porhyritic textures are characteristic of gabbros and diabasic intrusives.

The full petrographic descriptions of the 200 samples examined by the Project, are included in **Annex 3.**

6.2.2 Mineralogical Analyses of Rocks

Representative mineralogical bulk analyses of rocks by XRD are illustrated in **Annex 3**. The major rock forming minerals of ultrabasic rocks are olivine (mainly forsterite), orthopyroxene (mainly enstatite), clinopyroxene (mostly diopside), tremolite and serpentinite (mainly lizardite). Accessory minerals include magnetite, spinel, chromite, talc, brucite, chrysotile, chlorite, pyroaurite and andradite.

The isotropic gabbros are dominated by feldspars, actinolite and diopside and they may contain other minerals such as quartz, chlorite, smectite, epidote, clinozoisite and zeolites (laumontite, analcime and natrolite). The granitic and plagiogranitic rocks contain feldspars and amphibole and certain sub-types are saturated with quartz.

6.2.3 Mineralogical Analyses of Soils

Soil samples collected from relatively thick soils developed over gabbros and diabase are dominated by amphibole, feldspar, quartz and smectite with subordinate zeolites (laumontite), clinopyroxenes (diopside) and goethite-maghemite. Samples from poorly developed soils over gabbros are characterized by amphibole, feldspar, clinopyroxene, smectite, zeolites and locally by quartz and talc. Except of clinoryroxenes and talc all the above minerals have been identified in poorly developed soils over diabase. Soils over plagiogranites are relatively rich in quartz and feldspars.

Quite contrasting mineralogy is displayed by soils developed over ultrabasic rocks. Serpentinite soils are rich in lizardite and contain various amounts of chrysotile. The harzburgite-periodotite-wehrlite assemblage is also characterized by lizardide and locally by traces of chrysotile. Unlike these, soils over pyroxenites are rich in clinopyroxenes and amphibole.

6.2.4 Microanalysis of Rock Samples

Representative rock samples namely of serpentinite, harzburgite, peridotite, dunite and wehrlite have been microanalysed using the standard procedures described in Section 5 of this Report. A complete set of microanalytical results are included in **Annex 3**.

Although beyond the scope of this Project an attempt was made to evaluate these results. The MgO content of forsterite in the investigated rocks ranges from 49% to 51.5%. On average it increases from 49% in the serpentinites through 50.3% in the harzburgite-peridotite-wehrlite assemblage to 51.2% in the dunite. In the serpentine the MgO content ranges between 36% and 41% and is relatively higher in dunite and serpentinized dunite. In the orthopyroxenes the MgO content varies from 32.5% to 35% and is relatively lower in the pervasively serpentinized rocks.

Although the chromite of the dunite samples is relatively rich in chromium, on average the Cr:Fe ratio for the different ultrabasic rock is about 2:1. The chemistry of the chromite grains in most rock samples is relatively narrow. Small compositional variations displayed between dunite and the harzburgite-peridotite assemblage are given below.

Ratio	Harzburgite/Peridotite	Dunite
Cr/Cr+Al	0.71	0.85
Mg/Mg+Fe	0.34	0.24
Mg/Al	0.60	0.87

6.2.5 Chrysotile Asbestos in Rock Samples

Although chrysotile, has been detected in several samples, this mineral may not be always classified as asbestos. Chrysotile consists of flexible fibres with greater length than width, equal diameter and very easily separated.

Chrysotile asbestos has been detected exclusively in serpentinites and in a sample of highly serpentinized harzburgite (HAR06PPL) and in a sample of completely serpentinized dunite (DUN10KAK). However, all of the samples containing asbestos are completely serpentinized, as shown in the relevant tables of mineralogical analyses by XRD (**Annex 3).** A map showing the distribution of the laboratory results with asbestos occurrence is shown in **Annex 6.**

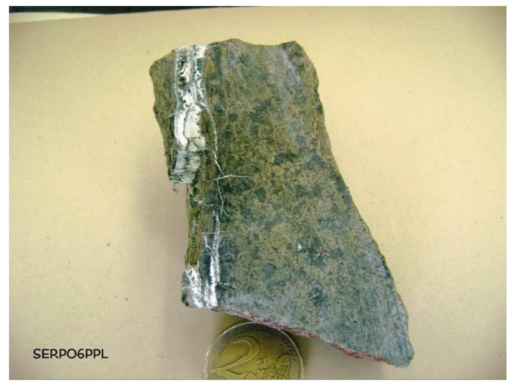

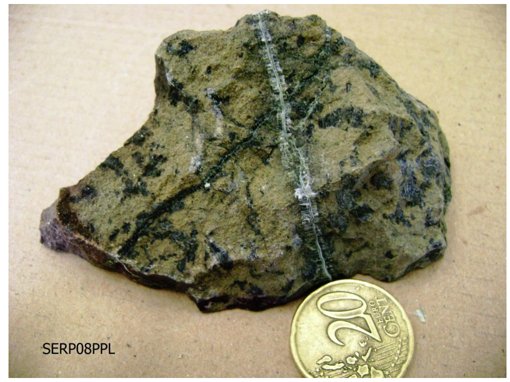

Figure 15: Examples of asbestos veins in serpentinite samples, all found near Pano Amiantos: SERP06PPL (Serpentinized harzburgite) , SERP05PPL (Serpentinized peridotite) , SERP08PPL (Serpentinized peridotite), SERP15PAM (Serpentinite).

The asbestos-bearing samples do not contain any of the original minerals: olivine (forsterite), orthopyroxene (enstatite/bronzite-hypersthene) or clinopyroxene (diopside/diallage-augite). In contrast, they mainly comprise of serpentine minerals (chrysotile and lizardite), with minor amounts of magnetite, goethite, brucite, andradite etc. The dominant serpentine mineral is **lizardite**. Chrysotile occurs primarily in veins as asbestos, but also in a microcrystalline form (apparent fibre), while antigorite has limited development. There is only one “serpentinite” sample (SERP13PAM-Serpentinized peridotite) not containing asbestos. This sample contains orthopyroxene, clinopyroxene and amphibole (tremolite), and some serpentine minerals (chrysotile and lizardite). Therefore, it cannot be regarded as a typical serpentinite sample (See **Annex 3**).

In completely serpentinized rock samples, asbestos occurs as veins or veinlets. Veins have small dimensions. Their width is usually a few millimetres or smaller and rarely exceeds one hundredth of the examined sample (e.g. the sample SERP15PAM-Serpentinite). Representative pictures of asbestos veins in serpentinite samples are shown in **Figure 15**. The veins in the serpentinite samples may consist mainly of asbestos fibres or may be composites.

In order to identify the minerals occurring in the asbestos veins, material extracted from the veins, was studied by means of XRD, after pulverization in a medium of liquefied nitrogen. As concluded from the study of the resulting XRD patterns, the asbestos mineral is chrysotile (2Mc1 type). One representative chrysotile asbestos XRD diagram, is presented in **Figure 16**.

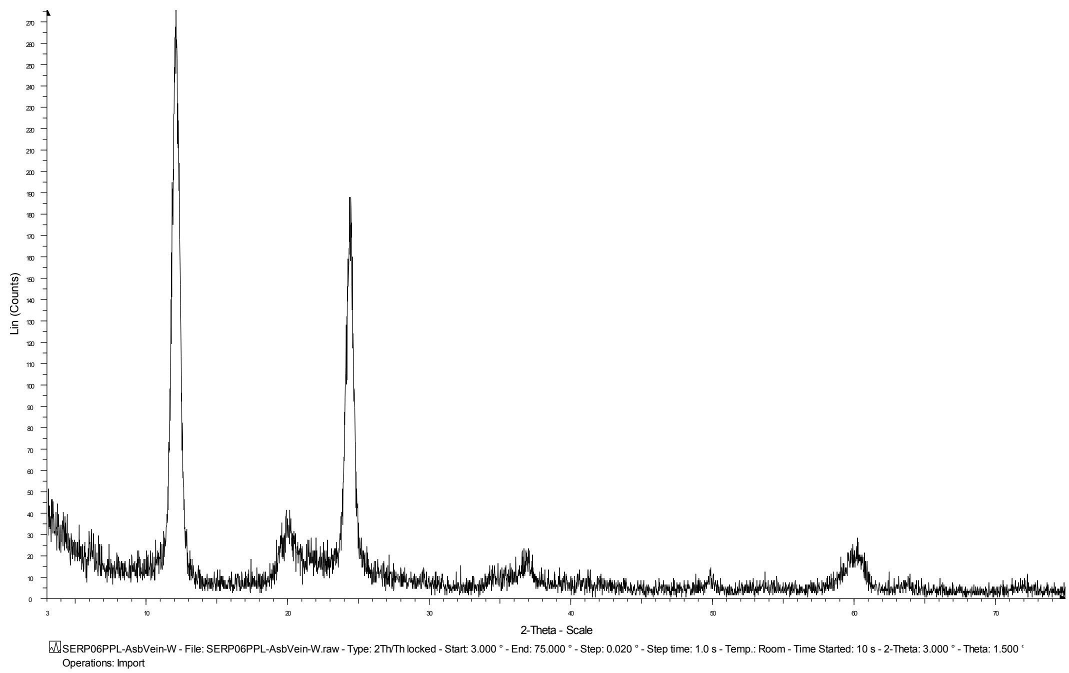

Figure 16: XRD-diagram for the material gained from an asbestos vein in sample SERP06PPL (Serpentinised harzburgite found near Pano Amiantos).

The composite veins contain mixtures of intimately associated chrysotile and lizardite and sometimes garnets (andradite mainly). In all of the studied samples the asbestos veins are cross-fibre type.

The microanalyses of the chrysotile asbestos are presented in the **Annex 3**. These results show that the chemical composition is generally as expected, but the iron content is somewhat higher. The characteristics of the asbestiform fibres and asbestos veins are well illustrated in the corresponding SEM micrographs and PLM photos. Examples are shown in **Figure 17** (SEM) an **Figure 18** (PLM).

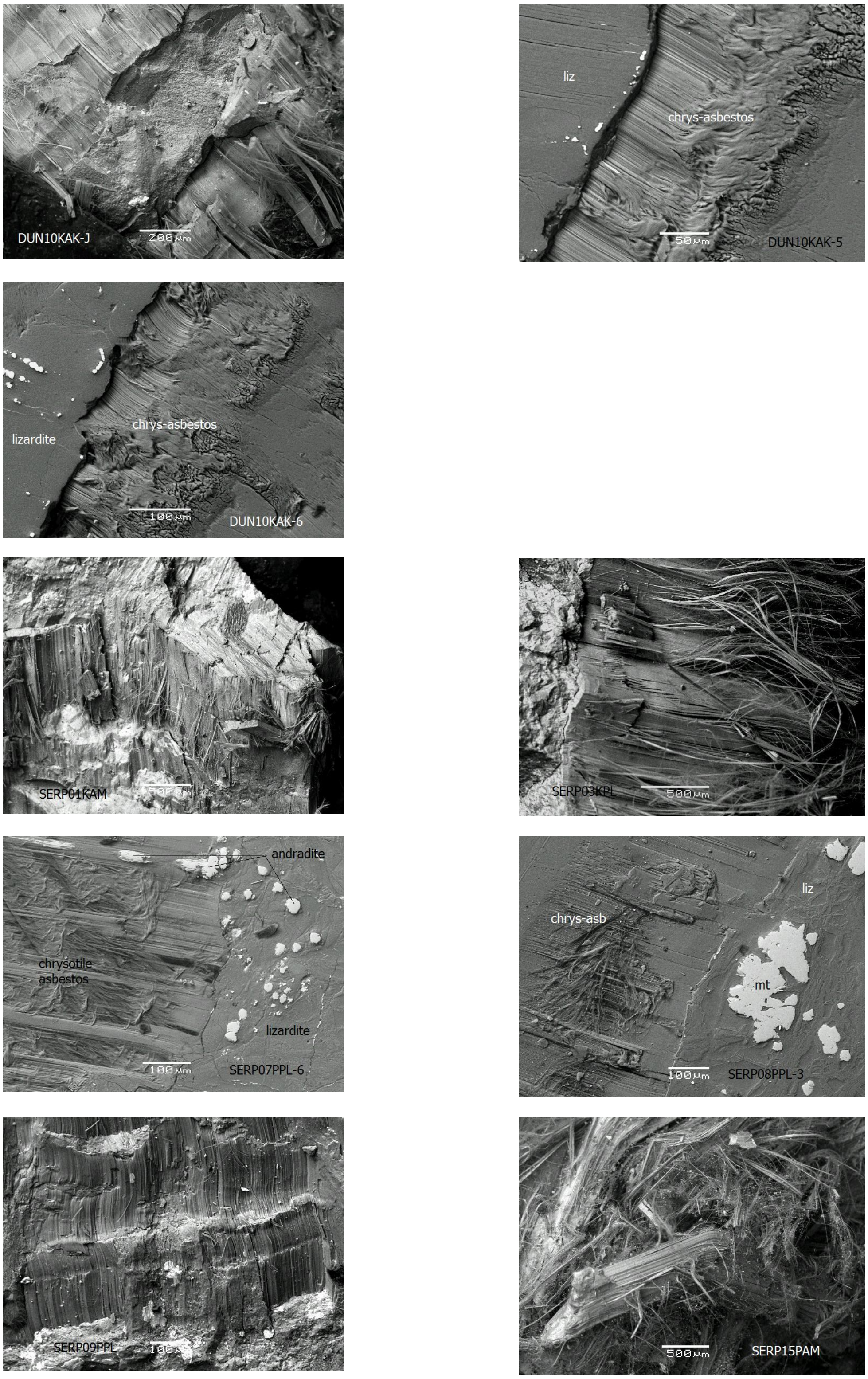

Figure 17: SEM micrographs for some representative asbestos fibres. One Dunite sample: DUN10KAK (near Agios Nikolaos). Six Serpentinite samples from the Pano Amiantos area: SERP01KAM, SERP03KPL, SERP07 PPL, SERP08PPL, SERP09PPL, SERP15PAM.

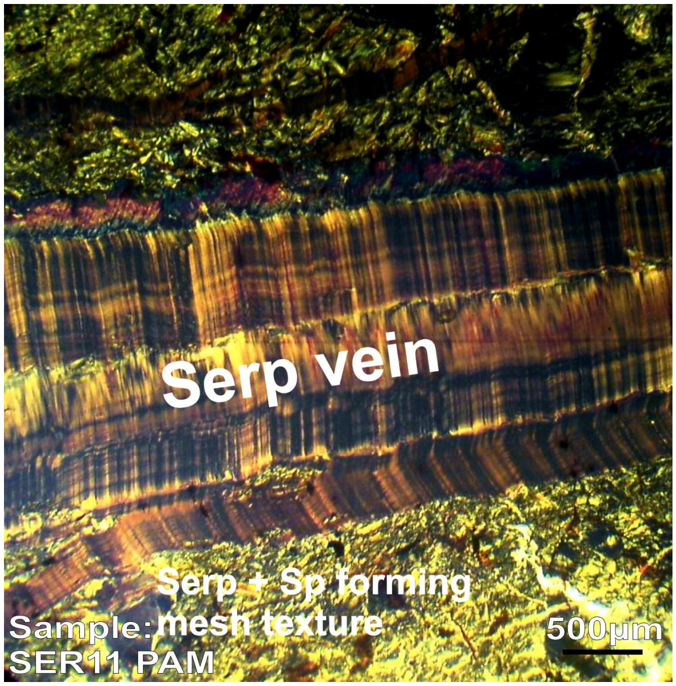

Figure 18: PLM Photo of a representative asbestos fibre. Sample SER11PAM (Serpentinite.)

6.2.6 Chrysotile Asbestos in Soil Samples

The presence of asbestos in the **soil samples** was visually checked and examined in detail under a binocular microscope in the 3mm – 200 mesh sieve fraction. The mineralogical identification was done with the XRD method. In addition, the morphological characteristics and microanalyses were done by SEM (**Figure 19**).

Only three samples (SER01KAM, SER02PPL and SER05PPL) show a sufficient quantity of asbestos fibres and few show traces (See **Annex 3**).

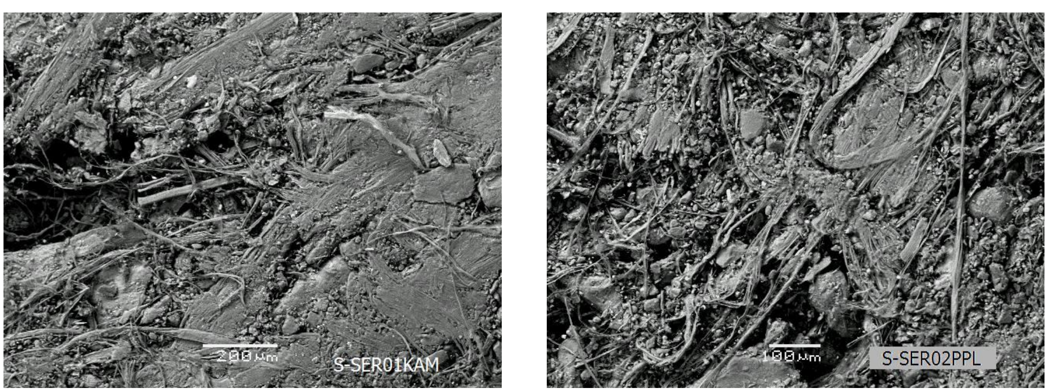

Figure 19: Morphological study of soil samples (grains in conductive tape) containing asbestos fibres, by SEM. Soil samples SER01KAM (Serpentinised peridotite) and SER02PPL (Serpentinised peridotite).

6.2.7 Other types of asbestos

In each case the asbestos present in the studied samples is chrysotile (2Mc1 type). Amphibolitic asbestos was not found. Although in some petrographic specimen amphiboles were observed with PLM or SEM - or in soil samples with SEM – these amphiboles were never asbestiform.

The amphiboles in most cases appear to replace the clinopyroxenes; These minerals sometimes show fibrous growth, but they are never asbestiform (**Figure 20)**. The mineralogy of these amphiboles as concluded from the PLM, SEM and/or XRD, is commonly **actinolite-tremolite** or hornblende type (see **Annex 3**).

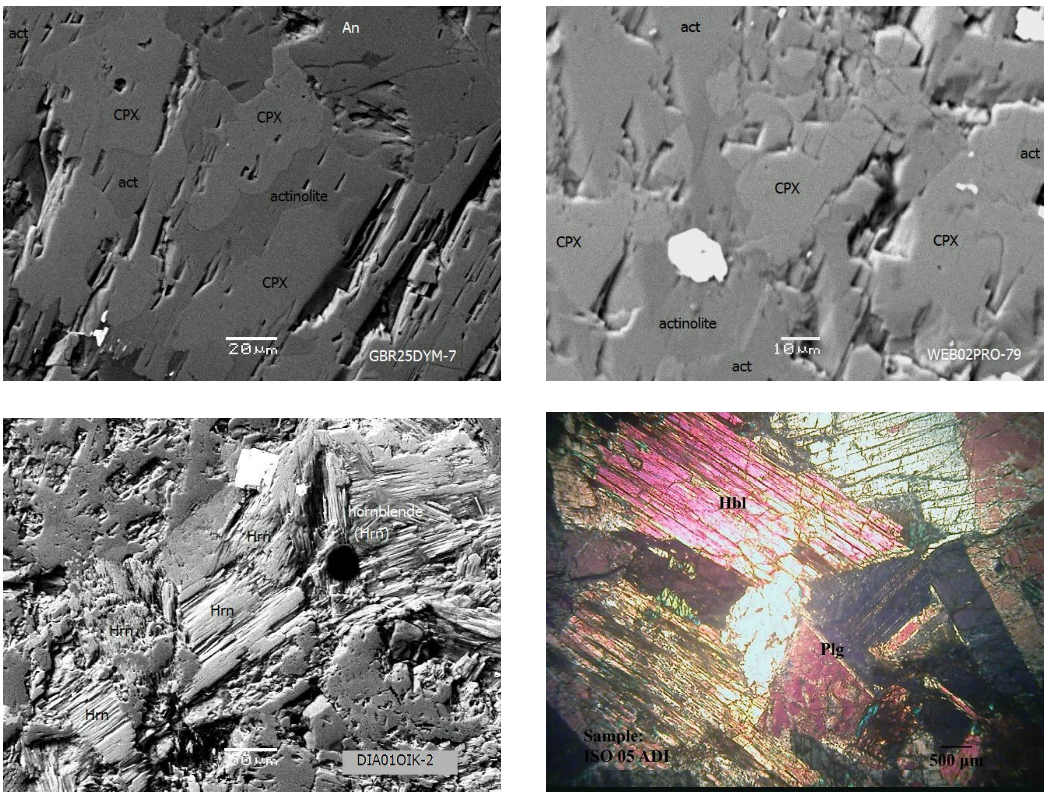

Figure 20: Amphiboles (clinopyroxenes) in the studied rock samples. Gabbro sample GBR25DYM, Websterite sample WEB02PRO, Diabase sample DIA01OIK and Isotropic Gabbro sample ISO05ADI.

In the corresponding **soil-samples** (except of these of SER, HAR, DUN) fibrous amphibole minerals are also actinolite-tremolite or hornblende type, and **never asbestiform** (**Figure 21**).

Figure 21: Non-asbestiform amphibole minerals in soil samples from the Troodos Area. Samples S18 and S23 originate from agricultural soils. Samples GBR22MON (Hornblendic Gabbro) and PLA02KAK (Granitic) are respectively associated to Gabbro and Plagiogranite parent material.

7 RISK ANALYSIS

7.1 Introduction

The potential environmental hazards and associated public health issues related to the exposure to naturally occurring asbestos have recently gained the regulatory and media spotlight in many areas. Fibrous rocks or sediments may be present in a variety of geological formations. It has been suggested in previous reports that airborne asbestos may be released from natural deposits, and that the absence of appropriate engineering controls may pose a potential health hazard if these rocks are crushed or exposed to natural weathering and erosion or to human activities that create dust.

Actual health risks can be questioned. In fact, there is need for (1) clear standards that establish a scientific basis for risk evaluation and assessment of naturally occurring fibrous materials in rocks and sediments; and (2) effective public policies for managing NOA, minimizing potential hazards, and protecting public health. Some of these key issues involved with the study of rocks containing fibrous minerals will be discussed in this chapter.

7.2 Definitions

Before presenting the risk assessment methodology, some terms are explained. First, it is important to point to the difference between the terms “hazard” and “risk”. The **"hazard"** associated with a substance is its intrinsic ability to cause adverse effects to human health or the environment. The **"risk"**, on the other hand, is the probability that such harmful effects will occur in various exposure scenarios.

Risk assessment aims to characterize the nature and magnitude of health risks to humans (e.g., residents, workers, recreational visitors) and ecological receptors (e.g., birds, fish, wildlife) from chemical contaminants and other stressors that may be present in the environment. Risk assessment generally involves hazard identification, exposure assessment, dose-response assessment and risk characterisation.

Hazard identification involves gathering and evaluating data on the types of health injury or disease that may be produced by a chemical and on the conditions of exposure under which injury or disease occurs. It may also involve characterisation of the behaviour of a chemical within the body and the interactions it undergoes with organs, cells, or even parts of cells. This can be of help in determining whether the forms of toxicity known to be produced by a substance in one population group or in experimental settings are also likely to be produced in humans (e.g., are substances found to be carcinogenic or teratogenic in experimental animals also likely to have the same results in humans).

Exposure assessment involves (1) describing the nature and size of the population exposed to a substance, (2) the magnitude and (3) duration of their exposure. It may concern current exposure, or exposures anticipated in the future. For example, the duration of exposure differs considerably between long-term residents and tourists visiting the area of exposure even though the momentary average intensity may be similar.

Dose-response assessment involves describing the quantitative relationship between the amount of exposure to a substance and the extent of toxic injury. Data can be derived from animal studies or, less frequently, from studies in exposed human populations. There may be different dose-response relationships for a substance if it produces different toxic effects under different conditions of exposure.

For **risk characterisation**, whatever the suspected harmful agent, the following endpoints can be considered:

- human health: ADI[2], TDI[3] and cancer risk levels are used to quantify this endpoint;
- ecological risk: is quantified by the use of NOEC[4] values from toxicity experiments;
- groundwater risk: this risk is related to the dispersion of pollution in groundwater. Criteria do vary among countries and so do protection levels. In some countries groundwater is protected as a resource that has to remain pure. Other countries will use risk based protection levels.

At a general level the framework for ecological risk assessment may be very similar to the framework for the assessment of human health risk. The target of the assessment which may be defined as “ecosystem health” is however more complex than human health, since it involves a large number of organisms and phenomena operating at various spatial and temporal scales. Ecological risk assessment should also make a distinction between two types of ecological risks: those occurring at the contaminated site itself, and the impact of the site on the surroundings, either by transport of pollution or for instance by the loss of an important habitat.

Data and analysis results from the previous steps will be integrated in order to determine the likelihood that humans will experience any of the various forms of toxicity associated with the fibrous materials, incorporated in rocks and sediments.

7.3 Methodology for hazard indentifiction

7.3.1 Hazard Identification

In section 2.2.2, a summary of some relevant epidemiologic studies related to asbestos exposure is given. From literature, it is clear that exposure to free asbestos fibres can give rise to the following diseases:

- Asbestosis (a scarring of the lungs which makes breathing difficult);
- Mesothelioma (a rare cancer of the lining of the chest or abdominal cavity);
- Bronchial carcinoma (lung cancer);

---

[2] ADI: Acceptable Daily Intake
[3] TDI: Total Daily Intake
[4] NOEC: No Observed Effect Concentration

The link between exposure to asbestos and other types of cancers is less clear. It is obvious that asbestos poses health risks only when fibres are present in the air that people breathe.

7.3.2 Exposure assessment

Several conditions exist under which man can be exposed to naturally occurring fibrous material present in soils that have been disturbed. The impact of exposure to asbestos depends on:

- the concentration of asbestos fibres in the air;
- the amount of time since the initial exposure, or how long the exposure lasted;
- how often you were exposed;
- the size of the asbestos fibres inhaled.

Techniques available for assessing environmental exposure are:

- biological monitoring;
- air monitoring;
- analysis of materials;
  - fibre content;
  - fibre release;
- computer-based modelling.

In the WHO air quality guidelines (2000), the following general concentration patterns are given for background levels of asbestos in the air:

- Rural areas (remote from asbestos emission sources): below 100 fibres /m^3;
- Urban areas: general levels may vary from below 100 to 1.000 fibres /m^3;

These results were obtained by comparison of various sets of data with restriction of quantifications to orders of magnitude.

Near various emission sources the following values have been measured as yearly averages:

- Downwind from an asbestos-cement plant at 300 m: 2,200 fibres/m^3; at 700 m: 800 fibres/m3; at 1,000 m: 600 fibres/m^3;
- At a street crossing with heavy traffic, 900 fibres/m^3;
- On an express-way, up to 3,300 fibres/m^3;
- Indoor air, in buildings without specific asbestos sources, concentrations are generally below 1,000 fibres/m^3;
- Indoor air, in buildings with friable asbestos, concentrations vary irregularly; usually less than 1,000 fibres/m^3 are found, but in some cases exposure reaches 10,000 fibres/m^3.

For this study, potential exposure will be estimated based on the asbestos content present in the geological formations and soils in the Troodos region. In order to estimate the probability of these fibres becoming airborne, computer-based modelling and GIS-analysis will be applied. During this exercise, the

The probability of exposure will thus be the result of an extensive GIS-analysis, based on the basic information shown in **Error! Reference source not found.22** will be taken into account.

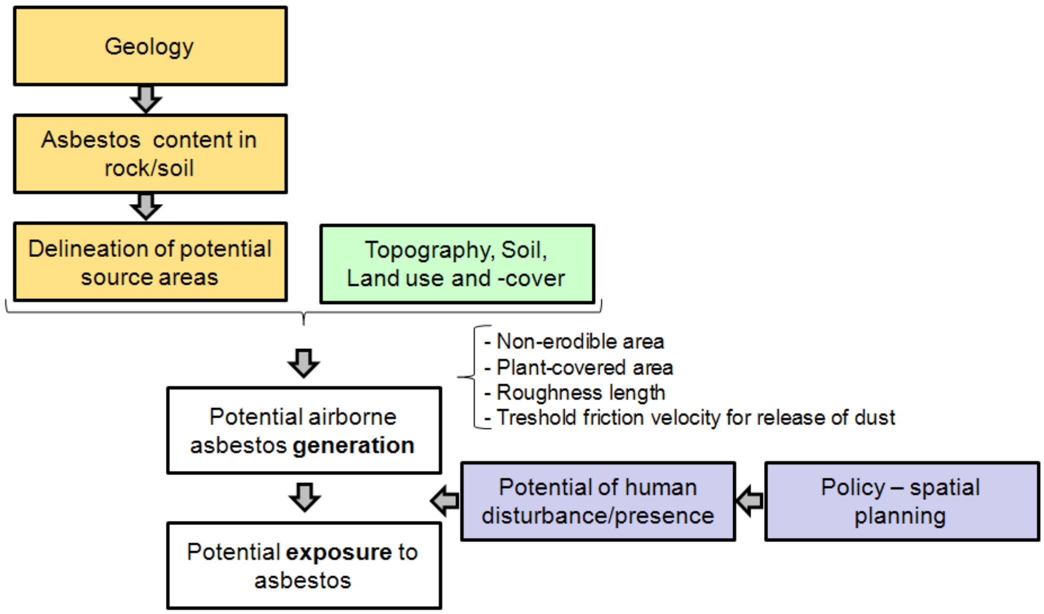

Figure 22: Factors taken into account for the risk assessment.

Each of these elements and the methodology for deriving the according GIS-layers will be discussed in the following sections.

7.3.2.1 Geology – asbestos content

The revised geological map shows the distribution of rock types. Based on the laboratory analyses that were performed, an average content of fibrous minerals can now be allocated to each formation. One should however bear in mind that the quantitative mineralogical analysis (by XRD) is a complicated procedure. The intensity (or height) and the sharpness of each peak in the XRD-pattern caused by the presence of a mineral in a sample is a function of many factors such as: the percentage of this mineral in the sample, the crystallinity, the orientation of the particles, the particle sizes, the mass coefficient etc. The crystallinity (the degree of order-disorder in the structures and/or the disorder in layers or mineral sheets) can cause problems with the interpretation. Quantitative mineralogical analysis results obtained from XRD should therefore be addressed with caution.

In this case, the conversion rules in **Table 55**Error! Reference source not found. were applied to obtain quantitative estimates for asbestos content in the samples (**always**

taking into consideration the specific characteristics of the mineral content in the sample[5]).

Table 5 : Quantification of asbestos concentrations in samples.

Estimated content - XRD (Chrysotile)	Concentration (interval) (%w)	Assumed concentration (%w)
Trace (+)	1-2	2
Minor (++)	2-10	7
Medium (+++ / ++++)	10-40	25
Major (+++++ or higher)	80-90	85

The average content (%w) in each formation is calculated as the average content of fibrous minerals measured in the collected samples for that particular formation. The resulting figures are shown in Error! Reference source not found.**6.**

Table 6: Average content (%w) of fibrous minerals (and standard deviation) for the geological formations of the study area.

Geological formation	Avg. conc. (%w)	St.dev.	Avg. conc. in rock (%w)	Avg. conc. in soil (%w)
Wehrlite	1.06	1.72	0.57	2.75
Serpentinite	12.08	10.8	16.87	4.9
Pyroxenite	0	0	0	0
Plagiogranite	0	0	0	0
Peridotite	1.29	2.43	0.75	4.5
Oliv. Gabbro	0	0	0	0
Isotr. Gabbro	0.05	0.32	0.17	0
Harzburgite	1.88	5	1.89	1.88
Dunite	0.94	1.78	1.25	0
Diabase	0	0	0	0

These averages are in the first place used to assess relative differences in fibrous mineral content between the geological formations in the area. In fact, in order to obtain an idea of the total fibrous mineral content of the rocks and soils in each geological unit, a correction factor should be applied for the extrapolation from the micro-scale of the laboratory sample to the macro-scale of the landscape in the study area. This correction factor can be estimated from the comparison between the calculated averages for the Serpentinite samples from the Amiantos Mine area, and the average grade of asbestos in the mined rock, as known from reports on the former mining activities:

$$F = C_{\text{avg, Serpentinite lab}}/C_{\text{avg, mined material}}$$

Using this correction factor F, the average content of fibrous minerals is then calculated as:

$$C_{\text{real, formation}} = C_{\text{avg, samples lab}}/F.$$

[5] Example: if a sample appears to contain only one mineral, then Major (+++++) can correspond to 80 - 90%. If we have two constituents in the sample, e.g. one MJ and one MD, obviously the MJ cannot be 80 or 90%, because of the existence of the MD constituent. Moreover, there is also a possible occurrence of amorphous minerals, not reflected in the XRD-pattern, and lowering the real content of cristaline minerals.

Where $C_{real,\ formation}$ = the estimated average concentration of fibrous minerals in a geological formation (%);$C_{avg,\ samples\ lab}$ = the calculated average concentration of fibrous minerals in the samples collected in a particular formation (%); and, F = the correction factor for upscaling of laboratory results.

Records that are available from the Amiandos asbestos mine show that the asbestos mine developed within an area of asbestos mineralization (highly serpentinized rock) and exploited a deposit with an **average grade of 0.8-1.0%w** (Howard Humprey & Partners, 1981). In the samples collected during this project in the Serpentinite core of the Troodos Ophiolite, the measured asbestos concentration in the laboratory was approximately 25%w. **This indicates that a correction factor in the order of magnitude of 25 should be applied in order to link the laboratory results to available concentrations on the landscape scale.**

The fibrous mineral concentrations were converted into a risk factor, representing the chance of finding fibrous material in an area. The risk factors, used per geological formation are shown in **Table** 9**7**. The map showing the distribution of these risk factors is added in **Annex 9.**

Table 7: Risk factors for the occurrence of fibrous minerals (higher values represent higher occurrence).

Geological formation	Risk factor
Wehrlite	1
Serpentinite	5
Pyroxenite	0
Plagiogranite	0
Peridotite	1
Oliv. Gabbro	0
Isotr. Gabbro	1
Harzburgite	1
Dunite	1
Diabase	0

7.3.2.2 *Erodibility of the surface (soil)*

Erodibility of the surface is an important factor for assessing the potential for loosening fibrous minerals from their matrix.

Weathering conditions of the outcrops on the sampling locations were estimated qualitatively during the field surveys. Classification categories were: 0 (not weathered, in situ bedrock), 1 (moderately weathered, loose rock), 2 (loose material, soil). Yet, in order to obtain information about the erodibility of the soil on the landscape scale, a map was produced based on the soil map for the area.

Erodibility is indeed a soil's inherent tendency to be transported by water or wind. One measure of erodibility (the resistance of a soil to sheet and rill erosion) is the K-factor (used in the Universal Soil Loss Equation - USLE), which is a function of:

- Texture of the soil (specifically, soil fraction with grain size less than 0.125 mm);
- Amount of organic matter in the soil; and
- Permeability (how well water drains).

Fine grained soils are more erodible than sands. Erodibility depends on the structural stability of the soil, and its capacity to transmit water downward. Structural stability is a function of soil particle size distribution (texture), mineralogy and organic matter content. Soils with high organic matter content are less erodible than those with low organic matter content.

Only the topsoil is subject to erosion, except where gullying is extreme, so a map of estimated erodibility has been produced only for the topsoil.

The K factor has been estimated from field plot experiments. Typical values are shown in **Table** 10**8**.

Table 8: Erodibility and K-factors.

Erodibility	K-factor
Very low	<0.02
Low	0.04
Moderate	0.06
High	0.08
Very high	>0.08

Comparing erodibility with the soil map shows that heavy clay soils are highly erodible as are structurally unstable, chemically dispersible sodic soils. Calcisols with sandy topsoil are slightly less erodible. Rocky soils (Leptosols) and weakly developed soils (Cambisols) are least erodible.

In the study area, 4 soil complexes are found. Their characteristics are summarized in Error! Reference source not found.**9**. Based on these characteristics, a risk correction factor for erodibility can now be allocated to each of these soil complexes.

Table 9: Soils in the study area, and their erodibility.

Soil type (WRB-classification)	Characteristics	Risk Correction factor
Eutric Cambisols and Eutric Anthropic Regosols	Weakly to moderately developed soils. Soils with very limited soil development, influenced by anthropogenic disturbance.	1.0
Calcaric rendzic Leptosols and Calcaric leptic Cambisols	Very shallow soils over hard calcareous rock or in unconsolidated very gravelly material, and having a mollic horizon (10-25 cm thick). Weakly to moderately developed stony and calcareous soils, with hard rock at a depth between 25 and 100 cm.	0.75
Eutric lithic Leptosols and Eutric skeletic Regosols	Very shallow soils over hard rock or in unconsolidated very gravelly material. Soils with very limited soil development, and 40-90% gravel or coarse material.	0.5
Skeletic calcaric Regosols and	Soils with very limited soil development, calcareous at least between 20 and 50 cm from the surface, and 40-90% gravel or	0.2

Calcaric lithic Leptosols	coarse material. Very shallow soils over hard calcareous rock or in unconsolidated very gravelly material.	

7.3.2.3 *Soil cover*

Similar to the erodibility of the soil material, the percentage of covered soil (plants, trees, buildings, streets) in the target zones is important.

The percentage of plant covered area can be estimated from CORINE land use data (**See ANNEX 9**), satellite images, and expert knowledge, gained through the fieldwork. Any thick coverage that can reduce wind and rain erosion is considered as plant cover. Grass, shrubs and forest are not treated separately.

The land use categories occurring in the study area, according to the CORINE Land Cover 2000 (CLC2000) GIS-layer for Cyprus, are listed in **Error! Reference source not found.11.** For each of these categories, the percentage of land cover was estimated, based on aerial photographs. An overlay was made from these photographs and the CORINE-map, for 8 contrasting representative sub-regions, each with an area of approximately 1.3 km². In these sub-regions, the percentage of covered land areas (trees, dense shrubs, sealed surfaces) was estimated for each of the land use categories, by counting (50x50m) grid-cells occupied by covered and non-covered soil, on a 1:5,000 scale map. Sub-regions that were addressed are listed in

Table 10**10**, and the methodology is further illustrated in **ANNEX 9.**

Table 10: Land cover assessment in the study area, based on CORINE and aerial photograph interpretation.

Sub-region	**Land use**	**CORINE**	**Covered cells counted**	**Non-covered cells counted**	**% soil cover**
Bare rock area	Bare rock	332	19	115	14
	Coniferous forest	312	74	48	61
Pano Platers	Sport and Leisure	142	52	20	72
	Sparsely vegetated areas	333	20	62	24
	Coniferous forest	312	53	18	75
	Coniferous forest	312	40	14	74
Kato Platres	Sclerophylous vegetation	323	29	89	25
	Discontinuous urban fabric	112	10	5	67
	Coniferous forest	312	44	7	86
	Complex cultivation pattern	242	42	64	40
Mandria	Principally agric, sign. Nature	243	17	78	18
	Transitionale woodland	324	16	57	22
	Broad-leaved forest	311	7	3	70
	Complex with scattered	242	52	56	48

	houses				
	Non-irrigated arable land	211	6	16	27
	Discontinuous urban fabric	112	6	5	55
Zoopigi	Fruit trees and berry plantations	222	60	57	51
	Complex with scattered houses	242	37	52	42
	Vineyards	221	14	14	50
Saittas	Discontinuous urban fabric	112	71	21	77
	Coniferous forest	312	28	15	65
	Complex with scattered houses	242	36	32	53
Pano Amiandos	Mineral extraction site	131	13	101	11
	Transitional woodland/shrub	324	53	51	51
Sinaoros	Sclerophereous vegetation	323	26	29	47
	Permanently irrigated	212	76	24	76
	Discontinuous urban fabric	112	21	16	57

Soil cover percentages derived from this exercise are listed in **Error! Reference source not found.**.

Table 11: Land use categories in the study area.

Code	LUSE type	Main characteristics	Soil cover (%)
112	Discontinuous urban fabric	Areas mainly occupied by dwellings and buidings used by administrative/public utilities or collevtivities, including their connected areas. 30 to 80% of the area is impermeable urban fabric	60
131	Mineral extraction sites	Artificial areas mainly occupied by extractive activities. This category excludes associated land of mines where barren materials are dumped, scree covered areas, …	10
142	Sport and leisure facilities	Areas volunarily created for recreational use. Includes areas of sport compounds, camping sites, ski resorts (except ski pistes), forest parks in the periphery of settlements, …	70
211	Non-irrigated arable land	Includes cereals, legumes, fodder crops, root crops, fallow land, vegetables, whether open field, under plastic or glass	30
212	Permanently irrigated land	This category excludes drainage networks to rehabilitate wet soils, crops under greenhouses, spray and rotary sprinkler lines, rice fields	80
221	Vineyards	At least 50% of the area occupied by vineyards	50
222	Fruit trees and Berry plantations	Parcels with fruit trees or shrubs: single or mixed fruit species, fruit trees associated with permanently grassed surfaces,...	50
241	Annual crops associated with permanent crops	Non-permanent crops (arable land or pasture) associated with permanent crops on the same parcel. The occupation rate of non-permanent crops is more than 50%.	50
242	Complex cultivation pattern with scattered houses	Juxtaposition of small parcels of diverse annual crops, pasture and/or permanent crops. Includes mixed parcels of pemanent crops (fruit trees, …), complex cultivation pattern areas with scattered houses within a patchwork structure when built-up parcels cover less than 30% of the patchwork area, parcels of grassland,…	50
243	Land principally occupied by agriculture, with significant areas areas of natural vegetation	Agricultural land use is more than 25% but less than 75% and semi-natural areas occupy more than 25% but less than 75%.	20
311	Broad-leaved forest	Forests have a height of at least 5 m, and a canopy closure of at least 30%. Broad-leaved	70

Code	LUSE type	Main characteristics	Soil cover (%)
		forest includes areas with a crown cover of more than 30% or a 500 subjects/ha density for plantation structures. Broad-leaved trees represent more than 75% of the planting pattern.	
312	Coniferous forest	Vegetation formation composed mainly of trees, including shrub and bush understoreys, where coniferous species predominate. Coniferous trees represent more than 75% of the formation.	70
323	Sclerophylous vegetation	Bushy sclerophyllous vegetation: maquis and garrigue.	40
324	Transitional woodland/shrub	Bushy or herbaceous vegetation with scattered trees. Can represent either woodland degradation or forest regeneration / recolonisation. Includes natural grassland areas with small forests (<25ha) and/or with trees intermixed which cover more than 30% of the surface (scattered trees or small plots of forests), young plantations, bare rocks with scattered trees that cover more than 10% of the surface. Canopy closure is <50%.	40
332	Bare rocks	Open spaces with little or no vegetation. Scree, cliffs, rock outcrops, including active erosion, rocks and reef flats above the high-water mark. At least 75% of the land surface is covered by unvegetated rocks. Excludes bare rocks where scattered trees cover more than 10% of the surface.	10
333	Sparsely vegetated areas	Steppes, badlands, scattered high-altitude vegetation. Includes sparsely vegetated and unstable areas of stones, boulders or rubble on steep slopes, where the vegetation layer covers between 15 and 50% of the surface.	20
512	Water bodies	Water bodies	100

The soil cover map was re-classed according to the decision rules in **Table 12**, in order to obtain a “soil cover risk correction factor” map, showing the following risk factors for release of fibrous material due to the lack of soil cover. (See ANNEX 9).

Table 12: Risk factors due to (lack of) land cover.

Land cover	Risk factor
<20%	0.9
20-50%	0.7
50-75%	0.5
>75%	0.3

7.3.2.4 Roughness length

From the CORINE maps, also the so-called “roughness length (Z0)” is derived in each polygon. The following values were used, from literature **(Table 13)**. The resulting map is shown in **ANNEX 9.**

Table 13: Rougness length for CORINE land use categories.

Code	LUSE type	Roughness (m)
111	Continuous urban fabric	1.2
311; 312; 313	Broad-leaved forest; coniferous forest; mixed forest	0.75
141;324;334	Green urban areas; Transitional woodland/shrub; Burnt areas	0.6
112; 133; 121; 142; 123	Discontinuos urban fabric; Construction sites; Industrial or commercial units; Sport and leisure facilities; Port areas	0.5
242;243;244	Agro-forestry areas; Complex cultivation patterns; Land principally occupied by agriculture, with significant areas of natural vegetation	0.1 - 0.5
241;221; 222;223	Annual crops associated with permanent crops; Fruit trees and berry plantations; Vineyard; Olive groves	0.1 - 0.3
122	Road and rail networks and associated land	0.05 - 0.1
211;212;213; 411,421	Non-irrigated arable land; Permanently irrigated land; Rice fields; Salt marshes	0.005
321;322; 323;231	Sclerophylous vegetation; Moors and heathland; Natural grassland; Pastures	0.03 - 0.1
131;132;124; 332;333	Dump sites; Mineral extraction sites; Airports; Bare rock; Sparsely vegetated areas	0.0005
335	Glaciers and perpetual snow	0.001
422;412;423	Peatbogs; Salines; Intertidal flats	0.0005
331	Beaches, dunes, and sand plains	0.0003
511;512;523; 522;521	Water courses; Water bodies; Coastal lagoons; Estuaries; Sea and ocean	0

Source: Julieta Silva, Carla Ribeiro, Ricardo Guedes (2007). Roughness length classification of CORINE land cover classes. EWEC 2007

The “roughness map” was re-classified in order to obtain a risk correction factor for roughness. The following scheme was applied **(**Error! Reference source not found.**4):**

Table 14: Rougness length risk factor.

Roughness length	Risk correction factor
0.005	1.0
0.03	0.9
0.1	0.5
0.3	0.4
0.5	0.3
0.6	0.2
0.75	0.1

7.3.2.5 Topography

From the topographical map, a digital terrain model with a 50 m resolution was created for the study area, through the (spline) interpolation of the topographical isolines. From this model, datalayers showing slope inclination (in %) and aspect (in ° relative to the north) were produced. These raster layers all have a 50 m resolution. A map of the digital terrain model, the slope map and the aspect map are included in **ANNEX 9**.

For small study areas, the digital terrain model can be used in order to calculate a risk factor based on the threshold friction velocity for dust raising. For this study, however, this risk factor was set to an average of 1 for the whole study area, because of the variability of the complex mountainous topography. This complexity and the large size of the project area tend to cancel out increased erosion on wind prone areas and reduced erosion from wind-shade areas.

7.3.2.6 Potential anthropogenic disturbances

The potential for anthropogenic disturbances of the soil or bedrock depends on the distance to human settlements or infrastructure, and local development policies.

7.3.3 Dose-response relations

7.3.3.1 Effects of lifetime or long-term exposure as reported in literature

Numerous past studies among populations exposed to asbestos at work have provided estimations concerning the magnitude of risk under such conditions. The major problem regarding environmental exposure to asbestos, is that very few studies are available to assess directly the magnitude of risk caused by such exposures. And for exposures of low level unrealistically large studies would be needed to assess directly the risk. Therefore, regulatory and other health authorities have been obliged to base their conclusions on extrapolations of dose-exposure relationships from relatively high exposures, some observations addressing the low exposure risks, and animal studies. The authorities have been obliged to objectively assess the somewhat discrepant findings of the vast number of scientific studies and the sometimes conflicting conclusions presented by different scientist.

For lung cancer and mesothelioma, EPA (1986) calculated by extrapolation that lifetime exposure to asbestos air concentrations of 0.0001 fibre/ml could result in up to 2-4 cancer deaths (lung cancer or mesothelioma) per 100,000 people. This air concentration is within reported ranges of ambient air levels (0.00001 to 0.0001 fibre/ml). The EPA analysis has been extensively discussed and reviewed in the scientific literature. EPA continuously reviews their cancer risk estimated for asbestos.

The Integrated Risk Information System (IRIS), prepared and maintained by the U.S. EPA, is an electronic database containing information on human health effects that may result from exposure to various chemicals in the environment. Health assessment information concerning asbestos is also included in IRIS. The sheet does include the carcinogenicity assessment for lifetime exposure.

The quantitative estimate of carcinogenic risk from inhalation exposure is presented in two ways. The unit risk is the quantitative estimate in terms of risk per µg/m3 air breathed. The second form in which risk is presented is an air concentration providing cancer risks of 1 in 10,000, 1 in 100,000 or 1 in 1,000,000 (Error! Reference source not found.**5**).

The inhalation Unit Risk is 2.3 E-1 per (fibre/ml). This means that 2,3 excess cancer cases are expected to develop per 10 people if they are continuously exposed for a lifetime to 1 fibre per ml air breathed.

Risk levels for specific air concentrations are specified in Error! Reference source not found.**5**. They form a good basis for risk assessment, although they do not differentiate between fibre type, fibre size or type of exposure. The only parameter is the airborne concentration of asbestos fibres.

Table 15: The lifetime risk of cancer (excess case of cancer per number of exposed persons) associated with life-long exposure to given airborne concentrations of asbestos (EPA).

Risk Level	Air concentration
E-4 (1 in 10,000)	4 E-4 fibre/ml
E-5 (1 in 100,000)	4 E-5 fibre/ml
E-6 (1 in 1,000,000)	4 E-6 fibre/ml

Estimated health risks for exposures shorter than a lifetime are listed in Error! Reference source not found.**6** (Health Effects Institute, 1991).

Table 16: Estimated risks associated to exposures shorter than the life-time.

Conditions	**Risk level (*)**
Exposure in a school containing asbestos-containing material. From age 5 to 18 years, 180 days/year, 5 hours/day.	
0.0005 f/cm^3	6

0.005 f/cm^3	60
Exposure in a public building containing asbestos-containing material. Age 25 to 45 years, 240 days/year, 8 hours/day.	
0.0002 f/cm^3	4
0.002 f/cm^3	40
Occupational exposure from age 25 to 45	
0.1 f/cm^3	2000
10 f/cm^3	200,000

(*) Number of Premature deaths, per million exposed persons.

In the Air Quality Guidelines from the WHO (Second Edition, 2000, and Global update, 2005) guidelines are given aiming to provide a basis for protecting public health from adverse effects of air pollutants and to eliminate or reduce exposure to those pollutants that are known or likely to be hazardous to human health or wellbeing. For some substances these guidelines encompass recommendations of a more general nature that will help to reduce human exposure to harmful levels of air pollutants. For some pollutants no guideline values are recommended, but risk estimates are indicated instead.

Indicative figures for risk and exposure assist risk managers in deciding either to prohibit a substance or to regulate it at levels that result in an acceptable degree of risk. Air quality guidelines are therefore given in terms of incremental unit risks with respect to those carcinogens that are considered to be genotoxic. The WHO provides concentrations of carcinogenic air pollutants associated with an excess lifetime cancer risk of 1 per 10.000, 1 per 100.000 and 1 per 1.000.000. For asbestos, the risk estimates are presented in **Error! Reference source not found.**. According to these guidelines, asbestos is a proven human carcinogen. No safe level can be proposed for asbestos because a threshold is not known to exist. Exposure therefore should be kept as low as possible.

Table 17: Risk estimates for asbestos, according to WHO.

Concentration	Range of lifetime risk estimates	
500 fibres */m3 (0,0005 fibres/ml)	10-6 - 10-5	Lung cancer in a population where 30 % are smokers
	10-5 - 10-4	Mesothelioma**

* fibres measured by optical methods

*** based on the formula of Peto, used for approximation of excess incidence of mesothelioma.*

These risk estimates were based on estimates of mesothelioma and lung cancer risk resulting from lifetime exposure to asbestos from various publications. With a lifetime exposure to as 1.000 fibres/ m^3 in a population of whom 30% are smokers, the excess risk due to lung cancer would be in the order of 10^{-6} -10^{-5}. For the same lifetime exposure, the mesothelioma risk for the general population would be in the range of 10^{-5} - 10^{-4}.

7.3.3.2 *Threshold values specified in regulation*

For occupational exposure, several standards and guidelines have been set up by different national and international authorities and institutes. These standards define the maximum doses to which a worker may be exposed to. When this action level is exceeded, special precaution measures need to be taken.

The EU directive (2009/148/EC)[6] regulates that "Employers shall ensure that no worker is exposed to an airborne concentration of asbestos in excess of 0,1 fibres per cm^3 as an 8-hour time-weighted average (TWA). This directive adds that for the purpose of measuring asbestos in the air, only fibres with a length of more than 5 micrometres, a breadth of less than 3 micrometres and a length/breadth ratio greater than 3:1 shall be taken into consideration.

Article 7 suggests that "fibre counting shall be carried out wherever possible by PCM (phase-contrast microscope) in accordance with the 1997 WHO (World Health Organisation) recommended method [7] or any other method giving equivalent results.

The EU-directive further states that "although current scientific knowledge is not such that a level can be established below which risks to health cease to exist, a reduction in exposure to asbestos will nonetheless reduce the risk of developing asbestos-related disease."

For the purposes of this Directive, 'asbestos' means the following fibrous silicates:
(a) asbestos actinolite, CAS No 77536-66-4;
(b) asbestos grunerite (amosite), CAS No 12172-73-5;
(c) asbestos anthophyllite, CAS No 77536-67-5;
(d) chrysotile, CAS No 12001-29-5;
(e) crocidolite, CAS No 12001-28-4;
(f) asbestos tremolite, CAS No 77536-68-6.

Similarly, according to OSHA[8], employee exposure to asbestos must not exceed 0,1 fibre per cubic centimetre of air (0,1 fibres/cc), averaged over an 8-hour work shift. Short-term exposure must also be limited to not more than 1 f/cc, averaged over 30 minutes. An action level of 0,1 fibres/cc is the level US EPA has established in which employers must initiate such activities as air monitoring, employee training, and medical surveillance.

Historically, exposure evaluation methods utilized optical microscopy and a variety of dust-sampling techniques. From the 1960's onwards, the techniques for dust sampling changed with the advances in membrane filter technology and analytical techniques switched from a count of all particles to a count of only those particles meeting a given "fibre" definition. In the last 2 decades, there has been a shift in focus from manufacturing and production environments to non-occupational exposures in ambient air and commercial buildings and schools. This shift has also resulted in the diminished use of optical microscopy and the development of electron microscopic techniques for air sample analysis.

---

[6] DIRECTIVE 2009/148/EC OF THE EUROPEAN PARLIAMENT AND OF THE COUNCIL of 30 November 2009 on the protection of workers from the risks related to exposure to asbestos at work
[7] Determination of airborne fibre concentrations. A recommended method, by phase-contrast optical microscopy (membrane filter method), WHO, Geneva 1997 (ISBN 92 4 154496 1).
[8] OSHA: US Department of Labor - Occupational Safety and Health Administration.

Electronmicroscopy is the most reliable method for identifying asbestos fibres. The resolution is sufficient to measure also small fibres. Disadvantage for these method is, beside the price, the lack of exposure data based on this method in epidemiological studies.

7.4 Risk analysis results and discussion

7.4.1 Risk map for the study area

The risk assessment results in a ranking system which allows to estimate the relative threat associated with actual or potential release of fibrous substances to the environment and allows to set priorities for further evaluation and eventual remedial action. The analysis concentrates on airborn asbestos, which constitutes the main pathway to human exposure.

Estimating asbestos related risk (ARR) can be accomplished on a receptor-specific or a susceptible area basis. In the present case, ARR was calculated for the wider area of Troodos thus a specific receptor approach was not possible. Instead, a stepwise approach is adopted via which the areas where fibrous minerals are found in soils are mapped and considered for further assessment. Subsequently the risks for dust raising are assessed and a potential airborne asbestos generation risk map is produced. Lastly areas prone to airborn asbestos occurrence are mapped by considering atmospheric dispersion influences. Human exposure risks are thus qualitatively examined via overlaying fibrous mineral dispersion prone areas with inhabited areas and other sites that exhibit human activity.

As discussed above, the following maps have been prepared:

1. Rock type and associated fibrous mineral content;
2. Soil erodibility map depicted in 4 categories;
3. Corine Land Use (reclassified to obtain soil cover risk classes and roughness length risk classes);
4. Soil cover depicted in 4 categories;
5. Roughness length (Z_0);
6. Threshold friction velocity.

Risk factors associated to each of these layers have been multiplied in order to obtain the risk map for the study area. The result is shown in **ANNEX 10**.

7.4.2 Interpretation of results and discussion on the risk map

7.4.2.1 Mapping of rock type and associated fibrous mineral content

Areas containing fibrous minerals were initially mapped through the examination of existing maps, examination of satellite images and extensive fieldwork which was supported by petrological analysis of selected samples. The geology of the area was thus delineated and described. Subsequently a sampling programme was designed and implemented which aimed at assessing the presence of fibrous minerals in each geological formation and in producing a semi-quantitative estimation of the concentration of fibrous minerals in the examined areas.

The delineation of geology is presented in **Annex 9.**

Of the above formations only Serpentine has been found to contain fibrous minerals at a concentration that can produce exposure risk. In this discussion we will thus further focus on the serpentine areas.

7.4.2.2 Calculation of the basic dust emission factor

The dust emission factor can be estimated for the serpentine areas. For the purposes of the analysis these areas are subdivided in two categories, namely the asbestos mine area and areas outside the mine.

The mine area is characterized by disturbed materials and mine waste, which are void of vegetation, mixed with rehabilitated areas with foreign soils and vegetation that approximates a surface coverage of 15%. The disturbed surfaces have a high propensity to form an upper crust. Empirically it is assumed that this crust has a depth of 2 mm.

The remaining areas are characterized by undisturbed soils with a well established vegetation cover, which is estimated to occupy 40% of the area.

For the Amiantos mine, a size distribution mode of 1 mm is assumed. For the remaining areas a size distribution mode of 2 mm is assumed. For the areas outside the mine we use this mode to determine threshold friction velocity by applying the following graph **(Figure 23).**

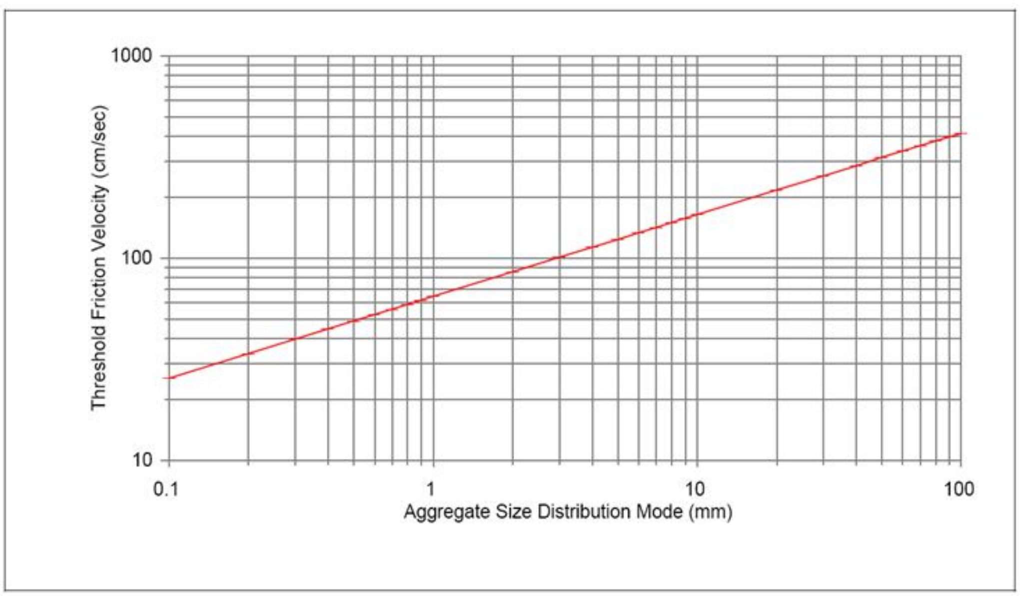

Figure 23: Graph of threshold friction velocity to aggregate size distribution mode

For the Amiantos mine the threshold friction velocity calculation is based on the recommendation of Gillette et al. (1980) who suggested that for crusty disturbed soils the threshold friction velocity can be estimated from the following equation:

$U^*t = 48 + 59$ (thickness), cm/s

in which U*t is the uncorrected threshold friction velocity and "thickness" is the thickness of the surface crust in cm. It is noted that utilizing the above graph **(Figure 23)** would give a threshold friction velocity value of 65 cm s^{-1}, while the selected method provides for a more conservative estimate.

The resulting Threshold Friction Velocities are as follows:

Table 18: Uncorrected Friction Velocity

Area	**Uncorrected friction velocity (U*t) (m s^{-1})**
Type 1 (Amiantos Mine)	0.486
Type 2	0.85

Corrected Friction (Ut) is calculated by correcting the threshold velocity to a height of 10m from U*. Correction is based on roughness length Zo, as follows **(Table 19).**

Table 19: Corrected friction velocity

Area	**Zo (cm)**	**A**	**U*t (m s^{-1})**	**Ut_{10} (m s^{-1})**
Amiantos Mine	0.05	0.075	0.486	6.4
Forested Serpentine Area	1	0.086	0.85	9.9

Z_o is determined from the literature as per the table presented below (**Table 20.)**

Table 20: Terrain classification in terms of effective surface roughness length, Z0.

Terrain description	**Zo (m)**
Open sea, fetch at least 5 km	0.0002
Open flat terrain; grass, few isolated obstacles	0.03
Low crops, occasional large obstacles	0.10
High crops, scattered obstacles	0.25
Parkland, bushes, numerous obstacles	0.50
Regular large obstacle coverage (suburb, forest)	0.50 – 1.0

Thus, in order for a dust event to occur, wind values at the 10 m level need to exceed 6.4 m s^{-1} in the Amiantos mine and 9.9 m s^{-1} in the case of the surrounding serpentine areas.

The emission per disturbance from a "limited reservoir" open area is described by the following equation (Eq. 6-3, EPA Manual, Cowherd et al.,1988):

$$E = k \sum_{i=1}^{N} P_i$$

where E is the emission rate (g/m2/year) per event; k is a particle size multiplier (k = 1 for PM_{30} / TPM and k =.4 for PM10).

Pi is the erosion potential for the period between disturbances (g/m2), in which
$P = 58(U^* - U^*t)^2) + 25(U^* - U^*t)$, where U* and U*t are the friction velocity and the threshold friction velocity (units: m/s); N is the number of disturbances per year.

In order to calculate the risk of dust creation at the study areas, the integral of emissions in all potential dust events should be calculated. In accordance with wind data from the meteorological service, the characteristic wind for the area can be taken as 8 m s^{-1}. For the purposes of the study it is assumed that this characteristic wind correlates with the average dust emission rate and it that it occurs for 5% of the time. For the purpose of estimating emissions for the areas outside the Amiantos mine it is estimated that a wind speed of 14 m s^{-1} or faster occurs with a frequency of 2%.

It is noted that these are conservative estimates of frequency based on wind statistics at Saittas.

The above emission rate variables are applied to determine the potential emission per m^2 for the representative bare areas. These potential values, however, need to be adjusted in order to account for the presence of areas not prone to erosion such as areas covered by vegetation or by non-erodable objects or structures. Thus, the final emission factors for the two areas are calculated as follows (**Table 21)**:

Table 21: Dust mission rates.

Area	Plant cover	% non-erodible elements	Ut	Event emission g/m^2	Annual Emission g/m2	Annual average hourly emission ($g/m^2/h$)
Amiantos Mine	15	30	6.4	2.1	900	0.1
Forested Serpentine Area	40	40	9.9	2.3	400	0.05

An explanation of the estimation of correction factors is provided below.

7.4.2.2.1 Percentage of non-erodable area

This parameter can have a significant impact on dust raising. Non erodable material is in principle defined as any material with a diameter larger than 1 cm. The values were estimated semi-quantitatively via satellite image examination, existing bibliography and field visits. As a result the assessment relied to a large extent on expert judgment.

For the purposes of this discussion it is assumed that the percentage non-erodable area is in the 20-50 % range for the Asbestos Mine and approximated as 30%. It is assumed to be in the 20-50% range for the remaining areas and is approximated as 40%. These values were estimated from on-site visual inspections and expert judgment.

7.4.2.2.2 Percentage of plant covered area

This parameter affects dust raising both by the area from where dust may be raised as well as reducing wind speed near the ground. The values were estimated semi-quantitatively via satellite image examination and the Corine Level II Land Use map. Results are depicted in 4 categories of erodable area: <20%, 20%-50%, >50%-75%, >75%. Level II Corine Land Use has been prepared by the Department of Environment. The latest version of 2006 has been used.

Here we assumed that the percentage of area not covered by vegetation is 75% for the Amiantos mine and 60% for the remaining areas. These values were estimated from coarse analysis of satellite images and expert judgment.

7.4.2.2.3 Asbestos related risk

At present there are no correlations between dust and asbestos fibre concentrations. A fully quantitative assessment of airborne asbestos can therefore not be made. Utilizing data from this study and the “Risk Assessment due to the presence of the Asbestos mine”, however, some quantitative initial assessments are undertaken which provide a first measure of risks associated with the presence of fibrous minerals.

7.4.2.2.4 Estimation of fiber concentrations in the air from natural sources

In order to calculate dust concentrations, screen level modeling has been applied. It was assumed that the Mine area had a size of 1X1 km and the remaining Sepemtine an area of 5X5 km.

In order to calculate the ambient asbestos concentration it is assumed that the concentration of fibers in soils is maintained in dust raised in the air. This is of course a rough approximation but a more accurate method cannot be applied considering the current availability of data. From existing data it is deduced that the soil asbestos fiber content in the general serpentine area ranges around 50-150 fibers per litter where an average of 90 fibers per liter (~0.25 fibers / μg.) is assumed. Utilising the In the mine area, fiber concentrations can be as high as 1000 fibers /liter (~2.5 fibers / μg.)

Utilising these values, dust and fiber concentrations from the two serpentine areas are as follows:

Table 22: Estimated concentrations.

Area	Dust Annual Average (μg m^{-3})	Dust event Average (μg m^{-3})[1]	Fibers Annual Average (fiber m^{-3})	Event based Fibers (fibers m^{-3})
Amiantos Mine	120	1100	300	2750
Forested Serpentine Area	45	125	113	313

The above estimates **(Table 22)** were based on a screening level application of the SCREEN dispersion model where the following assumptions were made.

Area	Wind speed (ms^{-1})	Cross sectional area (km)
Amiantos Mine	8	1X1
Other Serpentine Area	14	3X3

7.4.2.2.5 Estimation of fiber concentrations from human induced dust raising

PM10 concentrations can be calculated from the USEPA guide AP42. A screening level calculation results in PM10 concentrations in the order of 1100 μg m^{-2}. In accordance with the *«Technical Background Document on Control of Fugitive Dust at Cement Manufacturing facilities, EPA, March 20, 1998»*, the PM10 value can be correlated to a PM_{30} value through the k factor which in this case is equal to 2. Thus ground works can be assumed to produce dust concentrations in excess of 2200 μg/m^3. This may be an easier parameter to correlate with fiber counts as it approaches TPM which is at present collected by the GSD.

7.4.2.2.6 Accuracy of the resulting concentrations

The present study is based on numerous assumptions regarding dust raising, ration of the number of asbestos fibers to dust weight and dispersion parameters. These factors therefore limit the accuracy of the results. Considering both the data gaps and the range of air born concentrations the following range of concentrations are considered to be a more appropriate interpretation of expected fiber concentrations in the study area.

Table 23: Ranges of fibre concentrations in the air.

Area	Concentration (Fibres m^{-3})
Amiantos Mine	100-500 (annual average); 2,000 - 10,000 per event
Remaining Serpentine Area	Up to 200 (annual average); Up to 2,500 per event

Utilising the criteria of 1000 fibers per m^3 we can conclude that the asbestos mine constitutes a moderate risk from naturally occurring asbestos while the remaining serpentine areas constitute a marginal risk.

7.4.2.2.7 Asbestos related risk from ground works

It is noted that the above analysis pertains only to dust raising resulting solely by natural erosion. Events concerning construction or other intensive ground works can result in significantly high dust / fiber concentrations in the air and thus can potential present a significantly higher risk.

By applying the EPA AP42 guideline for dust production from ground works we estimate that within the mine, intensive mining can in principle produce dust concentrations in the range of 1,100 µg/m3 (PM10) for medium intensity works such as the works undertaken within the Amiantos mine. Assuming the ratio of 20 fibers per µg we can then deduce that during ground works, air born asbestos concentrations can exceed 22,000 fibres cm^{-3}.

7.4.2.3 <u>Risk map for the Troodos area: accuracy and use</u>

As discussed earlier, the following layers are incorporated in the risk map

1. Rock type and associated fibrous mineral content;
2. Soil erodibility, depicted in 4 categories;
3. Corine Land Use (reclassified to obtain soil cover risk classes and roughness length risk classes);
4. Soil cover depicted in 4 categories;
5. Roughness length (Z0);
6. Threshold friction velocity factor.

The fibrous mineral content map constitutes the main tool for identifying areas of risk. For the calculatios it is assumed that the area of each feological formation is homogenious. Also ia is noted that for areas outside the studied geological formations and for a more localized distribution of concentrations, full scale dispersion models are needed.

Asbestos concentrations are indicatively calculated in the previous sections. At this stage it may be inferred that the calculated concentrations occur in the whole of each geological formation in the study area. In the absence of a dispersion model however, expected airborne concentrations resulting from wind dispersion are not mapped.

7.4.2.3.1 Comparison to earlier studies

Ambient asbestos concentrations in the air have been monitored earlier at several locations. Levels of asbestos detected in these samples typically ranged from 10-1000 within the mine, 0-500 in the remaining serpentine areas and 0-100 in areas within 5 km around the serpentine area.

The above results are comparable with the results produced by the risk analysis. It is noted, however that the comparability of the results is in part due to the fact that several assumptions made in the analysis were based on the results of the prior measurements. The quantitative assessment is based on numerous assumptions that should be verified by additional research.

7.4.2.3.2 Accuracy

The accuracy of a geologic (rock type) boundary on a geologic map is dependent upon a number of factors. Some of these factors are directly related to geology, e.g.:

- The amount of geologic boundary, or contact, exposed for observation;
- The extent of rock outcrops in the area and the distances between them;
- The regularity and consistency in the occurrence of geologic units within an area;
- Whether the geologic unit is sufficiently consistent in appearance to be properly identified throughout the map area;
- Whether the unit is homogeneous or is intimately associated with occurrences of other rock types that cannot be readily separated at the scale of mapping;
- Whether an occurrence of the geologic unit is sufficient in size to show at the scale of mapping.

Observation of differences in the location of a given geologic boundary on different geologic maps can provide some insight into map boundary accuracy. Typically, the mapped boundaries for the maps are located within 0 to 200 m of each other. The worst case, in an area of poor exposure, had differences in contact locations of 10 to 500 m.

Finally, possibilities exist for the presence of unmapped (previously undiscovered) fibrous rock areas and for areas to be misidentified. The chance of these situations generally decreases with increasing size of the occurrence, but cannot be entirely eliminated.

7.4.2.3.3 Map use and limitations

This map indicates areas and major faults within the Troodos Ophiolite where geologic conditions are favorable for natural occurrences of chrysotile asbestos. It is based on a compilation of existing geologic data from various published and unpublished sources and extensive geologic field work by the Ecorem-Atlantis project team.

The purpose of this map is to provide information to local, regional and national authorities and the public as to where natural occurrences of fibrous rock are more likely to be found in the Troodos area. It does not indicate whether asbestos minerals are present or absent in bedrock or soil associated with a particular parcel of land. The determination of asbestos presence or absence for a parcel can only be made during a detailed site-specific examination of the property. Consequently, no representations or warranties as to the actual presence or absence of natural occurrences of asbestos at specific locations within the area covered by this map can be made. Further, no representations or warranties regarding the accuracy of the data from which these maps were derived are made.

This map should help responsible Authorities in determining where they may wish to consider actions that may help minimize generation of and exposure to asbestos dust. Because of the uncertainties in the map, it should however not be used as a tool for prescribing mitigation measures. Rather it is intended to be used as a tool for determining where it may be appropriate to require site-specific investigations prior to the issuance of grading and development permits to aid in the selection of appropriate, cost-effective mitigation measures.

Map uncertainties in rock boundary locations and fault zone widths may be addressed in one or more ways. The most conservative approach might be to apply whatever investigation requirements are adopted to a specified buffer zone around ultramafic rock areas of some width (250 m, for example). Such an approach will increase the odds of finding small or poorly exposed ultramafic rock occurrences where mitigation might prove beneficial.

A final point is that geologic maps often require modifications of rock unit boundaries and fault locations as new information becomes available. Regulations involving geologic maps related to asbestos issues should allow for such modifications so that decisions will always be made based upon the most accurate geologic map available at the time.

8 CONCLUSIONS AND RECCOMENDATIONS

The ultimate objectives of Project GSD/2008/26 within the Troodos region have been achieved in a satisfactory manner and the principal conclusions drawn from this multidisciplinary project work are given below:

1. The Project's geological map confirms the bulk of the lithological and structural elements reflected on the published geological map of the Geological Survey Department. Significant upgrading has been achieved with respect to the distribution and relationships of a number of lithological units as a result of detailed field work and petrographical investigations. The Project's geological map is supported by petrographic work on a total of two hundred (200) standard thin-sections from outcrops.

2. The more extensive rocks within the Project area are multigenerational gabbros surrounding the ultrabasic complex of the Troodos dome structure. The bulk of the ultramafic layered rocks occur within the central portion of the Troodos dome structure and are closely associated with the tectonised harzburgite of the mantle sequence. Smaller layered ultramafic and mafic units occur within co-genetic pyroxene gabbros and appear to represent higher stratigraphic horizons.

3. Apart from the main serpentinite mass (Bastite Serpentinite) that forms the core of the ultrabasic complex, much smaller and irregular bodies of serpentinite occur at numerous locations within narrow zones of variably serpentinised ultrabasic rocks, particularly with the harzburgite, peridotite and dunite.

4. Besides harzburgite and dunite the petrographic study of thin sections revealed additionally protoliths of lherzolite and peridotite within the Bastite Serpentinite. Also, small bodies of these rocks are found enclosed within the Harzburgite Unit.

5. Microanalytically, the dunite is distinguished from the harzburgite-peridotite assemblage by relatively higher contents of MgO in its forsterite and high Cr/Cr+Al and Mg/Al ratios of its chromite.

6. Field relationships within the ultrabasic rocks of the central and stratigraphically lower portion of the Troodos dome structure substantiate previous views that the complex consists of an early deformed suite and a late undeformed suite, the latter being dominated by poikilitic wehrlite.

7. Block faulting typifies the overall tectonic pattern of the Project area and numerous lithological contacts are characterized by steeply dipping fractures and brecciation. Tectonic fabrics in older and deformed rocks are commnly parallel to the compositional layering.

8. The dominant serpentine mineral is lizardite with local development of antigorite. Chrysotile occurs primarily as asbestos but also as microcrystalline

(apparent fibre). Tremolite and actinolite within the Project area does not possess the specific structural features of asbestiform minerals.

9. Asbestos veining was found only in 12% of the investigated samples in the laboratory and all these samples were completely serpentinised rocks. They occur mainly in the Bastite Serpentinite area (and also in the Harzburgite and Dunite areas). In addition, traces of chrysotile were found in rock samples originating from the Wehrlite, Peridotite and Isotropic Gabbro formations. Only a very small portion of the investigated soil samples indicated considerable quantities of asbestiform chrysotile.

10. Pervasive veining and well developed stringer and veinlet stockworks of chrysotile asbest are confined to the Bastite Serpentinite, particularly in its brecciated and smashed portion within Amiantos quarries and their immediate vicinity.

11. Hair-like stringers of both asbestiform and microcrystalline chrysotile are found erratically distributed within serpentinite zones developed elsewhere in the ultrabasic rocks.

12. The Potential Asbestos Related Risk (ARR) was identified on the basis of deliniating areas with surface rock outcrops and soils which contain asbestos fibers. Under this criterion the whole of the serpentine area is considered to carry a potential ARR.

13. Asbestos Related Risk, ARR, on the basis of risk of exposure to airborne asbestos fibers, is assessed by calculating the potential annual and peak hour concentration of fibers that can result from dust raising events in the serpentine areas.

14. The study has revealed that the serpentine area indeed constitutes a basic Asbestos Related Risk, ARR.

15. The study revealed that disturbed, un-restored areas of the mine constitute a moderate risk from the presence of airborne asbestos fibers. However, additional research is required, especially with regard to fiber emission rates from soils. Also it is noted that this conclusion pertains to asbestos concentrations produced by airborne asbestos from natural dust events. Human induced dust-raising such as ground works and off road driving are additional risks.

In addition, the following recommendations are given with regard to the management of the assessed risk:

1. Residents and regular users of the area should be informed of the levels of risk associated with various activities within the Troodos area.
2. A risk management guide should be prepared and disseminated to people involved in dust generating activities such as ground works and cultivation.

3. Activities involving ground works in the Risk areas as delineated in the basic risk map should undergo an asbestos impact assessment. Measures should be proposed to mitigate the derived impacts.
4. Off roads with bare in situ soil surfaces should be covered either by paving or by suitable imported material.
5. The following further investigations are suggested which will enrich the current knowledge and information for the study area and will help to improve the accuracy and reliability of the risk map:
   - asbestos fibers content in dust
   - Monitoring of airborne dust concentrations, preferable of both PM10 and TSP.
   - Research to improve calculations of dust raising and fiber raising from soils to air
6. Additional investigations are also suggested with regard to the geological mapping of the area in order to further enrich the existing geological map.
7. To conduct additional research, especially with regard to fiber emission rates from soils in the area of the Troodos Mountains, but also in geologically similar areas, including Limassol Forest.

30 November, 2010

For Ecorem NV and ATLANTIS Consulting Ltd.

Charalambos Panayiotou
Consortium representative

REFERENCES

Albin M, Pooley FD, Stromberg U, et al. (1994). Retention patterns of asbestos fibres in lung tissue among asbestos cement workers. Occup Environ Med 51: 205-211.

Allen C. R. (1972). The petrology of a portion of the Troodos plutonic complex, Cyprus. Unpubl. PhD Thesis.

Amandus HE & Wheeler R. 1987. The morbidity and mortality of vermiculite miners and millers exposed to tremolite-actinolite: PartII. Mortality. Am J Ind Med 11:15-26.

American Thoracic Society (1986). Statement on diagnosis of nonmalignant diseases related to asbestos. Am Rev Resp Dis 134:363-8.

Baris Y. (1987). Asbestos and erionite related chest diseases. Ankara, Turkey: Semih Ofset Mat Ltd Co.

Baris Y.I., Artvinli M., Sahin A.A., et al. (1988a). Non-occupational asbestos trelated chest diseases in small Anatolian village. Br J Ind med 45:841-842.

Batanova, V.G., Sobolev, A.,V. (2000). Compositional heterogeneity in subduction-related mantle peridotites, Troodos massif, Cyprus. Geology, 28, 1, 55-58.

Bazas T, Oakes D, Gilson JC, et al. (1985). Pleural calcification in northwest Greece Environ Res 38:239-247.

Bazas T. (1987). Pleural effects of tremolite in north-west Greece. Lancet 1 (8548):1490-1491.

Bloss, F.D., 1999, Optical crystallography: Mineralogical Society of America Monograph Series, Publication 5: Washington, D.C., Mineralogical Society of America, 239 p.

Boffetta, P. (1998). Health effects of asbestos exposure in humans: a quantitative assessment. Med Lav 89:471-80.

Boutin G., Viallat J.R., Steinbauer J., et al. (1989). Bilateral pleural plaques in Corsica: a marker of non-occupational asbestos exposure. IARC Sci Publ 90: 406-410.

Burragato, P., Monti, F., Papacchini, L., Sperduto, B. (2002). Affioramenti di minerali asbestiformi; il caso della Regione Basilicata. Mappatura e valutazione del rischio. Prima nota. Le giornate di Corvara VIII Convegno di Igiene Industriale, 159-161.

Camus, M., Siemiatycki, J. and Bette Meek (1998). Nonoccupational Exposure to Chrysotile Asbestos and the Risk of Lung Cancer. The New England Journal of Medicine, 338, 22, 1565-1571.

Case BW. 1991. Health effects of tremolite: now and in the future. Ann N Y Acad Sci 643:491-504.

Churchill, R.K., Higgins, C., Hill, B. (Eds.) (2000). Areas more likely to contain natural occurrences of asbestos in Western El Dorado County, California. Department of Conservation, Division of Mines and Geology – Open-file report 2000-02.

Churg A & Wright JL. 1989. Fibre content of lung in amphibole- and chrysotile-induced mesothelioma: implications for environmental exposure. IARC Sci Publ 90:314-318.

Churg A, Wright JL. 1994. Persistence of natural mineral fibres in human lungs: an overview. Environ Health Perspect Suppl 102(5):229-233.

Churg A. 1993. Asbestos, Asbestosis and lung cancer, Modern Pathology, 6: 509-511.

Clinckenbeard, J. P., Churchill, R. K., Lee, K. (Eds.) (2002). Guidelines for Geologic investigations of naturally occurring asbestos in California. California Geological Survey. Special Publication 124.

Coin P.G., Roggli V.L., Brody A.R. (1992). Deposition, clearance, and translocation of chrysotile asbestos from peripheral and central regions of the rat lung. Environ Res 58: 97-116.

Coleman R.G. (1977). Ophiolites. Ancient Oceanic Lithosphere ? Springer -Verlag, Berlin, Heidelberg, New York, 299 p.

Constantopoulos S.H., Goudevenos J.A., Saratzis N., Langer A.M., Selikoff I.J., Moutsopoulos H.M. (1985). Metsovo lung: pleural calcification and restrictive lung function in northwestern Greece. Environmental exposure to mineral fibre as etiology. Environ Res 38:319-331.

Constantopoulos S.H., Malamou-Mitsi V.D., Goudevenos J.A., Papathanasiou M.P., Pavlidis N.A., Papadimitriou C.S. (1987). High incidence of malignant pleural mesothelioma in neighboring villages of northwestern Greece. Respiration 51: 266 – 271.

Constantopoulos S.H., Theodoracopoulos P., Dascalopoulos G., et al. (1991). Metsovo lung outside Metsovo: endemic pleural calcifications in the ophiolite belts of Greece. Chest 99: 1158-1161.

Çoplü L., Dumortier P., Demir A.U., Selcuk Z.T., Kalyoncu F., Kisacik G., De Vuyst P., Sahin A.A., Baris Y.I. (1996). An epidemiologic study in an Anatolian village in Turkey environmentally exposed to tremolite asbestos. J Environ Pathol Toxicol Oncol 15(2-4): 177-182.

Cullen M.R. (1998). Chrysotile asbestos: enough is enough. Lancet 351:1377-8.

Davis J.M.G. (1989). Mineral fibres carcinogenesis: experimental data relating to the importance of fibre type, size, depositon, dissolution and migration. IARC Sci Publ 90: 33-45.

Davis JMG, Adison J, Bolton RE, et al. 1985. Inhalation studies on the effects of tremolite and brucite dust in rats. Carcinogenesis 6(5):667-674.

Davis JMG, Bolton RE, Donglas A, Jones AD & Smith T. 1988. The effects of electrostatic charge on the pathogenicity of chrysotile asbestos; Br J Ind Med 45: 337-345.

Dodson RF, O'Sullivan M, Corn CJ, et al. 1997. Analysis of asbestos fibre burden in lung tissue from mesothelioma patients. Ultrastruct Pathol 21:321-336.

Doll R. 1955 Mortality from lung cancer in asbestos workers. Br J Ind Med 12:81-86.

Douglas, V., Suer, C., Villalobos, S., McCormack, J. (Eds.) (2002). Implementation guidance document for the asbestos airborne toxic control measure for surfacing applications. Stationary Source Division Emissions Assessment Branch. California Environmental Protection Agency Air Resources Board.

Dumortier P, 2003. Corps asbestosiques et fibres d'asbeste dans les échantillons pulmonaires. Utilisation comme marqueurs d'expositions professionnelles ou environnementales. Thesis, Brussels 146p.

Dumortier P, Çoplü L, de Martelaer V, Emri S, Baris I, and De Vuyst P. 1998. Assessment of environmental asbestos exposure in Turkey by bronchoalveolar lavage. Am J Respir Crit Care Med 158:1815-1824.

Dumortier, P., Coplu, L., Broucke, I., Emri, S., Selcuk, T., de Maertelaer, V., De Vuyst, P., Baris, I. (2001). Erionite bodies and fibres in bronchoalveolar lavage fluid (BALF) of residents from Tukzoy, Cappadocia, Turkey. Occup Environ Med, 58, 261-266.

Ecorem nv (unpublished report, 2006) Risk assessment due to the Presence of the Asbestos Mine, Troodos. Final report. Ministry of Agriculture, Natural Resources and Environment, Geological Survey Department Nicosia – Cyprus (Contract No. GSD/15/2002).

EPA, Integrated Risk Information System, http://www.epa.gpv/iris

Erzen C, Eryilmaz M, Kalyoncu F, et al. 1991. CT findings in malignant pleural mesothelioma related to nonoccupational exposure to asbestos and finrous zeolite (erionite). J Comput Assist Tomogr 15(2):256-260.

Gass I.G., MacLeod C.J, Murton B.J, Panayiotou A., Simonian K.O and Xenophontos C. (1994). The Geology of the Southern Troodos Transform Fault Zone. Cyprus Geological Survey Memoir 9.

Gass et al. (1990) Ophiolites. Oceanic Crust Analogues, Proceedings of the Symposium "Troodos 1987". Cyprus Geological Survey.

George R. P. (1975). The internal structure of the Troodos ultramafic Complex, Cyprus. Unpubl. PhD Thesis.

Goldberg M (INSERM, France), 2001. Health effects of non occupational exposure to asbestos, Asbestos Health Effects Conference, EPA, Oakland.

Goldstein, J.I., Newbury, D.E., Echlin, P., Joy, D.C., Fiori, C. and Lifshin, E., 1981, Scanning electron microscopy and X-ray microanalysis: a text for biologists, materials scientists, and geologists: New York and London, Plenum Press, 673 p.

Greenbaum D. (1972). The geology and evolution of the Troodos Plutonic complex and associated chromite deposits Cyprus. Unpubl. PhD Thesis.

GSD (2010) – Geology of Cyprus: http://www.moa.gov.cy/

Health Effects Institute - Asbestos Research. Asbestos in public and commercial buildings: a literature review and synthesis of current knowledge. Cambridge, MA, Health Effects Institute,1991

Howard Humphrey & Partners (1980). Loumata Valley Tip: Investigation and Design.

Howard Humphrey & Partners (1981). Tip Stability. Reconnaissance Report.

Hurlbut CS Jr, Klein C. (1977). Manual of mineralogy. 19th ed. New York, NY: John Wiley and Sons, 338-339.

International Group of Experts (1997). Asbestos, Asbestosis and Cancer. Proceedings of an International Expert Meeting 20-22 January 1997, Helsinki, Finland. Finnish Institute of Occupational Health, Helsinki, Finland. People and work. Research reports 1997;14:1-98.

INVIS - Institut de Veille Sanitaire (2007). Exposition environnementale à l'amiante chez les personnes riveraines d'anciens sites industriels et d'affleurements naturels. Choix méthodologiques, analyse des données disponibles, modalités de recueil.

INVIS - Institut de Veille Sanitaire (2007). Recensement et classement des sites naturels amiantifères et des formations géologiques potentiellement amiantifères en France. Rapport final.

Iwatsubo Y, Pairon JC, Boutin C, et al. 1998. Pleural mesothelioma: Dose-response relation at low levels of asbestos exposure in a French population-based case-control study. Am J Epidemiol 148:133-42.

Jolicoeur, CR, Alary JF, Sokov A. (1992). Asbestos. In: Kroschwitz JI, Howe-Grant M, ed. Kirk-Othmer encyclopedia of chemical technology. New York: John Wiley & Sons, 659-688.

Kyrou, K., and G. Petrides. 2004. The rehabilitation of the asbestos mine, Cyprus. Water Development Department, Republic of Cyprus, Greece. 9 pp.

Langer AM, Nolan RP, Constantopoulos SH et al. 1987. Association of Metsovo lung and pleural meothelioma with exposure to tremolite-containing whitewash. Lancet 1 (8539):965-967.

Lippman, M. (1994). Deposition and retention of u-inhaled fibres: effects on incidence of lung cancer and mesothelioma. Occup. Environ. Med. 51, 793-798.

Luce D, Brochard P, Quenel P, et al. 1994. Malignant pleural mesothelioma associated with exposure to tremolite. Lancet 344:1777.

Luce D, Bugel I, Goldberg P, Goldberg M, Salomon C, Billon-Galland MA, Nicolau J, Quenel P, Fevotte J, Brochard P. 2000, environmental exposure to tremolite and respiratory cancer in New Caledonia: a case-control Study. Am J Epidemiol 151 (3): 259 – 65.

Lynch KM, Smith WA. 1935. Pulmonary asbestosis III: Carcinoma of the lung in asbestos silicosis. Am J Cancer 24:56-64.

Magee F, Wright JL, Chan N, et al. 1986. Malignant mesothelioma caused by childhood exposure to long-fibre low aspect ratio tremolite. AM J Med 9:529-533.

Magnani C, Agudo A, Gonzalez CA, Andrion A, Calleja A, Chellini E, Dalmasso P, Escolar A, Hernandez S, Ivaldi C, Mirabelli D, Ramirez J, Turuguet D, Usel M, Terracini B. 2000. Multicentric study on malignant pleural mesothelioma and non-occupational exposure to asbestos. Br J Cancer 83:104-111.

McCrone, W.C., 1987, Asbestos identification: Chicago, Illinois, McCrone Research Institute, G&C Printers Inc., 199 p.

McDonald AD, Case BW, Churg A et al. 1997. Mesothelioma in Quebec chrysotile miners and millers: epidemiology and aetiology. Ann Occup Hyg 41:707-19.

McDonald JC, Sebastien P, Armstrong B. 1986. Radiological survey of past and present vermiculite miners exposed to tremolite. Br J Ind Med 43:445-449.

Metintas M, Ozdemir N, Hillerdal G, et al. 1999. Environmental asbestos exposure and malignant pleural mesothelioma. Respir Med 93:349-355.

Michaelides A. (1983). The origin of Chromites of the plutonic complex of the Troodos, Cyprus. Unpubl. PhD Thesis.

Mossman BT, Bignon J, Corn M, et al. 1990. Asbestos: scientific developments and implications for public policy. Science 247:294-301.

Murray HM. Statement before the committee in the minutes of evidence. In: report of the Departmental Committee on Compensation for Industrial Disease. H. M. Stationery Office, London 1907:127.

Nesse, W.D., 1991, Introduction to optical mineralogy: 2nd Edition, New York, Oxford University Press, 335 p.

Nicolas A. (1989). Structures of Ophiolites and Dynamics of Oceanic Lithosphere. Petrology and structural geology. Kluwer Academic Publishers. 367 p.

NIOSH. 1999. Work-related disease surveillance report 1999. Washington, DC: U.S. Department of Health and Human Services, Public Health Service, Centres for Disease Control, National Institute for Occupational Safety and Health, Division of Respiratory Disease Studies. DHHS (NIOSH) Publication No. 96-134.

Nurminen M, Karjalainen A, Takahashi K. 2003. Estimating the Induction Period of Pleural Mesothelioma From Aggregate Data on Asbestos Consumption. J Occup Environ Med 45:1107-1115.

O'Hanley, D.S., 1996, Serpentinites: records of tectonic and petrological history: New York, Oxford University Press, 227 p.

Pan, X.-L., Day, H.W., Wang, W., Beckett, L.A., Schenker, M.B. (2005) Residential Proximity to Naturally Occurring Asbestos and Mesothelioma Risk in California. American Journal of Respiratory and Critical Care Medicine, 172; 1019-1025.

Panayiotou A, (1980). Ophiolites. Proceedings International Ophiolite Symposium, Cypeus 1979. Cyprus Geological Survey.

Pantazis Th. M. (1980). Ophiolites of Cyprus. Ofioliti, Vol. 2 Spec. Issue, 239-278.

Peto J., Decarli A., La Vecchia C., Levi F., Negri E. (1999). The European mesothelioma epidemic. Br J Cancer 79:666-72.

Peto J., Hodgson J.T., Matthews F.E., Jones J.R. (1995). Continuing increase in mesothelioma mortality in Britain. Lancet 345:535-9.

Pott F, Roller M, Ziem U, et al. 1989. Carcinogenicity studies on natural and man-made fibres with the intraperitoneal test in rats. IARC Sci Publ 90:173-179.

Potts, P.J., 1987, A handbook of silicate rock analysis: Glasgow: New York, Blackie; Chapman and Hall, 622 p.

Rey F., Boutin C., Steinbauer J., et al. (1993). Environmental pleural plaques in an asbestos exposed population in northeast Corsica. Eur Respir J 6: 978-982.

Rey F., Boutin C., Viallat J.R., et al. (1994). Environmental asbestotic pleural plaques in northeast Corsica: correlations with airborne and pleural mineralogic analysis. Environ Health Perspect 102 (Suppl 5):251-252.

Roggli, V. (2007). Environmental Asbestos Contamination. What are the risks? Chest, 131, 336-338.

Roller M, Pott F, Kamino K, et al. 1996. Results of current intraperitoneal carcinogenicity studies with mineral and vitreous fibres. Exp Toxicol Pathol 48:3-12.

Roller m, Pott F, Kamino K, et al. 1997. Dose-response relationship of fibrous dusts in intraperitoneal studies. Environ. Health Perspect 105(Suppl 5):1253-1256.

Ross, M. (1981) The geologic occurrences and health hazards of amphibole and serpentine asbestos. In: Veblen, D.R., ed., Amphiboles and other hydrous pyriboles—Mineralogy: Mineralogical Society of America, Reviews in Mineralogy, p. 279-323.

Ross, M., and Virta, R.L. (2001). Occurrence, production and uses of asbestos. In: Nolan, R.P., Langer, A.M., Ross, Malcolm, Wicks, F.J., and Martin, R.F., eds., The health effects of chrysotile asbestos—Contribution of science to risk-management decisions: The Canadian Mineralogist, Special Publication 5, p. 79-88.

Sakellariou K, Malamou-Mitsi V, Haritou A, Koumpaniou C, Stachouli C, Dimoliatis ID, Constantopoulos SH. 1996. Malignant pleural mesothelioma from non-occupational asbestos exposure in Metsovo (north-west Greece): slow end of an epidemic? Eur respir J 9:1206-1210.

Schneider J, Rodelsperger K, Bruckel B, et al. 1998. Environmental exposure to tremolite asbestos: pleural mesothelioma in two Turkish workers in Germany.Rev Environ. Health 13(4):213-220.

Sebastien P, Janson X, Gaudichet A. et al. 1980. Asbestos retention in human respiratory tissues: comparative measurements in lung parenchyma and in parietal pleura. IARC Sci Publ 30: 237-246.

Şenyiğit, A., Babayiğit, C., Gökirmak, M., Topçu, F., Asan, E., Coşkunsel, M., Işik, R., Ertem, M. (2000). Incidence of Malignant Pleural Mesothelioma due to Environmental Asbestos Fibre Exposure in the Southeast of Turkey. Respiration, 67, 610-614.

Smith WE, Hubert DD, Sobel HJ, et al. 1979. Biologic tests of tremolite in hamsters. In: Lemen R, dement JM Eds. Proc. Conf. Occup. Exp. Fibrous Part. Dust. Ther. Ext. Environ. Park Forest South IL: 335-339.

Stanton MF, Layard M, Tegeris A, et al. 1981. Relation of particle dimension to carcinogenicity in amphibole asbestoses and other fibrous minerals. J Natl Cancer Inst 67(5):965-975.

US Department of Health and Human Services (2001). Toxicological profile for asbestos.

Vainio H, Boffetta P. 1994. Mechanisms of the combined effect of asbestos and smoking in the etiology of lung cancer. Scand J Work Environ Health 20:235-242.

Veblen, D.R. and Wylie, A.G., 1993, Mineralogy of amphiboles and 1:1 layer silicates, in Guthrie, G.D. and Mossman, B.T., eds., Health effects of mineral dusts, Reviews in Mineralogy, v. 28, Washington, D.C., Mineralogical Society of America, p. 61-137.

Virta RL. 2001. Asbestos: Geology, Mineralogy, Mining and Uses, U.S. Department of the Interior U.S. Geological Survey

Wagner JC, Berry G, Skidmore JW & Timbrell V. 1974. The effects of the inhalation of asbestos in rats, Br J Cancer, 28:173-185.

Wagner JC & Skidmore JW. 1965. Asbestos dust depositon and retention in rats, Ann NY Acad Sci, 132:77-86.

Wagner JC, Sleggs CA, Marchand P. 1960. Diffuse pleural mesothelioma and asbestos exposure in North Western Cape Province. Br J Ind Med 17:260-71.

Whittaker E. and Zussman J. (1956). The characterization of serpentine minerals by X-ray diffraction. Miner. Mag. 31, 107-126.

WHO (1998). Chrysotile asbestos: Environmental health criteria. Geneva: Switzerland: World Health Organization.

Wicks F. (2000). Status of the reference X-ray powder diffraction patterns for the serpentine minerals in the PDF database-1997. Powder Diffraction 15, (1), 42-50.

Wicks F. and O'Hanlley D. (1988). Serpentine minerals: Structures and petrology, in Hydrous Phyllosilicates, eds. S.W. Bailey, Reviews in Mineralogy, Vol. 19 (Mineralogical Society of America), pp. 91-167.

Wilson, R.A.M. (1959). The geology of the Xeros-Troodos area. Cyprus Geological Survey Memoir 1, 184 p.

Wylie A.G., Bailey K.F., Kelse J.W. (1993). The importance of width in asbestos fibre carcinogenicity and its implications for public policy. Am Ind Hyg Assoc J 54(4):239-252.

Yazicioglu S, Ilcayto R, Balci K, et al. 1980. Pleural calcification, pleural mesotheliomas, and bronchial cancers caused by tremolite dust. Thorax 35: 564-569.

ANNEX 1

SAMPLES

Sampling Locations

Topography, land cover, geology

Sample characteristics

Sampling Codes

ANNEX 2

FIELD WORK DATA: PHOTOGRAPHS

ANNEX 3

SAMPLE ANALYSES

ANNEX 4

REVISED GEOLOGICAL BASE MAP OF THE TROODOS AREA

ANNEX 5

SPATIAL DISTRIBUTION OF SAMPLES CONTAINING NATURALLY OCCURRING FIBROUS MATERIAL IN THE TROODOS AREA – FIELD OBSERVATIONS

ANNEX 6

SPATIAL DISTRIBUTION OF SAMPLES CONTAINING NATURALLY OCCURRING FIBROUS MATERIAL IN THE TROODOS AREA – LABORATORY RESULTS

ANNEX 7

LABORATORY FINAL PROGRESS REPORT

ANNEX 8

LABORATORY FINAL PROGRESS REPORT – ADDITIONAL SAMPLES

ANNEX 9

RISK AND CORRECTION FACTORS

ANNEX 10

ENVIRONMENTAL EXPOSURE RISK MAP